

AD-A065 387

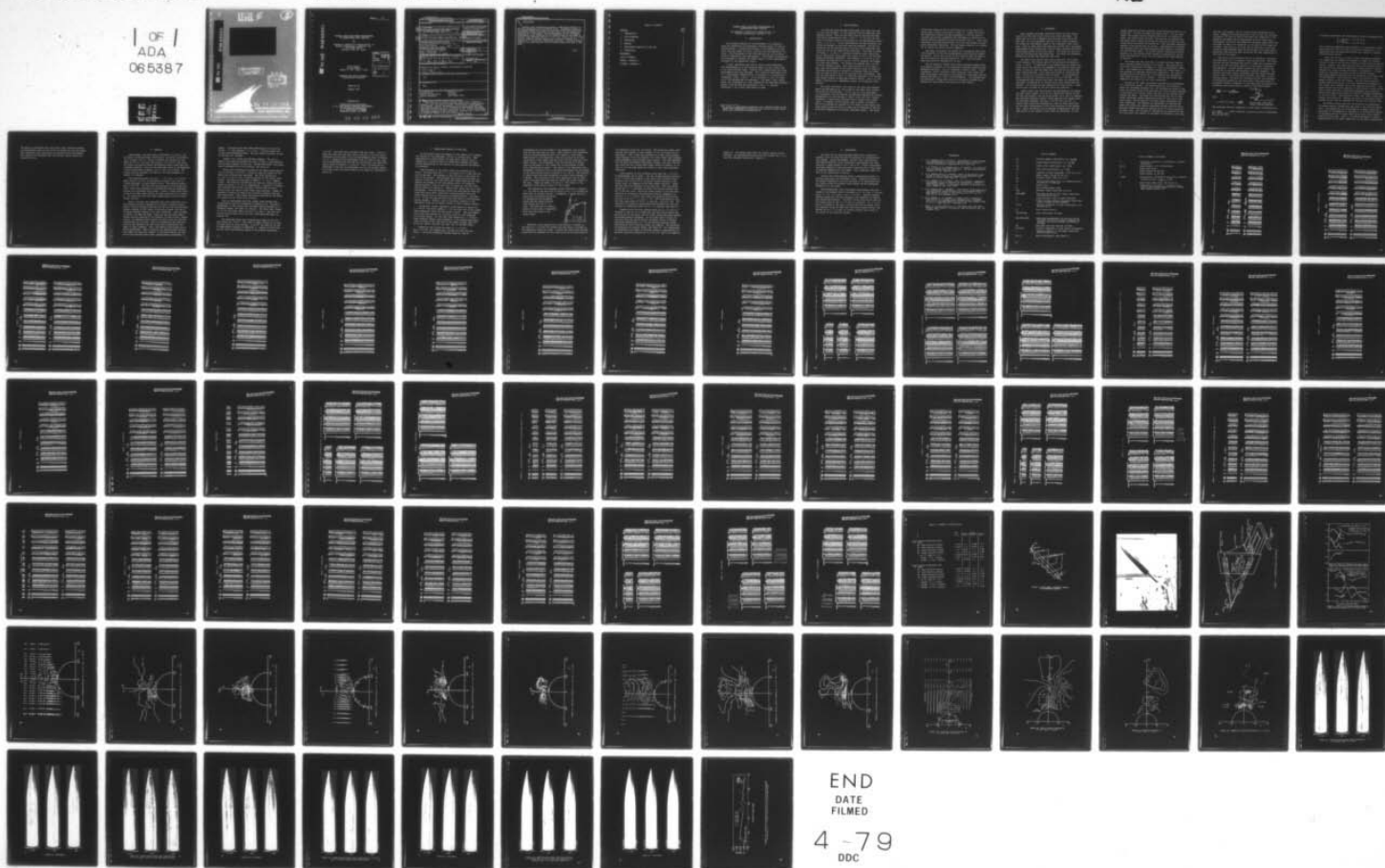
NIELSEN ENGINEERING AND RESEARCH INC MOUNTAIN VIEW CALIF F/G 20/4
FURTHER LASER VELOCIMETER MEASUREMENTS OF SLENDER-BODY WAKE VOR--ETC(U)
AUG 78 R G SCHWIND, J MULLEN
DAAK40-77-C-0070

UNCLASSIFIED

NEAR-TR-168

NL

OF /
ADA
065387



LEVEL II

5

AD A0 65387

DDC FILE COPY

DISTRIBUTION STATEMENT A

Approved for public release;
Distribution Unlimited



79 02 05 034

**NIELSEN ENGINEERING
AND RESEARCH, INC.**

OFFICES: 510 CLYDE AVENUE / MOUNTAIN VIEW, CALIFORNIA 94043 / TELEPHONE (415) 955-9457

COPY NO. 23

DDC FILE COPY AD A0 65387

FURTHER LASER VELOCIMETER MEASUREMENTS
OF SLENDER-BODY WAKE VORTICES

by

Richard G. Schwind and Joseph Mullen, Jr.
Nielsen Engineering & Research, Inc.
510 Clyde Avenue
Mountain View, CA 94043

Final Report
for the period
March 7, 1977 - May 7, 1978

Approved for public release;
distribution unlimited

ACCESSION for	
NTIS	Wallo Section
DDC	Diff Section
UNANNOUNCED	
JUSTIFICATION	
BY	
DISTRIBUTION/AVAILABILITY CODES	
Dist.	AVAIL. and/or SPECIAL
A	

NEAR TR 168

August 1978

Prepared for

Aeroballistics Directorate
U. S. Army Missile Research Development,
and Engineering Laboratory
U. S. Army Missile Command
Redstone Arsenal, AL 35809

79 03 05 034

Unclassified

SECURITY CLASSIFICATION OF THIS PAGE (When Data Entered)

REPORT DOCUMENTATION PAGE		READ INSTRUCTIONS BEFORE COMPLETING FORM
1. REPORT NUMBER	2. GOVT ACCESSION NO.	3. RECIPIENT'S CATALOG NUMBER
4. TITLE (and Subtitle) FURTHER LASER VELOCIMETER MEASUREMENTS OF SLENDER-BODY WAKE VORTICES		5. TYPE OF REPORT & PERIOD COVERED Final Technical Report 3/7/77 - 5/7/78
7. AUTHOR(s) Richard G. Schwind and Joseph Mullen, Jr		6. PERFORMING ORG. REPORT NUMBER NEAR-TR-168
9. PERFORMING ORGANIZATION NAME AND ADDRESS Nielsen Engineering & Research, Inc. 510 Clyde Avenue Mountain View, CA 94043 389 783		8. CONTRACT OR GRANT NUMBER(s) DAAK40-77-C-0070
11. CONTROLLING OFFICE NAME AND ADDRESS U.S. Army Missile Command ATTN: DRSMI-RDK Redstone Arsenal, AL 35809		10. PROGRAM ELEMENT, PROJECT, TASK AREA & WORK UNIT NUMBERS
14. MONITORING AGENCY NAME & ADDRESS (if different from Controlling Office) Final technical rept. 7 Mar 77 - 7 May 78		12. REPORT DATE August 1978
16. DISTRIBUTION STATEMENT (of this Report) Approved for public release; distribution unlimited. (12) 98 p.		13. NUMBER OF PAGES 87
17. DISTRIBUTION STATEMENT (of the abstract entered in Block 20, if different from Report) N/A		15. SECURITY CLASS. (of this report) Unclassified
18. SUPPLEMENTARY NOTES None		15a. DECLASSIFICATION/DOWNGRADING SCHEDULE N/A
19. KEY WORDS (Continue on reverse side if necessary and identify by block number) Aerodynamics Missiles Bodies of revolution Vortices Laser Anemometer Wind Tunnel Test		
20. ABSTRACT (Continue on reverse side if necessary and identify by block number) The flow over an ogive-cylinder model with a length-to-diameter ratio of seven has been investigated at incompressible flow speeds. Forces and moments, surface flow visualization, and three-dimensional laser velocimeter measurements have been obtained at pitch angles of 22.5° and 37.5°. Forces and moments have been compared to data previously obtained over a wide range of Reynolds numbers with this model. 389 783 <i>elt</i>		

DD FORM 1 JAN 73 1473

EDITION OF 1 NOV 65 IS OBSOLETE

Unclassified

SECURITY CLASSIFICATION OF THIS PAGE (When Data Entered)

Unclassified

SECURITY CLASSIFICATION OF THIS PAGE(When Data Entered)

20. (Continued)

Surface flow visualization shows a complicated pattern of multiple separation and attachment lines. Asymmetric breaks in the primary separation lines are believed to be associated with the tearing loose of attached vortex sheets and the subsequent formation of a new sheet. Three-dimensional laser velocimeter measurements were performed on the leeward side of the model at several cross sections and at $X = 2.8, 4.9, \text{ and } 6.3$ for $\alpha = 37\frac{1}{2}^\circ$. Vortical regions rapidly become more and more diffusive and asymmetric in nature with downstream distance. Crossflow vector plots do not show distinct vortex centers toward the rear of the model.

alpha

Unclassified

SECURITY CLASSIFICATION OF THIS PAGE(When Data Entered)

TABLE OF CONTENTS

<u>Section</u>	<u>Page No.</u>
1. INTRODUCTION	1
2. TEST APPARATUS	2
3. PROCEDURES	4
4. RESULTS	9
5. PRELIMINARY ANALYSIS OF THE DATA	12
6. CONCLUSIONS	16
REFERENCES	17
LIST OF SYMBOLS	18
TABLES 1 THROUGH 9	20
FIGURES 1 THROUGH 23	60

FURTHER LASER VELOCIMETER MEASUREMENTS OF SLENDER-BODY WAKE VORTICES

by Richard G. Schwind and Joseph Mullen, Jr.
Nielsen Engineering & Research, Inc.

1. INTRODUCTION

The rational modeling of flow phenomena is an effective means for predicting the aerodynamic characteristics of missile configurations. A significant portion of the modeling for moderate and high angles of attack concerns the body separation vortices. The correctness of the flow modeling can only be determined by comparisons with measurements. The present investigation was performed to increase the meager amount of flow measurements available in the separation region.

A laser velocimeter was used to obtain three-dimensional flow measurements in a non-intrusive manner on the leeward side of an ogive-cylinder model. Surface flow visualization and force measurements were also obtained. This study was sponsored by the U. S. Army Missile Command and is an extension of a previous investigation (refs. 1 and 2). As in reference 1, this is a data report for documenting the experiment. The model, laser velocimeter, and instrumentation were supplied by the NASA Ames Research Center,* and the test was performed in the U. S. Army R&T Laboratory 7- by 10-Foot Wind Tunnel at Ames.

*The author is particularly grateful to Dr. Kenneth Orloff of the Large Scale Aerodynamics Branch for the use of his laser velocimeter and associated instrumentation.

2. TEST APPARATUS

An existing ogive-cylinder wind-tunnel test model was used for this test program. It was borrowed from the NASA Ames Aerodynamics Branch. This was the model used in the previous NEAR flow field investigation (refs. 1 and 2). It has been the subject of extensive testing by personnel of the Aerodynamics Branch (refs. 3, 4, 5, 6). In the investigations by Ames personnel the forces and moments on the body have been measured and the surface flow and the vortical flow field have been visualized, the latter by use of the vapor-screen technique. The model is shown in Figure 1. It has a 3.5 length-to-diameter ratio ogive nose with a sharp point (nose apex total angle of 32.9°) and the same length cylindrical afterbody. The diameter is 15.24 cm (6 in.). The model was mounted on a 3.81-cm (1.5-in) diameter six-component task force balance. The balance was mounted into a 5.7-cm (2.25-in) diameter sting. This sting pivoted in pitch about a post that was attached to the tunnel floor as shown in Figure 2. The model centerline was located 4.5 diameters from the tunnel wall in order to make use of an existing laser velocimeter. The test was performed in the U. S. Army R&T Laboratory 7- by 10-Foot Wind Tunnel located at NASA Ames Research Center. This is a low speed, closed-circuit, atmospheric tunnel of rectangular cross section.

The laser velocimeter (LV) used for the flow field measurements was designed by Dr. Ken Orloff of the Large Scale Aerodynamics Branch of NASA Ames. It was lent for this experiment. It incorporates two dual-scatter crossed-beam systems that operate independently at wave-lengths of 488.0 (blue) and 514.5 (green) nanometers. These beams originate from a single 4-watt argon laser. A schematic of the optical path is shown in Figure 3. The two LV systems are mounted at a 30° angle to each other (the green system above the blue) to make the LV sensitive to the two cross-flow components of velocity (described later). The three

fixed-focus lenses of the LV (the center one is the receiving optics) show through the window in Figure 2. Except for use of the fixed-focus lenses and the arrangement of the two sets of transmitting optical components the instrument is similar to an earlier version designed by Grant and Orloff (ref. 7). Also, this instrument contained acousto-optic cells in each channel to eliminate directional ambiguity. The top (green) channel was rotated 90° to obtain the axial velocity component.

The laser velocimeter was placed on a traversing table that could translate in the three perpendicular directions by operating motors. The LV was tilted on this table so that the axis of the blue beams was inclined upwards at 7.74° (thus the green beams were directed downwards at 22.26°).

The LV frequency signals were either analyzed automatically by frequency trackers, or the frequency determined manually using frequency analyzers. This is discussed in detail later. The LV frequencies, three traversing table positions, four normal and side force gages, and tunnel Q were sensed by transducers and the signals delivered to a PDP 11-05 minicomputer. The computer system contained a floppy disk drive for accessible storage and a cathode ray tube display with copier for hard copies.

3. PROCEDURES

Upon assembly the model contained several surface irregularities in the form of bolt holes, pin holes and seams. The seams came at $2/3$ of a diameter from the nose (the end of the nose cap), at $3-1/2$ diameters (the end of the ogive forebody), and along the longitudinal seams of the clam-shell style afterbody. Most of these holes and seams were filled with a polyester resin-based filler (body putty) and the model smoothed and buffed before being placed in the wind tunnel. Two holes for mounting pins and the nose seam were waxed over. The model was frequently washed with solvent and wiped dry with rags.

Two model pitch angles were used in the test, $22-1/2$ and $37-1/2$ degrees, the same as used in the previous investigation (refs. 1 and 2). To establish at the higher angle of attack from which side of the missile the asymmetric flow pattern would originate, a strip of tape was added near the nose on the left hand side looking upstream. This tape strip helped to stabilize the flow. It was 0.5 cm wide by 0.026 cm thick. It was placed between 1.75 and 10.3 cm behind the tip (0.11 to $0.68 X/D$). The six-component body balance upon which the model was mounted was previously calibrated by an outside group using established procedures. Its calibration was checked in the wind tunnel. Interactions were included in the data reduction equations.

Carbon black flow visualization was performed at two different wind tunnel speeds, 18.2 and 36.4 meters per second (60 and 120 feet per second), and two pitch angles, 22.5 and 37.5 degrees. The resulting Reynolds numbers, based upon the free stream velocity and model diameter, are $Re_D = 0.18 \cdot 10^6$ and $0.37 \cdot 10^6$. A carbon black recipe was developed for each of those conditions for the best visualization of the fine structure of the surface flow. Since the mixture and its method of application may have some effect on the results, these items are described. At the

higher speed the solvent consisted of 60% kerosene and 40% no. 10 weight oil. To this was added 25% carbon black. For the lower speed, the solvent was 87% kerosene and 13% no. 10 weight oil. Again, 25% carbon black was used. The mixture was painted onto the model with a bristle brush and the painting process was continued while the tunnel was started up. This procedure minimized sagging of the mixture due to gravity. Approximately 20 seconds was required after the painting process was stopped to establish the desired flow speed. The surface pattern established itself quickly, but the solvent either gradually evaporated or ran off along the separation lines; and this process took approximately 45 minutes.

The tunnel was then shut down, the nose carefully removed and a carrying handle attached to the model. The model was removed from the balance and taken to a special photographic chamber. This chamber was a framework covered with cheese cloth. It was designed to eliminate destructive highlights. The nose was reinstalled once the model was in the chamber and photographs were taken at every 60° of rotation. The nose was always reassembled to the model with the same orientation.

Setting up the laser velocimeter required the establishment of a coordinate system. The three-dimensional LV traversing table was repeatedly adjusted until the intersection point of the laser velocimeter laser beams followed thin nylon strings attached to plum bobs at the front, middle and rear of the vertical plane through the model. The model was then mounted and the LV wind tunnel coordinate system established using the nose tip at zero pitch angle. The LV position and model angle transducers were then calibrated. The computer was programmed to translate between wind tunnel and missile coordinate systems and vice versa. Position checks were made by aligning the LV on various parts of the model body. The accuracy in determining the position of the LV focus point with respect to the model is believed to have been

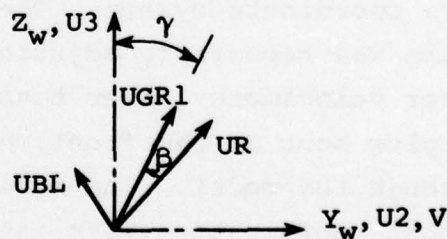
± 0.8 mm (.030 inches, .005 D) in each of the coordinate directions. Because of the configuration of the LV with its two sets of beams at 30° , the far side of the model was completely in the shadow of the beams and no measurements could be taken there. Furthermore, the top of the shadow zone extended upward away from the model at about an 8° angle due to the angle of the lower set of beams. The limit on how close the LV focus point could approach the body depended upon the reflections into either photomultiplier tube from any beam reflecting off some combination of the body and the window.

Data points were obtained with the LV system by traversing each horizontal row in a missile cross section twice. The first time the row was traversed both sets of beams were oriented vertically and two cross-flow vectors in wind tunnel coordinates were measured. For the repeat traverse the top LV beams were rotated 90° to measure the horizontal velocity component. The position was nearly always reproduced upon the second traverse within $\pm .001$ D in the horizontal position, and $\pm .006$ D in the vertical plane. The basis for resolving the two non-orthogonal LV velocities measured in the wind tunnel cross flow plane to orthogonal velocity components in the same plane was through the following relationship which is based on the sketch shown:

$$\frac{UGR1}{\cos\beta} = UR = \frac{UBL}{\cos(\beta+30^\circ)}$$

Thus:

$$\beta = \tan^{-1} \left(1.7320 - 2 \frac{UBL}{UGR1} \right)$$



Wind tunnel cross flow plane, looking upstream

The resulting velocity components in wind tunnel coordinates are:

$$\begin{aligned} U1 &= UGR2 && \text{(axial component, positive direction downstream)} \\ U2 &= UR \sin (\beta+\gamma) \\ U3 &= UR \cos (\beta+\gamma) \end{aligned}$$

In missile coordinates the dimensionless velocity components are:

$$\begin{aligned}U &= (U_1 \cos \alpha - U_3 \sin \alpha) / U_\infty \\V &= U_2 / U_\infty \\W &= (U_1 \sin \alpha + U_3 \cos \alpha) / U_\infty\end{aligned}$$

While velocity components were measured in a wind-tunnel coordinate system and then resolved into missile coordinates, it is emphasized that the measurement points were located in missile cross-sectional planes.

There were two ways to obtain laser velocimeter readings. The simpler was to command the computer to sample the tracker values 19 times in one-thirtieth second intervals and average the values. However, the signal-to-noise ratio was generally poor in the region of the flow with moderate to large vorticity levels. Tracking the signals became unreliable or impossible. In these cases the frequency was manually read on Hewlett Packard 141T-8443A spectrum analyzers and the resulting values typed into the minicomputer. Each crossflow vector was plotted in its proper location on the CRT display. The data point could be retaken before continuing. This was occasionally necessary if the tracker quit tracking just before sampling took place. In a cross section the lateral position of data points in each row was nearly always the same, simplifying subsequent data reduction. The vertical spacing was chosen to obtain an adequate definition of the flow field. Obtaining data points near vortex centers was usually very difficult. Reading one point in that region could consume as much time as required for the rest of the entire row.

The design concept used for the crossflow two-dimensional LV system created a system that was bulky in the vertical dimension. This particular LV was designed for another tunnel and could only be accommodated at the Army 7- by 10-Foot Wind Tunnel by replacing one of the large tunnel doors with a full length piece of plate glass. Even so, to take measurements in planes perpendicular to the model centerline, as was done, required that

the model be translated along the tunnel axial direction between the measurements taken in the front two planes and the rear plane. Upon completing this translation the balance forces and moments were checked for agreement with the previous values before continuing the test.

4. RESULTS

Model normal- and side-force coefficients, C_N and C_Y , and pitching- and yawing-moment coefficients, C_m and C_n , are presented in Figures 4 and 5. Figure 4 presents the results for the model at $22\text{-}1/2^\circ$ (no tape) and Figure 5, for $37\text{-}1/2^\circ$ with tape. The values are plotted versus the Reynolds number based upon the crossflow velocity. Data for the same body taken in the NASA/Ames 12-Foot Wind Tunnel by Keener, et al. (ref. 6) is shown. The reason for poor agreement in Figure 4, but good agreement in Figure 5 is unknown.

The crossflow vector plot for $X = 6.3$ ($x/L = .9$) at the model angle of $22\text{-}1/2^\circ$ is presented in Figure 6 (the view is looking upstream in cross-section plots). The Reynolds number, Re_D is $0.37 \cdot 10^6$. The dots show the positions of the vortex centers. These were obtained by interpolating velocity components between the surrounding data points. Figure 7 shows axial velocities at the same cross section and same conditions as in Figure 6. All velocities have been made dimensionless using the free-stream velocity.

Table 1 contains the individual data point positions X, Y, Z , and measured velocity components U, V, W both in missile coordinates. The raw frequency data $UB1$ and $UG1$ are the blue and green channel readings in the tunnel cross section plane, and $UG2$ is the green channel reading in the axial direction. Also included in Table 1 are $RMSB$ and $RMSG$. These are the root mean square values from the sampling of the trackers for $UB1$ and $UG1$, respectively. By comparing these values for these cases the relative unsteadiness can be noted. When the frequencies were read manually on the analyzers the rms values were automatically set equal to these readings. Thus, the manually read values can be easily determined. Table 2 contains the dimensionless circulation (GAM) and vorticity ($VORTIC$) in the cross section for each set of four adjacent data points (approximately rectangular in

shape). Circulation has been made dimensionless by using the factor: $\pi \times \text{body diameter} \times V_\infty \times \sin \alpha$. Positive values are in the counterclockwise sense. The grid center location, XC and YC and area are included.

Tables 1 and 2 have row and point numbers. The row in Table 2 lies half way between the rows in Table 1, and similarly for the point numbers on each row. Values from Table 2 have been used to determine vorticity contours, see Figure 8.

Three cross sections were probed at the model pitch angle of $37\text{-}1/2^\circ$ and $Re_D = 0.23 \cdot 10^6$. A strip of tape was located on the model nose as previously described. The cross sections at $X = 2.8, 4.9$ and 6.3 (40, 70 and 90 percent of the length) were probed. The data are contained in Tables 3, 5, and 7, respectively. The resulting circulation and vorticity values are presented in Tables 4, 6, and 8, respectively. Figures 9-17 contain the crossflow vector plot, and axial velocity and vorticity contour plots for each of these three cross sections. Figure 18 presents an overlay of some of the vorticity contours from the same three cases. This shows the relative position of the vortical regions in the three cross sections.

Sets of photographs from four carbon black surface flow visualization cases are presented in Figures 19-22. The set of photographs in each figure show the model surface pattern at 6 different angles, 60° apart in rotation. The first case, Figure 19, is for the pitch angle of $22\text{-}1/2^\circ$ (no tape). The flow conditions are the same as for the flow field described above in Figures 6-8.

The remaining three flow visualization cases are for the pitch angle for $37\text{-}1/2^\circ$. The first of these (Figure 20) is with the tape strip in place and $Re_D = 0.18 \cdot 10^5$, the same as for the LV measurements reported in Reference 1. Figures 21 and 22 are for the cross flow Reynolds number of the present experiment,

$0.37 \cdot 10^5$. The first case is without the tape strip. Figure 22 shows the case with the tape strip in place, so the flow field conditions are the same as for the measurements shown in Figures 9 to 17. Separation and attachment lines as shown in this last set of photographs were read and are indicated on the cross flow vector plots in Figures 9, 12 and 15. Also, the positions as indicated in this set of photographs for the two primary separation lines along the entire length of the model are indicated in Figure 23.

5. PRELIMINARY ANALYSIS OF THE DATA

As previously noted the purpose of this report is to present the results of the experiment, and not to analyze them. Some observations on these results are made here, however, but no comparisons to previous tests or theoretical methods are made. Further manipulation of the results is also possible and should be performed.

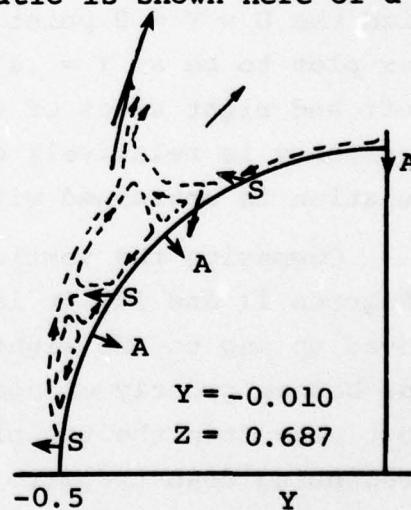
Some blemishes in the carbon black oil surfaces can be noted. The blank spot near $\theta = 0$ in Figure 22 is a spot that did not get painted. This appears to have had only a very local effect on the pattern. The uniformly dark areas, particularly in Figures 19 and 20, are areas where the carbon black did not flow. Smudges and scrapes of the flow pattern after its formation - during handling - show on the nose in Figure 21, and just above the mid section of Figure 22. These do not affect the use of the photographs. The flow patterns across the longitudinal seams and large bolt holes (both filled with polyester-based resin and sanded smooth) show no indication of discontinuities. The seam at $X = .50$ and the body pin hole does show signs of discontinuous surface heights. However, none of the major features in the separation lines can be readily traced to these junction effects.

The primary (first) separation lines showing in Figure 19, $\alpha = 22-1/2^\circ$, are quite symmetric. For the first 55% of the length these separation lines are very close to $\pm 100^\circ$. Then the separation lines move further aft to nearly $\pm 120^\circ$ for the remainder of the body length. For the next case (Figure 20, $\alpha = 37-1/2^\circ$, lower Reynolds number) large asymmetry in the primary separation lines is noted on the rear half of the model, greater than $+90^\circ$ in the 60° photo, and much less than -90° in the 240° photo.

Figures 21 and 22 show the model at $\alpha = 37-1/2^\circ$, $Re_D = 0.37 \cdot 10^6$, and respectively, without and with the tape strip. A striking difference between these two sets of

photographs are the two breaks in the separation line on each side for the case with the tape. These breaks in the separation lines are placed asymmetrically with respect to each other. These breaks in the separation lines are believed to be associated with vortex sheets tearing loose from the body and a new sheet forming. The attachment lines were marked with dashed lines on the model in this latter set of photographs to make their identification easier. The angles of the separation and attachment lines were read on enlarged photographs and are marked on the cross vector plots in Figures 9, 12, and 15. The location of these points has been determined to within three quarters of a degree. The locations of the first separation line on each side of the model has been read for nearly the entire length of the body. These are shown in Figure 23. The breaks in the separation lines show in detail in this figure.

The separation and attachment points indicated in Figure 9 ($X = 2.8$) and on the left side of Figure 12 ($X = 4.9$) contain an extra pair of singular points. A schematic is shown here of a local flow field which satisfies all separation and attachment points and the nearby measured flow vectors for the $X = 4.9$ case. The extra set of singular points in this case is associated with the first break in the vortex sheet.



Returning to the surface flow visualization in Figure 21, the case at $\alpha = 37\text{-}1/2^\circ$ but without the tape strip, no breaks in the separation lines are noted. Possibly the severe flow unsteadiness that was observed for this case is due to an oscillation of

the separation lines for the breaks. The resulting carbon black surface flow pattern of some average for the flow would not be meaningful. Also, since one placement of a tape strip produced large changes in the flow pattern, one could reason that possibly other placements would produce other results. The good agreement for the force and moment coefficients between this test with the tape strip and the 12-Foot Wind Tunnel results of Keener, et al (ref. 6) for the same model but without a tape strip indicates otherwise.

Some analysis of the crossflow plots from the $\alpha = 37-1/2^\circ$ LV measurements are in order. The two counter-rotating vortices at $X = 2.8$ that are evident in the vector and vorticity plots, Figures 9 and 11, have 15 to 25 percent excess velocity in the vortex cores (as compared to the free-stream velocity). These vortices have the character of swirling jets. The circulation inside the $\Omega = \pm 0.5$ contours and above the bottom traverse line are -0.169 and $+0.306$. While the vortex center on the left side could not be located by interpolating velocity components to find the $U = V = 0$ point, the center was selected from the vortex plot to be at $Y = .17$ and $Z = .61$. The circulations on the left and right sides of the $\Omega = 0$ line are $-.151$ and $+.291$. The vorticity is relatively concentrated and virtually all the circulation is contained within the $\Omega = \pm 0.5$ contours (see Table 9).

Comparing the vorticity contour plots for $X = 2.8$ and 4.9 (Figures 11 and 14) it is noted that the left vortex center has moved up and to the right, and the right vortex has moved upwards and become greatly elongated. In the lower left of Figure 14 vorticity from the top of another clockwise vortex is evident. Continuing downstream to $X = 6.3$ the vortical regions enlarge significantly while vorticity levels are reduced. The resulting circulations are actually larger (see Table 9). For convenience in visualizing the growth of vortical regions a superposition of selected vorticity contours for $X = 2.8, 4.9$, and 6.3 is shown in

Figure 18. The shaded areas show the central regions of the vortices. No concentrated vortex cores are evident at $X = 6.3$ from the crossflow vector plot, Figure 15.

6. CONCLUSIONS

The flow over an ogive-cylinder model with a length-to-diameter ratio of seven has been investigated at incompressible flow speeds. Forces and moments, surface flow visualization, and three-dimensional laser velocimeter measurements have been obtained at pitch angles of 22.5° and 37.5° . Forces and moments have been compared to data previously obtained over a wide range of Reynolds numbers with this model. This comparison shows the flow to be transitional in nature.

Surface flow visualization shows a complicated pattern of multiple separation and attachment lines. Asymmetric breaks in the primary separation lines are believed to be associated with the tearing loose of attached vortex sheets and the subsequent formation of a new sheet.

Three-dimensional laser velocimeter measurements were performed on the leeward side of the model at $X = 6.3$ for $\alpha = 22\text{-}1/2^\circ$, and at $X = 2.8, 4.9$, and 6.3 for $\alpha = 37\text{-}1/2^\circ$. Vortical regions rapidly become more and more diffusive and asymmetric in nature with downstream distance. Crossflow vector plots do not show all the vortex cores at the $X = 4.9$ and 6.3 locations. At $X = 2.8$, which is located on the nose, the vortices have a greater velocity component along the body axis than free-stream velocity, but farther aft at $X = 4.9$ and 6.3 velocity defects are evident in the center of the vortical regions.

REFERENCES

1. R. G. Schwind and D. M. Kline: Data Report on Laser Anemometer Measurements of Missile Body-Separation Vortices. Nielsen Engineering & Research TR 91, June 1975.
2. J. E. Fidler, R. G. Schwind and J. N. Nielsen: An Investigation of Slender-Body Wake Vortices. Nielsen Engineering & Research TR 108, February 1976.
3. E. R. Keener and G. T. Chapman: Onset of Aerodynamic Side Forces at Zero Sideslip on Symmetric Forebodies at High Angles of Attack, AIAA Paper No. 74-770.
4. G. T. Chapman, E. R. Keener, and G. N. Malcolm: Asymmetric Aerodynamic Forces on Aircraft at High Angles of Attack - Some Design Guides, in Stall/Spin Problems of Military Aircraft, AGARD CP 199, June 1976.
5. E. R. Keener and J. Taleghani: Wind Tunnel Investigations of the Aerodynamic Characteristics of Five Forebody Models at High Angles of Attack at Mach Numbers from 0.25 to 2.0, NASA TMX 73,076, December 1975.
6. E. R. Keener, G. T. Chapman, L. Cohen, and J. Taleghani: Side Forces on a Tangent Ogive Forebody with a Fineness Ratio of 3.5 at High Angles of Attack and Mach Numbers from 0.1 to 0.7, NASA TMX-3437, February 1977.
7. Grant, G. R. and Orloff, K. L.: Two-Color Dual-Beam Backscatter Laser Doppler Velocimeter, Applied Optics, Vol. 12, December 1973.

LIST OF SYMBOLS

C_m	Pitching moment coefficient, $C_m = M_m/SQD$
C_n	Yawing moment coefficient, $C_n = M_n/SQD$
C_N	Normal force coefficient, $C_N = N/SQ$
C_Y	Side force coefficient, $C_Y = Y/SQ$
D	Diameter of model afterbody, 15.24 cm (6 in.)
L	Model length, 106.68 cm (42 in.)
M_m	Pitching moment about $x/L = 0.5$
M_n	Yawing moment about $x/L = 0.5$, positive force on nose in +Y direction
N	Normal force
Q	Free stream dynamic head
Re_D	Reynolds number based upon U_∞ and D
$RMSB, RMSG$	Root mean square of blue, green, beam laser velocimeter raw data
S	Cross sectional area of model afterbody
s	Distance along a path in the model cross flow plane, divided by body diameter
U, V, W	Velocity components in body coordinates X, Y, Z divided by U_∞
U_∞	Free stream velocity
$UB1, UG1, UG2$	Laser velocimeter raw data
$UBL, UGR1, UGR2$	Velocities perpendicular to the axis and in the plane of the blue, green (oriented vertically), and green (rotated horizontally) LV beams
UR	Resultant velocity from UBL and $UGR1$
$U1, U2, U3$	Velocity components in wind tunnel coordinates
v	resultant velocity in the model cross flow plane divided by U_∞
X, Y, Z	Body coordinates/D (see Figure 1)

LIST OF SYMBOLS (concluded)

Y	Side force (positive in Y-direction), lateral coordinate
YC,ZC	Vortex center in Y, Z coordinates
α	Model pitch angle
β	Angle between UR and UGR
γ	Angle between Z_w and UGR
Γ, GAM	Dimensionless circulation, positive in counter-clockwise sense, $\frac{1}{\pi \sin \alpha} \int \bar{v} \cdot d\bar{s}$
θ	Angle about model axis, see Figure 23
Ω	Dimensionless vorticity, Γ divided by the area of the enclosed quadrilateral (lengths made dimensionless by D)

Table 1. Flow Field Velocities at 22.5° Pitch Angle and X = 6.3

MPT	RUN	IV	JZ	LUDIR		UT	P	U	UB1	UG1	UG2	RMSB	RMSG
				1	2								
26	017	8				36.540	16.846						
IPT	RUN	1	X	Y	Z	U	U	U	UB1	UG1	UG2	RMSB	RMSG
		1	6.307	-1.000	0.367	0.949	-0.010	0.495	178.3	129.8	764.1	138.4	129.0
		2	6.308	-0.988	0.384	0.934	-0.010	0.502	166.7	147.3	760.1	157.0	147.4
		3	6.309	-0.840	0.369	0.942	-0.015	0.526	169.3	178.2	762.1	168.5	178.3
		4	6.301	-0.700	0.356	0.947	0.022	0.552	194.2	206.2	762.1	194.8	209.5
		5	6.300	-0.631	0.358	0.932	0.059	0.570	206.5	247.9	762.1	208.0	248.2
		6	6.303	-0.560	0.355	0.947	0.063	0.556	176.5	222.7	768.1	177.0	223.1
		8	6.308	-0.480	0.359	0.941	0.141	0.571	152.1	257.0	758.1	152.7	257.4
	017					0.935	0.293	0.545	36.7	259.4	760.1	35.7	259.4
MPT	RUN	12	JZ	1	2	UT	P	U	UB1	UG1	UG2	RMSB	RMSG
		12				0.67082	0.58312E-02						
		1	X	Y	Z	U	U	U	UB1	UG1	UG2	RMSB	RMSG
		1	6.303	-1.001	0.439	0.945	-0.002	0.505	148.7	145.5	752.1	148.8	145.6
		2	6.302	-0.981	0.440	0.952	0.012	0.500	120.6	177.2	752.1	120.6	177.2
		3	6.302	-0.840	0.439	0.933	0.005	0.525	176.7	173.2	752.1	177.0	173.3
		4	6.301	-0.700	0.441	0.936	0.028	0.541	182.8	201.8	752.1	182.3	202.0
		5	6.302	-0.631	0.439	0.928	0.044	0.530	176.8	208.2	754.1	176.1	208.5
IPT	RUN	6	6.303	-0.560	0.441	0.933	0.084	0.544	156.1	218.0	754.1	156.4	218.1
		7	6.303	-0.480	0.438	0.932	0.069	0.543	163.9	219.3	754.1	164.9	219.5
		8	6.304	-0.420	0.434	0.935	0.119	0.535	123.5	213.3	758.1	123.5	213.3
		9	6.301	-0.350	0.439	0.896	0.334	0.475	74.0	181.0	710.0	74.0	181.0
		10	6.303	-0.314	0.438	0.815	0.350	0.462	-59.3	359.3	662.0	-59.3	359.3
		11	6.303	-0.279	0.438	0.800	0.376	0.444	-473.0	-413.6	601.0	-473.0	-413.6
		12	6.303	-0.243	0.438	0.803	-0.075	0.084	-497.2	-463.7	589.8	-497.2	-463.7

THIS PAGE IS BEST QUALITY PRACTICABLE
FROM COPY FURNISHED TO DDC

Table 1. Continued

[illegible]

NP	RT	IV	JZ	LUDIR	UT	P
26	015	20	5	1	2	0.54230
IPT	RUN	I	X	Y	Z	U
1	015	1	6298	-1.000	0.565	0.949
2	015	2	6298	-0.980	0.562	0.945
3	015	3	6297	-0.840	0.565	0.957
4	015	4	6299	-0.701	0.561	0.949
5	015	5	6299	-0.561	0.557	0.940
6	015	6	6297	-0.429	0.563	0.949
7	015	7	6298	-0.340	0.555	0.937
8	015	8	6299	-0.279	0.564	0.937
9	015	9	6298	-0.210	0.562	0.929
10	015	10	6299	-0.139	0.554	1.026
11	015	11	6299	-0.070	0.565	0.988
12	015	12	6297	-0.002	0.565	0.982
13	015	13	6297	0.070	0.563	0.995
14	015	14	6299	0.149	0.560	0.989
15	015	15	6299	0.209	0.560	0.976
16	015	16	6297	0.280	0.558	0.957
17	015	17	6297	0.340	0.561	0.984
18	015	18	6297	0.421	0.558	0.990
19	015	19	6294		0.578	0.956
20	015	20			0.578	0.956

22

[illegible]

Table 1. Continued

23

Table 1. Continued

WPT	RUM	IV	JZ	LUDIR	UT	P
78	012	26	9	2	35.964	16.558
IPT	53	1	X	Y	Z	U
54	012	1	6297	-1.001	0.765	0.52
55	012	2	6297	-0.989	0.762	0.52
56	012	3	6297	-0.841	0.756	0.55
57	012	4	6300	-0.700	0.757	0.55
58	012	5	6303	-0.559	0.754	0.58
59	012	6	6304	-0.490	0.753	0.59
60	012	7	6301	-0.420	0.759	0.67
61	012	8	6305	-0.385	0.759	0.73
62	012	9	6307	-0.280	0.767	0.77
63	012	10	6309	-0.210	0.762	0.75
64	012	11	6307	-0.140	0.755	0.73
65	012	12	6308	-0.071	0.754	0.71
66	012	13	6308	-0.000	0.764	0.65
67	012	14	6300	0.000	0.762	0.67
68	012	15	6309	0.130	0.763	0.70
69	012	16	6309	0.280	0.763	0.70
70	012	17	6309	0.350	0.763	0.51
71	012	18	6309	0.420	0.764	0.76
72	012	19	6309	0.490	0.757	0.70
73	012	20	6303	0.560	0.757	0.60
74	012	21	6306	0.630	0.763	0.75
75	012	22	6300	0.700	0.761	0.74
76	012	23	6307	0.841	0.765	0.57
77	012	24	6307	0.980	0.765	0.57
78	012	25	6305	0.980	0.765	0.63

THIS PAGE IS BEST QUALITY PRACTICABLE
FROM COPY FURNISHED TO DDC

Table 1. Continued

WPT	RUN	IV	JZ	LUDIR	UT	P	U	U1	U2	RMS	RMS
52	012	26	10	2	35.591	16.217					
1PT	012	1	1	00	0.846	0.02	0.447	1.144	722.0	54.4	84.0
27	012	2	2	00	0.846	0.35	0.457	55.2	722.0	93.1	93.1
28	012	3	3	00	0.846	0.34	0.454	55.3	722.0	91.5	91.5
29	012	4	4	00	0.846	0.03	0.449	55.3	722.0	107.0	107.0
30	012	5	5	00	0.847	0.03	0.450	55.3	722.0	96.6	96.6
31	012	6	6	00	0.846	0.16	0.450	55.3	722.0	101.6	101.6
32	012	7	7	00	0.848	0.11	0.448	55.3	722.0	109.6	109.6
33	012	8	8	00	0.839	0.14	0.447	55.3	722.0	99.7	99.7
34	012	9	9	00	0.841	0.16	0.447	55.3	722.0	27.0	27.0
35	012	10	10	00	0.836	0.25	0.450	55.3	722.0	68.0	68.0
36	012	11	11	00	0.834	0.34	0.391	55.3	722.0	19.2	19.2
37	012	12	12	00	0.842	0.32	0.315	55.3	722.0	15.2	15.2
38	012	13	13	00	0.838	0.09	0.021	55.3	722.0	7.4	7.4
39	012	14	14	00	0.837	0.36	0.141	55.3	722.0	5.0	5.0
40	012	15	15	00	0.844	0.55	0.102	55.3	722.0	7.4	7.4
41	012	16	16	00	0.837	0.33	0.017	55.3	722.0	1.0	1.0
42	012	17	17	00	0.838	0.62	0.155	55.3	722.0	1.0	1.0
43	012	18	18	00	0.836	0.21	0.100	55.3	722.0	1.0	1.0
44	012	19	19	00	0.837	0.16	0.385	55.3	722.0	1.0	1.0
45	012	20	20	00	0.836	0.37	0.405	55.3	722.0	1.0	1.0
46	012	21	21	00	0.838	0.34	0.409	55.3	722.0	1.0	1.0
47	012	22	22	00	0.838	0.69	0.409	55.3	722.0	1.0	1.0
48	012	23	23	00	0.838	0.60	0.411	55.3	722.0	1.0	1.0
49	012	24	24	00	0.839	0.72	0.404	55.3	722.0	1.0	1.0
50	012	25	25	00	0.828	0.84	0.415	55.3	722.0	1.0	1.0
51	012	26	26	00	0.843	0.84	0.427	55.3	722.0	1.0	1.0
52	012	27	27	00	0.843	0.64	0.427	55.3	722.0	1.0	1.0

Table 1. Continued

WPT	NUM	IV	JZ	LUDIR	UT	P
26	012	26	11	1	36.046	16.633
IPT	1	1	X	Y	Z	U
1	012	1	0311	-1.000	0.520	0.450
2	012	2	0307	-0.991	0.521	0.452
3	012	3	0303	-0.840	0.516	0.446
4	012	4	0297	-0.701	0.521	0.450
5	012	5	0310	-0.550	0.521	0.453
6	012	6	0306	-0.409	0.520	0.456
7	012	7	0308	-0.420	0.520	0.430
8	012	8	0311	-0.370	0.514	0.416
9	012	9	0303	-0.270	0.520	0.413
10	012	10	0304	-0.209	0.532	0.365
11	012	11	0305	-0.140	0.527	0.360
12	012	12	0307	-0.080	0.526	0.360
13	012	13	0310	0.000	0.521	0.355
14	012	14	0310	0.070	0.523	0.355
15	012	15	0310	0.130	0.520	0.341
16	012	16	0309	0.211	0.522	0.327
17	012	17	0308	0.270	0.526	0.332
18	012	18	0310	0.340	0.526	0.357
19	012	19	0310	0.411	0.521	0.388
20	012	20	0310	0.500	0.521	0.393
21	012	21	0310	0.631	0.519	0.404
22	012	22	0310	0.700	0.522	0.404
23	012	23	0310	0.790	0.522	0.413
24	012	24	0311	0.850	0.522	0.418
25	012	25	0311	0.900	0.522	0.418

THIS PAGE IS BEST QUALITY PRACTICABLE
FROM COPY FURNISHED TO DDC

Table 1. Continued

NPT	NUM	IV	JZ	LVDIR	UT	P	U	U1	U2	RMSB	RMSG
52	013	26	12	1	36.754	17.054					
1PT	013	1	6	Y	Z	U					
27	013	2	6	-1.000	1.002	0.551	0.425	0.007	736.1	25.7	46.1
28	013	3	6	-0.981	1.002	0.554	0.428	0.007	736.1	25.7	47.8
29	013	4	6	-0.840	1.079	0.945	0.433	0.007	736.1	25.7	69.1
30	013	5	6	-0.690	1.082	0.945	0.437	0.007	736.1	25.7	69.1
31	013	6	6	-0.559	1.076	0.567	0.417	0.007	736.1	25.7	69.1
32	013	7	6	-0.489	1.074	0.563	0.409	0.007	736.1	25.7	69.1
33	013	8	6	-0.419	1.078	0.949	0.392	0.007	736.1	25.7	69.1
34	013	9	6	-0.349	1.080	0.948	0.378	0.007	736.1	25.7	69.1
35	013	10	6	-0.279	1.077	0.948	0.358	0.007	736.1	25.7	69.1
36	013	11	6	-0.210	1.079	0.945	0.340	0.007	736.1	25.7	69.1
37	013	12	6	-0.140	1.076	0.945	0.320	0.007	736.1	25.7	69.1
38	013	13	6	-0.070	1.078	0.945	0.300	0.007	736.1	25.7	69.1
39	013	14	6	0.000	1.087	0.975	0.280	0.007	736.1	25.7	69.1
40	013	15	6	0.070	1.087	0.975	0.260	0.007	736.1	25.7	69.1
41	013	16	6	0.140	1.085	0.951	0.240	0.007	736.1	25.7	69.1
42	013	17	6	0.210	1.082	0.951	0.220	0.007	736.1	25.7	69.1
43	013	18	6	0.281	1.077	0.970	0.200	0.007	736.1	25.7	69.1
44	013	19	6	0.349	1.077	0.970	0.180	0.007	736.1	25.7	69.1
45	013	20	6	0.420	1.078	0.966	0.160	0.007	736.1	25.7	69.1
46	013	21	6	0.491	1.079	0.966	0.140	0.007	736.1	25.7	69.1
47	013	22	6	0.560	1.074	0.965	0.120	0.007	736.1	25.7	69.1
48	013	23	6	0.631	1.074	0.965	0.100	0.007	736.1	25.7	69.1
49	013	24	6	0.699	1.085	0.954	0.080	0.007	736.1	25.7	69.1
50	013	25	6	0.769	1.080	0.954	0.060	0.007	736.1	25.7	69.1
51	013	26	6	0.839	1.080	0.948	0.041	0.007	736.1	25.7	69.1
52	013	27	6	0.900	1.080	0.948	0.021	0.007	736.1	25.7	69.1

Table 1. Continued

WPT	SUM	IV	J2	LUDIR	UT	P
26	016	26	13	1	2	16.266
IPT	SUM	I	X	Y	Z	
1	016	1	03	097	1.166	
2	016	2	03	090	1.161	
3	016	3	06	084	1.161	
4	016	4	06	071	1.158	
5	016	5	06	061	1.156	
6	016	6	06	051	1.156	
7	016	7	06	040	1.154	
8	016	8	06	030	1.152	
9	016	9	06	020	1.153	
10	016	10	06	011	1.159	
11	016	11	06	003	1.156	
12	016	12	06	000	1.155	
13	016	13	06	000	1.155	
14	016	14	06	000	1.155	
15	016	15	06	000	1.157	
16	016	16	06	000	1.160	
17	016	17	06	020	1.160	
18	016	18	06	040	1.153	
19	016	19	06	058	1.160	
20	016	20	06	073	1.157	
21	016	21	06	088	1.157	
22	016	22	06	099	1.156	
23	016	23	06	097	1.157	
24	016	24	06	093	1.157	
25	016	25	06	096	1.159	
26	016	26	06	096	1.159	

Table 1. Concluded

29

Table 2. Vorticities and Circulations for 22.5° Pitch Angle and X = 6.3

POINT	ROW	VORTICITY AND CIRCULATION				VORTIC
		VC	ZC	AREA	GAM	
1	1	-0.991	0.403	0.001470	-0.000179	-0.1217
2	1	-0.910	0.403	0.010253	0.000701	0.0684
3	1	-0.770	0.401	0.010826	0.001565	0.1446
4	1	-0.665	0.399	0.006751	0.000694	0.1206
5	1	-0.595	0.398	0.005849	-0.000602	-0.1030
6	1	-0.525	0.398	0.005829	0.001962	0.1367
7	1	-0.454	0.397	0.005462	0.005921	1.0660

POINT	ROW	VORTICITY AND CIRCULATION				VORTIC
		VC	ZC	AREA	GAM	
1	2	-0.991	0.478	0.001474	0.000517	0.3509
2	2	-0.911	0.478	0.010920	-0.000676	-0.0619
3	2	-0.770	0.480	0.011225	-0.001206	-0.1148
4	2	-0.665	0.479	0.006445	-0.002100	-0.3856
5	2	-0.595	0.479	0.006424	-0.001787	-0.3295
6	2	-0.525	0.478	0.005560	-0.002943	-0.5893
7	2	-0.455	0.478	0.005854	-0.001302	-0.2225
8	2	-0.385	0.478	0.005767	0.004529	0.7853
9	2	-0.315	0.481	0.0059	-0.0226	-3.8
10	2	-0.253	0.483	0.0047	-0.0077	-1.6

POINT	ROW	VORTICITY AND CIRCULATION				VORTIC
		VC	ZC	AREA	GAM	
1	3	-0.990	0.540	0.000878	0.000719	0.8191
2	3	-0.910	0.540	0.00581	-0.002004	-0.3045
3	3	-0.770	0.541	0.005995	0.000335	0.0559
4	3	-0.665	0.540	0.002939	0.000455	0.1548
5	3	-0.595	0.537	0.002791	0.000286	0.1382
6	3	-0.525	0.538	0.002878	0.001800	0.6253
7	3	-0.454	0.539	0.002729	0.000506	0.1854
8	3	-0.385	0.540	0.002759	-0.000707	-0.2584
9	3	-0.315	0.543	0.002812	-0.005807	-3.3803
10	3	-0.245	0.544	0.002437	-0.005875	-2.4109
11	3	-0.175	0.537	0.002703	-0.004855	-1.7965
12	3	-0.106	0.540	0.002675	0.004025	1.5047
13	3	-0.037	0.543	0.002574	0.017644	6.5085
14	3	0.033	0.540	0.003060	0.014269	4.6622
15	3	0.103	0.541	0.002959	0.004665	1.6316

POINT	ROW	VORTICITY AND CIRCULATION				VORTIC
		VC	ZC	AREA	GAM	
1	4	-0.990	0.583	0.000776	0.000658	0.0852
2	4	-0.910	0.583	0.005414	-0.000238	-0.0440
3	4	-0.770	0.580	0.004966	-0.000187	-0.0377
4	4	-0.665	0.578	0.002392	0.000111	0.0481
5	4	-0.595	0.577	0.002722	0.001138	0.4181
6	4	-0.525	0.580	0.003105	-0.000044	-0.0142
7	4	-0.455	0.582	0.003130	0.000540	0.1725
8	4	-0.385	0.581	0.003103	0.001120	0.3610
9	4	-0.314	0.583	0.002821	-0.000532	-2.2801
10	4	-0.245	0.581	0.002760	-0.007836	-2.8362
11	4	-0.175	0.576	0.002644	-0.015301	-5.7873
12	4	-0.105	0.578	0.002617	-0.024486	-8.3584
13	4	-0.035	0.583	0.002791	-0.010884	-6.8030
14	4	0.035	0.582	0.002774	-0.009146	-3.2976
15	4	0.105	0.582	0.002809	-0.000813	-0.0757
16	4	0.175	0.581	0.003009	0.005573	2.2584
17	4	0.245	0.579	0.002886	0.008871	2.5860
18	4	0.314	0.578	0.002564	0.006875	2.6810
19	4	0.385	0.585	0.002421	0.003834	1.5833

POINT	ROW	VORTICITY AND CIRCULATION				VORTIC
		VC	ZC	AREA	GAM	
1	5	-0.990	0.621	0.000724	-0.000211	-0.2917
2	5	-0.910	0.620	0.005362	0.002922	0.5552
3	5	-0.769	0.621	0.006300	0.004082	0.6479
4	5	-0.665	0.617	0.003079	0.000646	0.2009
5	5	-0.595	0.617	0.002347	-0.000659	-0.0235
6	5	-0.525	0.621	0.002631	-0.000156	-0.0096
7	5	-0.455	0.621	0.002310	-0.001187	-0.5141
8	5	-0.385	0.621	0.002338	-0.00315	-0.9120
9	5	-0.315	0.623	0.002740	-0.001316	-0.4802
10	5	-0.245	0.621	0.002778	-0.006102	-2.1203
11	5	-0.175	0.618	0.002877	-0.005370	-1.9319
12	5	-0.105	0.623	0.002881	-0.005370	-2.0254
13	5	-0.035	0.623	0.002909	-0.000011	-1.0097
14	5	0.035	0.621	0.002909	0.000011	-0.0039
15	5	0.104	0.621	0.002828	0.010560	3.6175
16	5	0.175	0.621	0.002871	0.015588	5.8132
17	5	0.245	0.620	0.003016	0.016688	3.5438
18	5	0.314	0.618	0.002931	0.009146	2.1202
19	5	0.385	0.619	0.002520	0.005158	2.0553

THIS PAGE IS BEST QUALITY PRACTICABLE
FROM COPY FURNISHED TO DDC

Table 2. Concluded

POINT	ROW	VORTICITY	VC	AREA	CIRCULATION	GAM	VORTIC
1	1	0.900	0.900	0.00127	0.00039	0.00039	0.2836
2	2	0.910	0.910	0.00128	0.00128	0.00128	0.2836
3	3	0.920	0.920	0.00129	0.00129	0.00129	0.2836
4	4	0.930	0.930	0.00130	0.00130	0.00130	0.2836
5	5	0.940	0.940	0.00131	0.00131	0.00131	0.2836
6	6	0.950	0.950	0.00132	0.00132	0.00132	0.2836
7	7	0.960	0.960	0.00133	0.00133	0.00133	0.2836
8	8	0.970	0.970	0.00134	0.00134	0.00134	0.2836
9	9	0.980	0.980	0.00135	0.00135	0.00135	0.2836
10	10	0.990	0.990	0.00136	0.00136	0.00136	0.2836
11	11	0.995	0.995	0.00137	0.00137	0.00137	0.2836
12	12	0.998	0.998	0.00138	0.00138	0.00138	0.2836
13	13	0.999	0.999	0.00139	0.00139	0.00139	0.2836
14	14	0.999	0.999	0.00140	0.00140	0.00140	0.2836
15	15	0.999	0.999	0.00141	0.00141	0.00141	0.2836
16	16	0.999	0.999	0.00142	0.00142	0.00142	0.2836
17	17	0.999	0.999	0.00143	0.00143	0.00143	0.2836
18	18	0.999	0.999	0.00144	0.00144	0.00144	0.2836
19	19	0.999	0.999	0.00145	0.00145	0.00145	0.2836
20	20	0.999	0.999	0.00146	0.00146	0.00146	0.2836
21	21	0.999	0.999	0.00147	0.00147	0.00147	0.2836
22	22	0.999	0.999	0.00148	0.00148	0.00148	0.2836
23	23	0.999	0.999	0.00149	0.00149	0.00149	0.2836
24	24	0.999	0.999	0.00150	0.00150	0.00150	0.2836
25	25	0.999	0.999	0.00151	0.00151	0.00151	0.2836
26	26	0.999	0.999	0.00152	0.00152	0.00152	0.2836
27	27	0.999	0.999	0.00153	0.00153	0.00153	0.2836
28	28	0.999	0.999	0.00154	0.00154	0.00154	0.2836
29	29	0.999	0.999	0.00155	0.00155	0.00155	0.2836
30	30	0.999	0.999	0.00156	0.00156	0.00156	0.2836
31	31	0.999	0.999	0.00157	0.00157	0.00157	0.2836
32	32	0.999	0.999	0.00158	0.00158	0.00158	0.2836
33	33	0.999	0.999	0.00159	0.00159	0.00159	0.2836
34	34	0.999	0.999	0.00160	0.00160	0.00160	0.2836
35	35	0.999	0.999	0.00161	0.00161	0.00161	0.2836
36	36	0.999	0.999	0.00162	0.00162	0.00162	0.2836
37	37	0.999	0.999	0.00163	0.00163	0.00163	0.2836
38	38	0.999	0.999	0.00164	0.00164	0.00164	0.2836
39	39	0.999	0.999	0.00165	0.00165	0.00165	0.2836
40	40	0.999	0.999	0.00166	0.00166	0.00166	0.2836
41	41	0.999	0.999	0.00167	0.00167	0.00167	0.2836
42	42	0.999	0.999	0.00168	0.00168	0.00168	0.2836
43	43	0.999	0.999	0.00169	0.00169	0.00169	0.2836
44	44	0.999	0.999	0.00170	0.00170	0.00170	0.2836
45	45	0.999	0.999	0.00171	0.00171	0.00171	0.2836
46	46	0.999	0.999	0.00172	0.00172	0.00172	0.2836
47	47	0.999	0.999	0.00173	0.00173	0.00173	0.2836
48	48	0.999	0.999	0.00174	0.00174	0.00174	0.2836
49	49	0.999	0.999	0.00175	0.00175	0.00175	0.2836
50	50	0.999	0.999	0.00176	0.00176	0.00176	0.2836
51	51	0.999	0.999	0.00177	0.00177	0.00177	0.2836
52	52	0.999	0.999	0.00178	0.00178	0.00178	0.2836
53	53	0.999	0.999	0.00179	0.00179	0.00179	0.2836
54	54	0.999	0.999	0.00180	0.00180	0.00180	0.2836
55	55	0.999	0.999	0.00181	0.00181	0.00181	0.2836
56	56	0.999	0.999	0.00182	0.00182	0.00182	0.2836
57	57	0.999	0.999	0.00183	0.00183	0.00183	0.2836
58	58	0.999	0.999	0.00184	0.00184	0.00184	0.2836
59	59	0.999	0.999	0.00185	0.00185	0.00185	0.2836
60	60	0.999	0.999	0.00186	0.00186	0.00186	0.2836
61	61	0.999	0.999	0.00187	0.00187	0.00187	0.2836
62	62	0.999	0.999	0.00188	0.00188	0.00188	0.2836
63	63	0.999	0.999	0.00189	0.00189	0.00189	0.2836
64	64	0.999	0.999	0.00190	0.00190	0.00190	0.2836
65	65	0.999	0.999	0.00191	0.00191	0.00191	0.2836
66	66	0.999	0.999	0.00192	0.00192	0.00192	0.2836
67	67	0.999	0.999	0.00193	0.00193	0.00193	0.2836
68	68	0.999	0.999	0.00194	0.00194	0.00194	0.2836
69	69	0.999	0.999	0.00195	0.00195	0.00195	0.2836
70	70	0.999	0.999	0.00196	0.00196	0.00196	0.2836
71	71	0.999	0.999	0.00197	0.00197	0.00197	0.2836
72	72	0.999	0.999	0.00198	0.00198	0.00198	0.2836
73	73	0.999	0.999	0.00199	0.00199	0.00199	0.2836
74	74	0.999	0.999	0.00200	0.00200	0.00200	0.2836
75	75	0.999	0.999	0.00201	0.00201	0.00201	0.2836
76	76	0.999	0.999	0.00202	0.00202	0.00202	0.2836
77	77	0.999	0.999	0.00203	0.00203	0.00203	0.2836
78	78	0.999	0.999	0.00204	0.00204	0.00204	0.2836
79	79	0.999	0.999	0.00205	0.00205	0.00205	0.2836
80	80	0.999	0.999	0.00206	0.00206	0.00206	0.2836
81	81	0.999	0.999	0.00207	0.00207	0.00207	0.2836
82	82	0.999	0.999	0.00208	0.00208	0.00208	0.2836
83	83	0.999	0.999	0.00209	0.00209	0.00209	0.2836
84	84	0.999	0.999	0.00210	0.00210	0.00210	0.2836
85	85	0.999	0.999	0.00211	0.00211	0.00211	0.2836
86	86	0.999	0.999	0.00212	0.00212	0.00212	0.2836
87	87	0.999	0.999	0.00213	0.00213	0.00213	0.2836
88	88	0.999	0.999	0.00214	0.00214	0.00214	0.2836
89	89	0.999	0.999	0.00215	0.00215	0.00215	0.2836
90	90	0.999	0.999	0.00216	0.00216	0.00216	0.2836
91	91	0.999	0.999	0.00217	0.00217	0.00217	0.2836
92	92	0.999	0.999	0.00218	0.00218	0.00218	0.2836
93	93	0.999	0.999	0.00219	0.00219	0.00219	0.2836
94	94	0.999	0.999	0.00220	0.00220	0.00220	0.2836
95	95	0.999	0.999	0.00221	0.00221	0.00221	0.2836
96	96	0.999	0.999	0.00222	0.00222	0.00222	0.2836
97	97	0.999	0.999	0.00223	0.00223	0.00223	0.2836
98	98	0.999	0.999	0.00224	0.00224	0.00224	0.2836
99	99	0.999	0.999	0.00225	0.00225	0.00225	0.2836
100	100	0.999	0.999	0.00226	0.00226	0.00226	0.2836
101	101	0.999	0.999	0.00227	0.00227	0.00227	0.2836
102	102	0.999	0.999	0.00228	0.00228	0.00228	0.2836
103	103	0.999	0.999	0.00229	0.00229	0.00229	0.2836
104	104	0.999	0.999	0.00230	0.00230	0.00230	0.2836
105	105	0.999	0.999	0.00231	0.00231	0.00231	0.2836
106	106	0.999	0.999	0.00232	0.00232	0.00232	0.2836
107	107	0.999	0.999	0.00233	0.00233	0.00233	0.2836
108	108	0.999	0.999	0.00234	0.00234	0.00234	0.2836
109	109	0.999	0.999	0.00235	0.00235	0.00235	0.2836
110	110	0.999	0.999	0.00236	0.00236	0.00236	0.2836
111	111	0.999	0.999	0.00237	0.00237	0.00237	0.2836
112	112	0.999	0.999	0.00238	0.00238	0.00238	0.2836
113	113	0.999	0.999	0.00239	0.00239	0.00239	0.2836
114	114	0.999	0.999	0.00240	0.00240	0.00240	0.2836
115	115	0.999	0.999	0.00241	0.00241	0.00241	0.2836
116	116	0.999	0.999	0.00242	0.00242	0.00242	0.2836
117	117	0.999	0.999	0.00243	0.00243	0.00243	0.2836
118	118	0.999	0.999	0.00244	0.00244	0.00244	0.2836
119	119	0.999	0.999	0.00245	0.00245	0.00245	0.2836
120	120	0.999	0.999	0.00246	0.00246	0.00246	0.2836
121	121	0.999	0.999	0.00247	0.00247	0.00247	0.2836
122	122	0.999	0.999	0.00248	0.00248	0.00248	0.2836
123	123	0.999	0.999	0.00249	0.00249	0.00249	0.2836
124	124	0.999	0.999	0.00250	0.00250	0.00250	0.2836
125	125	0.999	0.999	0.00251	0.00251	0.00251	0.2836
126	126	0.999	0.999	0.00252	0.00252	0.00252	0.2836
127	127	0.999	0.999	0.00253	0.00253	0.00253	0.2836
128	128	0.999	0.999	0.00254	0.00254	0.00254	0.2836
129	129	0.999	0.999	0.00255	0.00255	0.00255	0.2836
130	130	0.999	0.999	0.00256	0.00256	0.00256	0.2836
131	131	0.999	0.999	0.00257	0.00257	0.00257	0.2836
132	132	0.999	0.999	0.00258	0.00258	0.00258	0.2836
133	133	0.999	0.999	0.00259	0.00259	0.00259	0.2836
134	134	0.999	0.999	0.00260	0.00260	0.00260	0.2836
135	135	0.999	0.999	0.00261	0.00261	0.00261	0.2836
136	136	0.999	0.999	0.00262	0.00262	0.00262	0.2836
137	137	0.999	0.999	0.00263	0.00263	0.00263	0.2836
138	138	0.999	0.999	0.00264	0.00264	0.00264	0.2836
139	139	0.999	0.999	0.00265	0.00265	0.00265	0.2836
140	140	0.999	0.999				

Table 3. Flow Field Velocities at 37.5° Pitch Angle and X = 2.8

NPT	RUN	IY	JZ	LUDIR	UT	P	UB1	UG1	UG2	RMSB	RMSG
138	025	7	1	1	2	36.168	16.747				
IPT	RUN	I	X	Y	Z	U	U	U	U	U	U
116	025	1	2.800	-0.979	0.500	0.816	0.041	129.5	787.4	129.5	159.2
117	025	2	2.800	-0.841	0.498	0.822	0.059	139.5	797.9	139.5	183.3
118	025	3	2.799	-0.701	0.501	0.842	0.075	149.4	822.2	149.4	205.3
119	025	4	2.802	-0.560	0.497	0.837	0.107	153.4	828.2	153.4	233.3
120	025	5	2.799	-0.490	0.499	0.832	0.141	147.4	838.2	147.4	253.4
121	025	6	2.798	-0.421	0.500	0.838	0.212	121.5	797.0	121.5	281.4
122	025	7	2.794	-0.352	0.510	0.781	0.364	65.6		65.6	341.5

NPT	RUN	IY	JZ	LUDIR	UT	P	UB1	UG1	UG2	RMSB	RMSG
115	025	17	2	1	2	36.353	16.919				
IPT	RUN	I	X	Y	Z	U	U	U	U	U	U
93	025	1	2.795	-0.979	0.556	0.850	0.009	81.1	793.5	81.2	86.9
94	025	2	2.798	-0.840	0.554	0.930	0.070	112.0	783.8	112.5	161.5
95	025	3	2.795	-0.699	0.556	0.843	0.070	100.1	797.2	110.8	152.2
96	025	4	2.797	-0.555	0.554	0.738	0.117	117.5	814.2	117.3	205.7
97	025	5	2.799	-0.490	0.552	0.822	0.147	117.3	816.2	117.3	227.3
98	025	6	2.801	-0.421	0.550	0.812	0.178	125.8	820.2	126.8	259.4
99	025	7	2.799	-0.349	0.552	0.877	0.215	159.4	820.2	159.4	321.5
100	025	8	2.802	-0.280	0.550	0.877	0.146	37.7	800.2	37.7	143.2
101	025	9	2.802	-0.210	0.548	1.130	-0.120	-73.0	872.0	-73.0	-563.8
102	025	10	2.804	-0.141	0.547	1.183	0.041	-100.7	589.8	-100.7	-568.4
103	025	11	2.799	-0.070	0.553	1.142	0.093	-117.4	589.8	-117.4	-1074.5
104	025	12	2.802	-0.001	0.558	1.064	0.201	-104.5	505.9	-104.5	-1046.5
105	025	13	2.804	0.071	0.547	1.036	0.422	-100.4	485.7	-100.4	-1000.4
106	025	14	2.804	0.140	0.546	1.089	0.509	-106.4	517.2	-106.4	-1464.5
107	025	15	2.797	0.210	0.556	0.983	0.756	-136.6	724.0	-136.6	-786.4
108	025	16	2.799	0.279	0.554	0.993	0.707	-176.0	808.2	-176.0	-263.4
109	025	17	2.795	0.351	0.555	0.933	0.462	-343.4		-343.4	13.0

Table 3. Continued

[illegible][illegible]

Table 3. Continued

35

36

[illegible]

Table 3. Continued

[illegible][illegible]

38

[illegible]

Table 4. Vorticities and Circulations for 37.5° Pitch Angle and X = 2.8

POINT	ROW	VC	AREA	GAM	VORTIC
1	1	-0.910	0.527	0.00731	-0.0591
2	1	-0.770	0.527	0.007768	0.3141
3	1	-0.630	0.527	0.007845	-0.0097
4	1	-0.525	0.526	0.008231	0.2742
5	1	-0.455	0.525	0.008563	0.2713
6	1	-0.385	0.528	0.008247	1.1321

POINT	ROW	VC	AREA	GAM	VORTIC
1	2	-0.910	0.578	0.006425	-0.4134
2	2	-0.770	0.577	0.006375	-0.0040
3	2	-0.630	0.576	0.005859	-0.0098
4	2	-0.525	0.575	0.005987	-0.3824
5	2	-0.455	0.576	0.003455	-0.5140
6	2	-0.385	0.578	0.003781	-0.3744
7	2	-0.314	0.577	0.003716	-1.2898
8	2	-0.245	0.576	0.003759	-3.6877
9	2	-0.175	0.573	0.003585	-4.4768
10	2	-0.105	0.573	0.003813	-3.3828
11	2	-0.036	0.572	0.002993	-1.7269
12	2	0.036	0.571	0.003287	-0.2393
13	2	0.105	0.572	0.002602	0.0806
14	2	0.175	0.574	0.003174	4.0289
15	2	0.244	0.576	0.002980	8.6638
16	2	0.315	0.578	0.003408	8.1096

POINT	ROW	VC	AREA	GAM	VORTIC
1	3	-0.910	0.626	0.006995	0.4316
2	3	-0.770	0.625	0.006946	0.4182
3	3	-0.630	0.623	0.007180	0.4440
4	3	-0.525	0.623	0.003743	0.3322
5	3	-0.455	0.625	0.003575	1.2832
6	3	-0.384	0.627	0.003237	0.8256
7	3	-0.314	0.628	0.003308	-0.0487
8	3	-0.244	0.627	0.003479	-3.0277
9	3	-0.174	0.625	0.003671	-7.0748
10	3	-0.104	0.623	0.003802	-5.6510
11	3	0.034	0.622	0.004020	-2.2144
12	3	0.105	0.622	0.003962	-2.1368
13	3	0.175	0.624	0.003500	1.1693
14	3	0.244	0.623	0.003625	3.3619
15	3	0.315	0.623	0.003564	5.2356
16	3	0.385	0.626	0.003429	3.4486
17	3	0.455	0.628	0.003551	-0.0932
18	3	0.525	0.625	0.003829	-0.5910
19	3	0.595	0.623	0.003894	-0.3842

POINT	ROW	VC	AREA	GAM	VORTIC
1	4	-0.910	0.730	0.007132	0.0844
2	4	-0.770	0.727	0.007223	-0.0337
3	4	-0.630	0.727	0.007017	0.0527
4	4	-0.525	0.728	0.003528	0.2214
5	4	-0.455	0.727	0.003499	-0.0315
6	4	-0.386	0.727	0.003777	-0.2472
7	4	-0.315	0.726	0.003578	-0.2708
8	4	-0.245	0.726	0.003378	-0.9528
9	4	-0.175	0.729	0.003388	-0.1673
10	4	-0.106	0.729	0.003819	0.01513
11	4	-0.035	0.728	0.003823	-0.0834
12	4	0.035	0.726	0.003857	-0.00358
13	4	0.106	0.727	0.003520	0.004768
14	4	0.175	0.728	0.003599	1.2599
15	4	0.245	0.727	0.003598	-0.01534
16	4	0.314	0.727	0.003602	0.01765
17	4	0.385	0.727	0.003439	0.015917
18	4	0.455	0.727	0.003088	0.004426
19	4	0.525	0.727	0.003012	0.00472
20	4	0.595	0.729	0.003088	0.00698
21	4	0.665	0.729	0.003383	0.001032
22	4	0.730	0.725	0.007429	-0.00448

POINT	ROW	VC	AREA	GAM	VORTIC
1	5	-0.909	0.730	0.007132	0.00602
2	5	-0.770	0.727	0.007223	-0.000244
3	5	-0.630	0.727	0.007017	0.000370
4	5	-0.525	0.728	0.003528	0.000781
5	5	-0.455	0.727	0.003499	0.000110
6	5	-0.386	0.727	0.003777	0.000934
7	5	-0.315	0.726	0.003578	0.000996
8	5	-0.245	0.726	0.003378	0.003219
9	5	-0.175	0.729	0.003388	-0.00567
10	5	-0.106	0.729	0.003819	0.001513
11	5	-0.035	0.728	0.003823	-0.00358
12	5	0.035	0.726	0.003857	-0.004768
13	5	0.106	0.727	0.003520	0.005546
14	5	0.175	0.728	0.003599	0.01534
15	5	0.245	0.727	0.003598	0.01765
16	5	0.314	0.727	0.003602	0.015917
17	5	0.385	0.727	0.003439	0.004426
18	5	0.455	0.727	0.003088	0.00472
19	5	0.525	0.729	0.003088	0.00698
20	5	0.595	0.729	0.003383	0.001032
21	5	0.665	0.725	0.007429	-0.00448
22	5	0.730	0.725	0.007429	-0.00448

THIS PAGE IS BEST QUALITY PRACTICABLE
FROM COPY FURNISHED TO DDC

Table 4. Concluded

POINT	ROW	VORTICITY	VC	AREA	ZC	GAM	VORTIC	POINT	ROW	VORTICITY	VC	AREA	ZC	GAM	VORTIC
1	6	-0.900	0.777	0.000461	-0.00117	-0.00117	-0.1843	1	8	-0.910	0.770	0.014370	0.000970	-0.000970	-0.0675
2	6	-0.770	0.776	0.000367	-0.000756	-0.000756	-0.1206	2	8	-0.770	0.770	0.014142	0.000959	-0.000959	-0.0641
3	6	-0.630	0.776	0.000374	-0.000756	-0.000756	-0.1206	3	8	-0.630	0.770	0.014142	0.000959	-0.000959	-0.0641
4	6	-0.490	0.777	0.000360	-0.000756	-0.000756	-0.1206	4	8	-0.490	0.770	0.014142	0.000959	-0.000959	-0.0641
5	6	-0.350	0.776	0.000363	-0.000756	-0.000756	-0.1206	5	8	-0.350	0.770	0.014142	0.000959	-0.000959	-0.0641
6	6	-0.210	0.774	0.000363	-0.000756	-0.000756	-0.1206	6	8	-0.210	0.770	0.014142	0.000959	-0.000959	-0.0641
7	6	-0.070	0.774	0.000363	-0.000756	-0.000756	-0.1206	7	8	-0.070	0.770	0.014142	0.000959	-0.000959	-0.0641
8	6	0.070	0.776	0.000363	-0.000756	-0.000756	-0.1206	8	8	0.070	0.770	0.014142	0.000959	-0.000959	-0.0641
9	6	0.210	0.776	0.000363	-0.000756	-0.000756	-0.1206	9	8	0.210	0.770	0.014142	0.000959	-0.000959	-0.0641
10	6	0.350	0.778	0.000363	-0.000756	-0.000756	-0.1206	10	8	0.350	0.770	0.014142	0.000959	-0.000959	-0.0641
11	6	0.490	0.778	0.000363	-0.000756	-0.000756	-0.1206	11	8	0.490	0.770	0.014142	0.000959	-0.000959	-0.0641
12	6	0.630	0.778	0.000363	-0.000756	-0.000756	-0.1206	12	8	0.630	0.770	0.014142	0.000959	-0.000959	-0.0641
13	6	0.770	0.774	0.000363	-0.000756	-0.000756	-0.1206	13	8	0.770	0.770	0.014142	0.000959	-0.000959	-0.0641
14	6	0.910	0.776	0.000363	-0.000756	-0.000756	-0.1206	14	8	0.910	0.770	0.014142	0.000959	-0.000959	-0.0641
15	6	1.050	0.776	0.000363	-0.000756	-0.000756	-0.1206	15	8	1.050	0.770	0.014142	0.000959	-0.000959	-0.0641
16	6	1.190	0.776	0.000363	-0.000756	-0.000756	-0.1206	16	8	1.190	0.770	0.014142	0.000959	-0.000959	-0.0641
17	6	1.330	0.776	0.000363	-0.000756	-0.000756	-0.1206	17	8	1.330	0.770	0.014142	0.000959	-0.000959	-0.0641
18	6	1.470	0.773	0.000363	-0.000756	-0.000756	-0.1206	18	8	1.470	0.770	0.014142	0.000959	-0.000959	-0.0641
19	6	1.610	0.775	0.000363	-0.000756	-0.000756	-0.1206	19	8	1.610	0.770	0.014142	0.000959	-0.000959	-0.0641
20	6	1.750	0.775	0.000363	-0.000756	-0.000756	-0.1206	20	8	1.750	0.770	0.014142	0.000959	-0.000959	-0.0641
21	6	1.890	0.774	0.000363	-0.000756	-0.000756	-0.1206	21	8	1.890	0.770	0.014142	0.000959	-0.000959	-0.0641
22	6	2.030	0.774	0.000363	-0.000756	-0.000756	-0.1206	22	8	2.030	0.770	0.014142	0.000959	-0.000959	-0.0641

POINT	ROW	VORTICITY	VC	AREA	ZC	GAM	VORTIC	POINT	ROW	VORTICITY	VC	AREA	ZC	GAM	VORTIC
1	7	-0.910	0.823	0.000304	0.001173	0.001173	0.1700	1	7	-0.910	0.823	0.000304	0.001173	0.001173	0.1700
2	7	-0.770	0.823	0.000304	0.001173	0.001173	0.1700	2	7	-0.770	0.823	0.000304	0.001173	0.001173	0.1700
3	7	-0.630	0.824	0.000304	0.001173	0.001173	0.1700	3	7	-0.630	0.824	0.000304	0.001173	0.001173	0.1700
4	7	-0.490	0.825	0.000304	0.001173	0.001173	0.1700	4	7	-0.490	0.825	0.000304	0.001173	0.001173	0.1700
5	7	-0.350	0.825	0.000304	0.001173	0.001173	0.1700	5	7	-0.350	0.825	0.000304	0.001173	0.001173	0.1700
6	7	-0.210	0.823	0.000304	0.001173	0.001173	0.1700	6	7	-0.210	0.823	0.000304	0.001173	0.001173	0.1700
7	7	-0.070	0.824	0.000304	0.001173	0.001173	0.1700	7	7	-0.070	0.824	0.000304	0.001173	0.001173	0.1700
8	7	0.070	0.824	0.000304	0.001173	0.001173	0.1700	8	7	0.070	0.824	0.000304	0.001173	0.001173	0.1700
9	7	0.210	0.825	0.000304	0.001173	0.001173	0.1700	9	7	0.210	0.825	0.000304	0.001173	0.001173	0.1700
10	7	0.350	0.825	0.000304	0.001173	0.001173	0.1700	10	7	0.350	0.825	0.000304	0.001173	0.001173	0.1700
11	7	0.490	0.825	0.000304	0.001173	0.001173	0.1700	11	7	0.490	0.825	0.000304	0.001173	0.001173	0.1700
12	7	0.630	0.823	0.000304	0.001173	0.001173	0.1700	12	7	0.630	0.823	0.000304	0.001173	0.001173	0.1700
13	7	0.770	0.823	0.000304	0.001173	0.001173	0.1700	13	7	0.770	0.823	0.000304	0.001173	0.001173	0.1700
14	7	0.910	0.822	0.000304	0.001173	0.001173	0.1700	14	7	0.910	0.822	0.000304	0.001173	0.001173	0.1700
15	7	1.050	0.822	0.000304	0.001173	0.001173	0.1700	15	7	1.050	0.822	0.000304	0.001173	0.001173	0.1700
16	7	1.190	0.822	0.000304	0.001173	0.001173	0.1700	16	7	1.190	0.822	0.000304	0.001173	0.001173	0.1700
17	7	1.330	0.824	0.000304	0.001173	0.001173	0.1700	17	7	1.330	0.824	0.000304	0.001173	0.001173	0.1700
18	7	1.470	0.824	0.000304	0.001173	0.001173	0.1700	18	7	1.470	0.824	0.000304	0.001173	0.001173	0.1700
19	7	1.610	0.824	0.000304	0.001173	0.001173	0.1700	19	7	1.610	0.824	0.000304	0.001173	0.001173	0.1700
20	7	1.750	0.821	0.000304	0.001173	0.001173	0.1700	20	7	1.750	0.821	0.000304	0.001173	0.001173	0.1700
21	7	1.890	0.820	0.000304	0.001173	0.001173	0.1700	21	7	1.890	0.820	0.000304	0.001173	0.001173	0.1700
22	7	2.030	0.822	0.000304	0.001173	0.001173	0.1700	22	7	2.030	0.822	0.000304	0.001173	0.001173	0.1700

Table 5. Flow Field Velocities at 37.5° Pitch Angle and X = 4.9

NPT	RUM	IY	JZ	LUDIR	UT	P	U	U1	U2	U3	U4	RMS	RMS
144	028	5	1	1	13.804	2.4345							
IPT	RUM	I	X	Y	Z	U	U1	U2	U3	U4	U5	RMS	RMS
127	028	1	4.896	-0.839	0.455	0.796	0.092	0.864	229.2	297.4	816.2	229.2	297.4
128	028	2	4.899	-0.559	0.451	0.780	0.174	0.965	307.5	437.6	848.2	307.5	437.6
129	028	3	4.897	-0.420	0.453	0.690	0.134	0.852	279.9	379.5	746.1	279.9	379.5
130	028	4	4.901	-0.348	0.451	0.964	-0.186	0.227	-459.1	-597.9	627.9	-459.1	-597.9
131	028	5	4.905	-0.281	0.442	0.321	-0.113	-0.404	-658.6	-742.1	5.1	-658.6	-742.1
NPT	RUM	IY	JZ	LUDIR	UT	P	U	U1	U2	U3	U4	RMS	RMS
162	028	9	2	1	36.600	17.115							
IPT	RUM	I	X	Y	Z	U	U1	U2	U3	U4	U5	RMS	RMS
145	028	1	4.896	-0.841	0.526	0.709	0.118	0.802	219.3	307.4	866.2	219.3	307.4
146	028	2	4.902	-0.560	0.525	0.758	0.112	0.944	305.0	437.6	866.2	305.0	437.6
147	028	3	4.901	-0.419	0.522	0.711	0.344	0.980	543.8	543.8	866.2	543.8	543.8
148	028	4	4.898	-0.281	0.524	0.960	0.399	0.339	-618.7	-381.5	618.7	-618.7	-381.5
149	028	5	4.906	-0.210	0.520	1.210	-0.223	0.144	-728.4	-922.3	742.1	-728.4	-922.3
150	028	6	4.903	-0.140	0.519	1.163	-0.341	0.069	-988.4	-988.4	666.0	-988.4	-988.4
151	028	7	4.902	-0.071	0.523	1.199	-0.336	-0.043	-872.1	-1122.6	666.0	-872.1	-1122.6
152	028	8	4.899	-0.000	0.524	1.266	-0.527	-0.082	-828.2	-1278.8	666.0	-828.2	-1278.8
153	028	9	4.902	0.072	0.527	1.256	-0.357	0.020	-846.1	-1114.6	710.0	-846.1	-1114.6
NPT	RUM	IY	JZ	LUDIR	UT	P	U	U1	U2	U3	U4	RMS	RMS
180	028	15	3	1	36.375	16.905							
IPT	RUM	I	X	Y	Z	U	U1	U2	U3	U4	U5	RMS	RMS
163	028	1	4.895	-0.841	0.607	0.794	0.098	0.832	207.3	307.4	866.2	207.3	307.4
164	028	2	4.896	-0.559	0.605	0.774	0.213	0.943	391.6	479.7	866.2	391.6	479.7
165	028	3	4.897	-0.421	0.606	0.748	0.360	0.943	479.7	479.7	866.2	479.7	479.7
166	028	4	4.897	-0.281	0.598	0.923	0.166	0.619	-69.1	-323.5	776.1	-69.1	-323.5
167	028	5	4.902	-0.209	0.598	1.066	0.026	0.339	-323.5	-323.5	776.1	-323.5	-323.5
168	028	6	4.900	-0.139	0.598	1.178	0.066	0.189	-814.2	-814.2	674.1	-814.2	-814.2
169	028	7	4.896	-0.069	0.605	1.136	0.110	0.189	-560.4	-560.4	674.1	-560.4	-560.4
170	028	8	4.899	0.001	0.601	1.136	-0.117	0.189	-1042.5	-1042.5	674.1	-1042.5	-1042.5
171	028	9	4.901	0.072	0.604	1.145	-0.193	-0.135	-1042.5	-1042.5	674.1	-1042.5	-1042.5
172	028	10	4.906	0.139	0.596	1.095	-0.161	-0.155	-1042.5	-1042.5	674.1	-1042.5	-1042.5
173	028	11	4.901	0.210	0.603	1.051	-0.170	-0.155	-1042.5	-1042.5	674.1	-1042.5	-1042.5
174	028	12	4.898	0.279	0.604	1.028	0.233	-0.089	-1042.5	-1042.5	674.1	-1042.5	-1042.5
175	028	13	4.906	0.349	0.593	0.993	0.255	0.104	-1042.5	-1042.5	674.1	-1042.5	-1042.5
176	028	14	4.902	0.419	0.599	0.876	0.338	0.265	-1042.5	-1042.5	674.1	-1042.5	-1042.5
177	028	15	4.898	0.489	0.607	0.837	-0.041	0.265	-1042.5	-1042.5	674.1	-1042.5	-1042.5

Table 5. Continued

WPT	RUN	IV	J2	LUDIR	UT	P
108	028	17	4	2	36.171	16.715
101	028	1	X	Y	Z	U
01	028	1	4	0	0.677	0.791
02	028	2	0	0	0.674	0.744
03	028	3	0	0	0.676	0.746
04	028	4	0	0	0.669	0.808
05	028	5	0	0	0.667	0.808
06	028	6	0	0	0.667	1.028
07	028	7	0	0	0.676	1.117
08	028	8	0	0	0.678	1.069
09	028	9	0	0	0.678	1.231
10	028	10	0	0	0.671	0.987
101	028	11	0	0	0.676	1.076
102	028	12	0	0	0.677	0.977
103	028	13	0	0	0.672	0.982
104	028	14	0	0	0.671	0.918
105	028	15	0	0	0.672	0.812
106	028	16	0	0	0.677	0.885
107	028	17	0	0	0.677	0.785
108	028	18	0	0	0.677	0.785
109	028	19	0	0	0.677	0.785
110	028	20	0	0	0.677	0.785
111	028	21	0	0	0.677	0.785
112	028	22	0	0	0.677	0.785
113	028	23	0	0	0.677	0.785
114	028	24	0	0	0.677	0.785
115	028	25	0	0	0.677	0.785
116	028	26	0	0	0.677	0.785
117	028	27	0	0	0.677	0.785
118	028	28	0	0	0.677	0.785
119	028	29	0	0	0.677	0.785
120	028	30	0	0	0.677	0.785
121	028	31	0	0	0.677	0.785
122	028	32	0	0	0.677	0.785
123	028	33	0	0	0.677	0.785
124	028	34	0	0	0.677	0.785
125	028	35	0	0	0.677	0.785
126	028	36	0	0	0.677	0.785
127	028	37	0	0	0.677	0.785
128	028	38	0	0	0.677	0.785
129	028	39	0	0	0.677	0.785
130	028	40	0	0	0.677	0.785
131	028	41	0	0	0.677	0.785
132	028	42	0	0	0.677	0.785
133	028	43	0	0	0.677	0.785
134	028	44	0	0	0.677	0.785
135	028	45	0	0	0.677	0.785
136	028	46	0	0	0.677	0.785
137	028	47	0	0	0.677	0.785
138	028	48	0	0	0.677	0.785
139	028	49	0	0	0.677	0.785
140	028	50	0	0	0.677	0.785
141	028	51	0	0	0.677	0.785
142	028	52	0	0	0.677	0.785
143	028	53	0	0	0.677	0.785
144	028	54	0	0	0.677	0.785
145	028	55	0	0	0.677	0.785
146	028	56	0	0	0.677	0.785
147	028	57	0	0	0.677	0.785
148	028	58	0	0	0.677	0.785
149	028	59	0	0	0.677	0.785
150	028	60	0	0	0.677	0.785
151	028	61	0	0	0.677	0.785
152	028	62	0	0	0.677	0.785
153	028	63	0	0	0.677	0.785
154	028	64	0	0	0.677	0.785
155	028	65	0	0	0.677	0.785
156	028	66	0	0	0.677	0.785
157	028	67	0	0	0.677	0.785
158	028	68	0	0	0.677	0.785
159	028	69	0	0	0.677	0.785
160	028	70	0	0	0.677	0.785
161	028	71	0	0	0.677	0.785
162	028	72	0	0	0.677	0.785
163	028	73	0	0	0.677	0.785
164	028	74	0	0	0.677	0.785
165	028	75	0	0	0.677	0.785
166	028	76	0	0	0.677	0.785
167	028	77	0	0	0.677	0.785
168	028	78	0	0	0.677	0.785
169	028	79	0	0	0.677	0.785
170	028	80	0	0	0.677	0.785
171	028	81	0	0	0.677	0.785
172	028	82	0	0	0.677	0.785
173	028	83	0	0	0.677	0.785
174	028	84	0	0	0.677	0.785
175	028	85	0	0	0.677	0.785
176	028	86	0	0	0.677	0.785
177	028	87	0	0	0.677	0.785
178	028	88	0	0	0.677	0.785
179	028	89	0	0	0.677	0.785
180	028	90	0	0	0.677	0.785
181	028	91	0	0	0.677	0.785
182	028	92	0	0	0.677	0.785
183	028	93	0	0	0.677	0.785
184	028	94	0	0	0.677	0.785
185	028	95	0	0	0.677	0.785
186	028	96	0	0	0.677	0.785
187	028	97	0	0	0.677	0.785
188	028	98	0	0	0.677	0.785
189	028	99	0	0	0.677	0.785
190	028	100	0	0	0.677	0.785
191	028	101	0	0	0.677	0.785
192	028	102	0	0	0.677	0.785
193	028	103	0	0	0.677	0.785
194	028	104	0	0	0.677	0.785
195	028	105	0	0	0.677	0.785
196	028	106	0	0	0.677	0.785
197	028	107	0	0	0.677	0.785
198	028	108	0	0	0.677	0.785
199	028	109	0	0	0.677	0.785
200	028	110	0	0	0.677	0.785
201	028	111	0	0	0.677	0.785
202	028	112	0	0	0.677	0.785
203	028	113	0	0	0.677	0.785
204	028	114	0	0	0.677	0.785
205	028	115	0	0	0.677	0.785
206	028	116	0	0	0.677	0.785
207	028	117	0	0	0.677	0.785
208	028	118	0	0	0.677	0.785
209	028	119	0	0	0.677	0.785
210	028	120	0	0	0.677	0.785
211	028	121	0	0	0.677	0.785
212	028	122	0	0	0.677	0.785
213	028	123	0	0	0.677	0.785
214	028	124	0	0	0.677	0.785
215	028	125	0	0	0.677	0.785
216	028	126	0	0	0.677	0.785
217	028	127	0	0	0.677	0.785
218	028	128	0	0	0.677	0.785
219	028	129	0	0	0.677	0.785
220	028	130	0	0	0.677	0.785
221	028	131	0	0	0.677	0.785
222	028	132	0	0	0.677	0.785
223	028	133	0	0	0.677	0.785
224	028	134	0	0	0.677	0.785
225	028	135	0	0	0.677	0.785
226	028	136	0	0	0.677	0.785
227	028	137	0	0	0.677	0.785
228	028	138	0	0	0.677	0.785
229	028	139	0	0	0.677	0.785
230	028	140	0	0	0.677	0.785
231	028	141	0	0	0.677	0.785
232	028	142	0	0	0.677	0.785
233	028	143	0	0	0.677	0.785
234	028	144	0	0	0.677	0.785
235	028	145	0	0	0.677	0.785
236	028	146	0	0	0.677	0.785
237	028	147	0	0	0.677	0.785
238	028	148	0	0	0.677	0.785
239	028	149	0	0	0.677	0.785
240	028	150	0	0	0.677	0.785
241	028	151	0	0	0.677	0.785
242	028	152	0	0	0.677	0.785
243	028	153	0	0	0.677	0.785
244	028	154	0	0	0.677	0.785
245	028	155	0	0	0.677	0.785
246	028	156	0	0	0.677	0.785
247	028	157	0	0	0.677	0.785
248	028	158	0	0	0.677	0.785
249	028	159	0	0	0.677	0.785
250	028	160	0	0	0.677	0.785
251	028	161	0	0	0.677	0.785
252	028	162	0	0	0.677	0.785
253	028	163	0	0	0.677	0.785
254	028	164	0	0	0.677	0.785
255	028	165	0	0	0.677	0.785
256	028	166	0	0	0.677	0.785
257	028	167	0	0	0.677	0.785
258	028	168	0	0	0.677	0.785
259	028	169	0	0	0.677	0.785
260	028	170	0	0	0.677	0.785
261	028	171	0	0	0.677	0.785
262	028	172	0	0	0.677	0.785
263	028	173	0	0	0.677	0.785
264	028	174	0	0	0.677	0.785
265	028	175	0	0	0.677	0.785
266	028	176	0	0	0.677	0.785
267	028	177	0	0	0.677	0.785
268	028	178	0	0	0.677	0.785
269	028	179	0	0	0.677	0.785
270	028	180	0	0	0.677	0.785
271	028	181	0	0	0.677	0.785
272	028	182	0	0	0.677	0.785
273	028	183	0	0	0.677	0.785
274	028	184	0	0	0.677	0.785
275	028	185	0	0	0.677	0.785
276	028	186	0	0	0.677	0.785
277	028	187	0	0	0.677	0.785
278	028	188	0	0	0.677	0.785
279	028	189	0	0	0.677	0.785
280	028	190	0	0	0.677	0.785
281	028	191	0	0	0.677	0.785
282	028	192	0	0	0.677	0.785
283	028	193	0	0	0.677	0.785
284	028	194	0	0	0.677	0.785
285	028	195	0	0	0.677	0.785
286	028	196	0	0	0.677	0.785
287	028	197	0	0	0.677	0.785
288	028	198	0	0	0.677	0.785
289	028	199	0	0	0.677	0.785
290	028	200	0	0	0.677	0.785
291	028	201	0	0	0.677	0.785
292	028	202	0	0	0.677	0.785
293	028	203	0	0	0.677	0.785
294	028	204	0	0	0.677	0.785
295	028	205	0	0	0.677	0.785
296	028	206	0	0	0.67	

WPT	18	19	20	21	22	23	24	25	26	27	28	29	30	31	32	33	34	35	36	37	38	39	40	41	42	43	44	45	46	47	48	49	50	51	52	53	54	55	56	57	58	59	60	61	62	63	64	65	66	67	68	69	70	71	72	73	74	75	76	77	78	79	80	81	82	83	84	85	86	87	88	89	90																	
1	1	2	3	4	5	6	7	8	9	10	11	12	13	14	15	16	17	18	19	20	21	22	23	24	25	26	27	28	29	30	31	32	33	34	35	36	37	38	39	40	41	42	43	44	45	46	47	48	49	50	51	52	53	54	55	56	57	58	59	60	61	62	63	64	65	66	67	68	69	70	71	72	73	74	75	76	77	78	79	80	81	82	83	84	85	86	87	88	89	90
2	1	2	3	4	5	6	7	8	9	10	11	12	13	14	15	16	17	18	19	20	21	22	23	24	25	26	27	28	29	30	31	32	33	34	35	36	37	38	39	40	41	42	43	44	45	46	47	48	49	50	51	52	53	54	55	56	57	58	59	60	61	62	63	64	65	66	67	68	69	70	71	72	73	74	75	76	77	78	79	80	81	82	83	84	85	86	87	88	89	90
3	1	2	3	4	5	6	7	8	9	10	11	12	13	14	15	16	17	18	19	20	21	22	23	24	25	26	27	28	29	30	31	32	33	34	35	36	37	38	39	40	41	42	43	44	45	46	47	48	49	50	51	52	53	54	55	56	57	58	59	60	61	62	63	64	65	66	67	68	69	70	71	72	73	74	75	76	77	78	79	80	81	82	83	84	85	86	87	88	89	90
4	1	2	3	4	5	6	7	8	9	10	11	12	13	14	15	16	17	18	19	20	21	22	23	24	25	26	27	28	29	30	31	32	33	34	35	36	37	38	39	40	41	42	43	44	45	46	47	48	49	50	51	52	53	54	55	56	57	58	59	60	61	62	63	64	65	66	67	68	69	70	71	72	73	74	75	76	77	78	79	80	81	82	83	84	85	86	87	88	89	90
5	1	2	3	4	5	6	7	8	9	10	11	12	13	14	15	16	17	18	19	20	21	22	23	24	25	26	27	28	29	30	31	32	33	34	35	36	37	38	39	40	41	42	43	44	45	46	47	48	49	50	51	52	53	54	55	56	57	58	59	60	61	62	63	64	65	66	67	68	69	70	71	72	73	74	75	76	77	78	79	80	81	82	83	84	85	86	87	88	89	90
6	1	2	3	4	5	6	7	8	9	10	11	12	13	14	15	16	17	18	19	20	21	22	23	24	25	26	27	28	29	30	31	32	33	34	35	36	37	38	39	40	41	42	43	44	45	46	47	48	49	50	51	52	53	54	55	56	57	58	59	60	61	62	63	64	65	66	67	68	69	70	71	72	73	74	75	76	77	78	79	80	81	82	83	84	85	86	87	88	89	90
7	1	2	3	4	5	6	7	8	9	10	11	12	13	14	15	16	17	18	19	20	21	22	23	24	25	26	27	28	29	30	31	32	33	34	35	36	37	38	39	40	41	42	43	44	45	46	47	48	49	50	51	52	53	54	55	56	57	58	59	60	61	62	63	64	65	66	67	68	69	70	71	72	73	74	75	76	77	78	79	80	81	82	83	84	85	86	87	88	89	90
8	1	2	3	4	5	6	7	8	9	10	11	12	13	14	15	16	17	18	19	20	21	22	23	24	25	26	27	28	29	30	31	32	33	34	35	36	37	38	39	40	41	42	43	44	45	46	47	48	49	50	51	52	53	54	55	56	57	58	59	60	61	62	63	64	65	66	67	68	69	70	71	72	73	74	75	76	77	78	79	80	81	82	83	84	85	86	87	88	89	90
9	1	2	3	4	5	6	7	8	9	10	11	12	13	14	15	16	17	18	19	20	21	22	23	24	25	26	27	28	29	30	31	32	33	34	35	36	37	38	39	40	41	42	43	44	45	46	47	48	49	50	51	52	53	54	55	56	57	58	59	60	61	62	63	64	65	66	67	68	69	70	71	72	73	74	75	76	77	78	79	80	81	82	83	84	85	86	87	88	89	90
10	1	2	3	4	5	6	7	8	9	10	11	12	13	14	15	16	17	18	19	20	21	22	23	24	25	26	27	28	29	30	31	32	33	34	35	36	37	38	39	40	41	42	43	44	45	46	47	48	49	50	51	52	53	54	55	56	57	58	59	60	61	62	63	64	65	66	67	68	69	70	71	72	73	74	75	76	77	78	79	80	81	82	83	84	85	86	87	88	89	90
11	1	2	3	4	5	6	7	8	9	10	11	12	13	14	15	16	17	18	19	20	21	22	23	24	25	26	27	28	29	30	31	32	33	34	35	36	37	38	39	40	41	42	43	44	45	46	47	48	49	50	51	52	53	54	55	56	57	58	59	60	61	62	63	64	65	66	67	68	69	70	71	72	73	74	75	76	77	78	79	80	81	82	83	84	85	86	87	88	89	90
12	1	2	3	4	5	6	7	8	9	10	11	12	13	14	15	16	17	18	19	20	21	22	23	24	25	26	27	28	29	30	31	32	33	34	35	36	37	38	39	40	41	42	43	44	45	46	47	48	49	50	51	52	53	54	55	56	57	58	59	60	61	62	63	64	65	66	67	68	69	70	71	72	73	74	75	76	77	78	79	80	81	82	83	84	85	86	87	88	89	90
13	1	2	3	4	5	6	7	8	9	10	11	12	13	14	15	16	17	18	19	20	21	22	23	24	25	26	27	28	29	30	31	32	33	34	35	36	37	38	39	40	41	42	43	44	45	46	47	48	49	50	51	52	53	54	55	56	57	58	59	60	61	62	63	64	65	66	67	68	69	70	71	72	73	74	75	76	77	78	79	80	81	82	83	84	85	86	87	88	89	90
14	1	2	3	4	5	6	7	8	9	10	11	12	13	14	15	16	17	18	19	20	21	22	23	24	25	26	27	28	29	30	31	32	33	34	35	36	37	38	39	40	41	42	43	44	45	46	47	48	49	50	51	52	53	54	55	56	57	58	59	60	61	62	63	64	65	66	67	68	69	70	71	72	73	74	75	76	77	78	79	80	81	82	83	84	85	86	87	88	89	90
15	1	2	3	4	5	6	7	8	9	10	11	12	13	14	15	16	17	18	19	20	21	22	23	24	25	26	27	28	29	30	31	32	33	34	35	36	37	38	39	40	41	42	43	44	45	46	47	48	49	50	51	52	53	54	55	56	57	58	59	60	61	62	63	64	65	66	67	68	69	70	71	72	73	74	75	76	77	78	79	80	81	82	83	84	85	86	87	88	89	90
16	1	2	3	4	5	6	7	8	9	10	11	12	13	14	15	16	17	18	19	20	21	22	23	24	25	26	27	28	29	30	31	32	33	34	35	36	37	38	39	40	41	42	43	44	45	46	47	48	49	50	51	52	53	54	55	56	57	58	59	60	61	62	63	64	65	66	67	68	69	70	71	72	73	74	75	76	77	78	79	80	81	82	83	84	85	86	87	88	89	90
17	1	2	3	4	5	6	7	8	9	10	11	12	13	14	15	16	17	18	19	20	21	22	23	24	25	26	27	28	29	30	31	32	33	34	35	36	37	38	39	40	41	42	43	44	45	46	47	48	49	50	51	52	53	54	55	56	57	58	59	60	61	62	63	64	65	66	67	68	69	70	71	72	73	74	75	76	77	78	79	80	81	82	83	84	85	86	87	88	89	90
18	1	2	3	4	5	6	7	8	9	10	11	12	13	14	15	16	17	18	19	20	21	22	23	24	25	26	27	28	29	30	31	32	33	34	35	36	37	38	39	40	41	42	43	44	45	46	47	48	49	50	51	52	53	54	55	56	57	58	59	60	61	62	63	64	65	66	67	68	69	70	71	72	73	74	75	76	77	78	79	80	81	82	83	84	85	86	87	88	89	90
19	1	2	3	4	5	6	7	8	9	10	11	12	13	14	15	16	17	18	19	20	21	22	23	24	25	26	27	28	29	30	31	32	33	34	35	36	37	38	39	40	41	42	43	44	45	46	47	48	49	50	51	52	53	54	55	56	57	58	59	60	61	62	63	64	65	66	67	68	69	70	7																			

Table 5. Continued

NPT	RUM	IV	JZ	LUDIR	UT	P
72	028	18	6	36.381		16.910
IPT	RUM	I	X	Y	Z	U
55	028	1	4.897	-0.839	0.828	0.805
56	028	2	4.903	-0.560	0.818	0.800
57	028	3	4.900	-0.422	0.835	0.776
58	028	4	4.902	-0.280	0.822	0.745
59	028	5	4.898	-0.211	0.826	0.791
60	028	6	4.900	-0.140	0.825	0.955
61	028	7	4.900	-0.067	0.824	0.975
62	028	8	4.907	0.000	0.819	0.946
63	028	9	4.901	0.070	0.826	0.944
64	028	10	4.905	0.141	0.816	0.916
65	028	11	4.900	0.209	0.824	0.915
66	028	12	4.898	0.280	0.820	0.878
67	028	13	4.903	0.350	0.819	0.964
68	028	14	4.898	0.420	0.828	0.853
69	028	15	4.899	0.491	0.826	0.790
70	028	16	4.899	0.560	0.826	0.786
71	028	17	4.898	0.630	0.825	0.759
72	028	18	4.899	0.840	0.825	0.759
UG1	0.807					
UG2	0.762					
UG3	0.786					
UG4	0.817					
UG5	0.785					
UG6	0.695					
UG7	0.495					
UG8	0.219					
UG9	-0.020					
UG10	-0.238					
UG11	-0.285					
UG12	-0.264					
UG13	-0.056					
UG14	-0.374					
UG15	-0.525					
UG16	-0.377					
UG17	-0.817					
UG18	-0.777					
UG19	-0.788					
UG20	-0.788					
UG21	-0.788					
UG22	-0.788					
UG23	-0.788					
UG24	-0.788					
UG25	-0.788					
UG26	-0.788					
UG27	-0.788					
UG28	-0.788					
UG29	-0.788					
UG30	-0.788					
UG31	-0.788					
UG32	-0.788					
UG33	-0.788					
UG34	-0.788					
UG35	-0.788					
UG36	-0.788					
UG37	-0.788					
UG38	-0.788					
UG39	-0.788					
UG40	-0.788					
UG41	-0.788					
UG42	-0.788					
UG43	-0.788					
UG44	-0.788					
UG45	-0.788					
UG46	-0.788					
UG47	-0.788					
UG48	-0.788					
UG49	-0.788					
UG50	-0.788					
UG51	-0.788					
UG52	-0.788					
UG53	-0.788					
UG54	-0.788					
UG55	-0.788					
UG56	-0.788					
UG57	-0.788					
UG58	-0.788					
UG59	-0.788					
UG60	-0.788					
UG61	-0.788					
UG62	-0.788					
UG63	-0.788					
UG64	-0.788					
UG65	-0.788					
UG66	-0.788					
UG67	-0.788					
UG68	-0.788					
UG69	-0.788					
UG70	-0.788					
UG71	-0.788					
UG72	-0.788					

NPT	RUM	IV	JZ	LUDIR	UT	P
54	028	18	7	36.215		16.756
IPT	RUM	I	X	Y	Z	U
37	028	1	4.897	-0.841	0.904	0.794
38	028	2	4.903	-0.560	0.900	0.790
39	028	3	4.907	-0.419	0.888	0.730
40	028	4	4.898	-0.280	0.901	0.711
41	028	5	4.902	-0.209	0.901	0.756
42	028	6	4.895	-0.133	0.893	0.750
43	028	7	4.897	-0.071	0.908	0.750
44	028	8	4.902	0.000	0.901	0.882
45	028	9	4.896	0.072	0.898	0.869
46	028	10	4.901	0.140	0.898	0.948
47	028	11	4.904	0.211	0.898	0.938
48	028	12	4.906	0.282	0.894	0.772
49	028	13	4.900	0.351	0.894	0.772
50	028	14	4.901	0.421	0.901	0.670
51	028	15	4.895	0.493	0.902	0.680
52	028	16	4.901	0.559	0.902	0.754
53	028	17	4.905	0.630	0.899	0.763
54	028	18	4.908	0.841	0.893	0.763
UG1	0.806					
UG2	0.726					
UG3	0.741					
UG4	0.759					
UG5	0.713					
UG6	0.621					
UG7	0.386					
UG8	0.166					
UG9	-0.028					
UG10	-0.180					
UG11	-0.331					
UG12	-0.531					
UG13	-0.731					
UG14	-0.931					
UG15	-1.131					
UG16	-1.331					
UG17	-1.531					
UG18	-1.731					
UG19	-1.931					
UG20	-2.131					
UG21	-2.331					
UG22	-2.531					
UG23	-2.731					
UG24	-2.931					
UG25	-3.131					
UG26	-3.331					
UG27	-3.531					
UG28	-3.731					
UG29	-3.931					
UG30	-4.131					
UG31	-4.331					
UG32	-4.531					
UG33	-4.731					
UG34	-4.931					
UG35	-5.131					
UG36	-5.331					
UG37	-5.531					
UG38	-5.731					
UG39	-5.931					
UG40	-6.131					
UG41	-6.331					
UG42	-6.531					
UG43	-6.731					
UG44	-6.931					
UG45	-7.131					
UG46	-7.331					
UG47	-7.531					
UG48	-7.731					
UG49	-7.931					
UG50	-8.131					
UG51	-8.331					
UG52	-8.531					
UG53	-8.731					
UG54	-8.931					
UG55	-9.131					
UG56	-9.331					
UG57	-9.531					
UG58	-9.731					
UG59	-9.931					
UG60	-10.131					
UG61	-10.331					
UG62	-10.531					
UG63	-10.731					
UG64	-10.931					
UG65	-11.131					
UG66	-11.331					
UG67	-11.531					
UG68	-11.731					
UG69	-11.931					
UG70	-12.131					
UG71	-12.331					
UG72	-12.531					

Table 5. Continued

[illegible]

WPT	RUN	IV	JZ	LUDIR	UT	P
18	028	18	9	1	35.790	:6.365
IPT	028	1	X	Y	Z	U
1	028	1	4.897	-0.850	1.206	0.793
2	028	2	4.899	-0.851	1.204	0.795
3	028	3	4.900	-0.852	1.200	0.805
4	028	4	4.907	-0.850	1.206	0.806
5	028	5	4.895	-0.851	1.199	0.836
6	028	6	4.903	-0.850	1.195	0.878
7	028	7	4.903	-0.850	1.137	0.878
8	028	8	4.903	-0.850	1.156	0.919
9	028	9	4.898	-0.851	1.206	0.916
10	028	10	4.898	-0.852	1.206	0.872
11	028	11	4.898	-0.852	1.206	0.874
12	028	12	4.898	-0.852	1.206	0.871
13	028	13	4.904	-0.849	1.197	0.764
14	028	14	4.898	-0.851	1.203	0.758
15	028	15	4.898	-0.851	1.205	0.683
16	028	16	4.898	-0.851	1.205	0.724
17	028	17	4.898	-0.852	1.206	0.741
18	028	18	4.898	-0.852	1.206	0.741

Table 5. Concluded

NET	RUN	IV	JZ	LUDIR	UT	P	U	UB1	UG1	UG2	RMSB	RMSG
126	028	18	10	2	36.290	16.826	0.336	-63.6	33.0	1.0	-63.6	33.0
127	028	1	4.894	-0.840	1.355	0.128	0.651	-157.0	74.0	7.28	-157.0	74.0
128	028	2	4.898	-0.590	1.354	0.190	0.610	-241.6	72.0	7.25	-241.6	72.0
129	028	3	4.898	-0.400	1.353	0.236	0.542	-355.3	68.0	6.88	-355.3	68.0
130	028	4	4.891	-0.200	1.352	0.240	0.471	-441.6	66.0	6.62	-441.6	66.0
131	028	5	4.896	-0.139	1.353	0.251	0.422	-511.6	64.0	6.47	-511.6	64.0
132	028	6	4.894	-0.066	1.355	0.263	0.365	-589.7	62.0	6.23	-589.7	62.0
133	028	7	4.897	-0.001	1.353	0.296	0.263	-683.9	60.0	6.00	-683.9	60.0
134	028	8	4.897	0.001	1.353	0.111	0.182	-712.4	58.0	5.83	-712.4	58.0
135	028	9	4.900	0.070	1.352	0.117	0.113	-820.2	56.0	5.60	-820.2	56.0
136	028	10	4.897	0.141	1.350	0.128	0.152	-820.2	54.0	5.40	-820.2	54.0
137	028	11	4.901	0.209	1.350	0.117	0.113	-710.9	52.0	5.20	-710.9	52.0
138	028	12	4.894	0.279	1.350	0.011	0.030	-540.9	50.0	5.00	-540.9	50.0
139	028	13	4.894	0.351	1.356	0.178	0.338	-325.4	48.0	4.80	-325.4	48.0
140	028	14	4.894	0.419	1.356	0.287	0.520	-34.1	46.0	4.60	-34.1	46.0
141	028	15	4.896	0.489	1.357	0.332	0.600	37.0	44.0	4.40	37.0	44.0
142	028	16	4.904	0.560	1.347	0.389	0.744	378.9	42.0	4.20	378.9	42.0
143	028	17	4.892	0.608	1.359	0.242	0.847	454.7	40.0	4.00	454.7	40.0
144	028	18	4.894	0.840	1.356	0.154	0.813	358.9	38.0	3.80	358.9	38.0

NET	RUN	IV	JZ	LUDIR	UT	P	U	UB1	UG1	UG2	RMSB	RMSG
17	027	17	11	2	36.228	16.966	0.813	-16.5	38.5	7.31	-16.5	38.5
18	027	1	4.897	-1.31	1.508	0.060	0.649	-182.1	44.5	7.25	-182.1	44.5
19	027	2	4.900	-0.91	1.502	0.083	0.639	-260.1	41.5	7.19	-260.1	41.5
20	027	3	4.903	-0.81	1.498	0.090	0.622	-341.3	38.5	7.15	-341.3	38.5
21	027	4	4.902	-0.700	1.498	0.111	0.614	-420.9	35.5	7.07	-420.9	35.5
22	027	5	4.903	-0.590	1.504	0.127	0.568	-500.9	32.5	6.97	-500.9	32.5
23	027	6	4.899	-0.420	1.506	0.143	0.524	-584.8	29.5	6.87	-584.8	29.5
24	027	7	4.898	-0.281	1.500	0.178	0.478	-671.1	26.5	6.75	-671.1	26.5
25	027	8	4.902	-0.140	1.498	0.200	0.402	-760.9	23.5	6.63	-760.9	23.5
26	027	9	4.901	0.002	1.498	0.208	0.359	-854.1	20.5	6.50	-854.1	20.5
27	027	10	4.904	0.172	1.499	0.243	0.300	-954.8	17.5	6.37	-954.8	17.5
28	027	11	4.910	0.345	1.499	0.266	0.256	-1061.1	14.5	6.23	-1061.1	14.5
29	027	12	4.909	0.420	1.499	0.281	0.206	-1174.4	11.5	6.09	-1174.4	11.5
30	027	13	4.902	0.559	1.502	0.322	0.156	-1293.2	8.5	5.94	-1293.2	8.5
31	027	14	4.902	0.700	1.501	0.371	0.105	-1418.4	5.5	5.79	-1418.4	5.5
32	027	15	4.909	0.840	1.499	0.420	0.072	-1549.9	2.5	5.63	-1549.9	2.5
33	027	16	4.909	0.979	1.499	0.468	0.036	-1688.0	0.5	5.47	-1688.0	0.5
34	027	17	4.912	1.055	1.489	0.521	0.000	-1833.1	0.5	5.31	-1833.1	0.5

POINT	ROW	VORTICITY	VC	AREA	GAM	VORTIC
1	1	-0.489	0.489	0.00372	0.002791	0.1370
2	2	-0.489	0.489	0.00389	-0.009021	-0.3049
3	3	-0.367	0.488	0.00748	-0.046000	-5.1763
4	4	-0.200	0.484	0.005173	-0.030311	-5.8508

POINT	ROW	VORTICITY	VC	AREA	GAM	VORTIC
1	1	-0.700	0.566	0.022645	0.004116	0.1818
2	2	-0.400	0.544	0.011511	-0.000033	-0.0810
2	2	-0.350	0.563	0.011054	-0.015181	-1.3734
2	2	-0.245	0.560	0.005460	-0.000366	-1.7300
4	4	-0.175	0.558	0.005476	-0.017036	-3.1119
5	5	-0.105	0.561	0.005636	-0.016518	-3.9308
6	6	-0.035	0.563	0.005582	-0.016870	-3.0168
7	7	0.036	0.564	0.005531	-0.010706	-1.9508

POINT	ROW	VORTICITY	VC	AREA	GAM	VORTIC
1	1	-0.700	0.787	0.020032	0.005112	0.2552
2	2	-0.490	0.706	0.010008	0.006616	0.6552
3	3	-0.351	0.708	0.009899	0.003545	0.7083
4	4	-0.246	0.700	0.004708	-0.000725	-0.1515
5	5	-0.175	0.705	0.005194	-0.009116	-1.7530
5	5	-0.105	0.705	0.005556	-0.006851	-1.2330
6	6	-0.034	0.705	0.005065	-0.014917	-3.0505
7	7	0.035	0.787	0.005000	-0.010082	-3.2163
8	8	0.106	0.787	0.004808	-0.006554	-1.3408
9	9	0.175	0.708	0.004454	-0.002834	-0.6363
10	10	0.244	0.700	0.005342	-0.007722	-1.4455
11	11	0.315	0.708	0.005351	0.012635	2.3570
12	12	0.305	0.706	0.006304	0.011181	2.1000
13	13	0.456	0.706	0.006564	0.017430	3.1304
14	14	0.506	0.708	0.006443	0.030034	3.6812
15	15	0.506	0.708	0.006443	0.030034	3.6812
16	16	0.506	0.708	0.006443	0.030034	3.6812
17	17	0.506	0.708	0.006443	0.030034	3.6812

POINT	ROW	VORTICITY	VC	AREA	GAM	VORTIC
1	1	-0.700	0.641	0.019474	0.002735	0.1494
2	2	-0.490	0.640	0.009856	0.006708	0.6947
3	3	-0.350	0.637	0.009777	0.000702	0.0779
4	4	-0.246	0.633	0.004980	-0.005207	-1.0456
5	5	-0.175	0.631	0.004752	-0.007792	-1.6307
5	5	-0.104	0.636	0.004850	-0.032118	-6.6526
6	6	-0.034	0.639	0.004876	-0.000328	-0.0659
7	7	0.036	0.639	0.005148	-0.005325	-0.9653
8	8	0.106	0.639	0.005266	-0.015872	-2.9903
9	9	0.175	0.637	0.005309	-0.023436	-4.4145
10	10	0.245	0.638	0.004802	-0.010162	-2.0731
11	11	0.315	0.637	0.005385	-0.002871	-0.5345
12	12	0.384	0.636	0.005493	0.014912	2.7144
13	13	0.454	0.637	0.004835	0.014912	2.6555
14	14	0.504	0.637	0.004835	0.012886	2.6555

POINT	ROW	VORTICITY	VC	AREA	GAM	VORTIC
1	1	-0.700	0.713	0.021307	0.000824	0.0387
2	2	-0.490	0.712	0.010564	-0.000485	-0.0950
3	3	-0.350	0.712	0.010594	-0.013109	-0.0590
4	4	-0.246	0.712	0.005231	-0.016683	-1.7382
5	5	-0.175	0.			

VORTICITY AND CIRCULATION						
POINT	ROW	VC	AREA	GAM	VORTIC	
1	1	-0.700	0.489	0.00372	0.002791	0.1370
2	2	-0.400	0.488	0.00389	-0.009021	-0.3049
3	3	-0.367	0.488	0.00748	-0.046000	-5.1763
4	4	-0.200	0.484	0.005173	-0.030311	-5.8508

VORTICITY AND CIRCULATION						
POINT	ROW	VC	AREA	GAM	VORTIC	
1	1	-0.700	0.566	0.022645	0.004116	0.1818
2	2	-0.400	0.544	0.011511	-0.000033	-0.0810
2	2	-0.350	0.563	0.011054	-0.015181	-1.3734
2	2	-0.245	0.560	0.005460	-0.000366	-1.7300
4	4	-0.175	0.558	0.005476	-0.017036	-3.1119
5	5	-0.105	0.561	0.005636	-0.016518	-3.9308
6	6	-0.035	0.563	0.005582	-0.016870	-3.0168
7	7	0.036	0.564	0.005531	-0.010706	-1.9508

VORTICITY AND CIRCULATION						
POINT	ROW	VC	AREA	GAM	VORTIC	
1	1	-0.700	0.641	0.019474	0.002735	0.1494
2	2	-0.490	0.640	0.009856	0.006708	0.6947
3	3	-0.350	0.637	0.009777	0.000702	0.0779
4	4	-0.246	0.633	0.004980	-0.005207	-1.0456
5	5	-0.175	0.631	0.004752	-0.007792	-1.6307
5	5	-0.104	0.636	0.004850	-0.032118	-6.6536
6	6	-0.034	0.639	0.004876	-0.000328	-0.0659
7	7	0.036	0.639	0.005148	-0.005325	-0.9659
8	8	0.106	0.639	0.005266	-0.015872	-2.9903
9	9	0.175	0.637	0.005309	-0.023436	-4.4145
10	10	0.245	0.638	0.004802	-0.010162	-2.0731
11	11	0.315	0.637	0.005385	0.002871	0.5345
12	12	0.384	0.636	0.005493	0.014912	2.7144
13	13	0.454	0.637	0.004835	0.014912	2.6555
14	14	0.504	0.637	0.004835	0.012886	2.6555

VORTICITY AND CIRCULATION						
POINT	ROW	VC	AREA	GAM	VORTIC	
1	1	-0.700	0.787	0.020032	0.005112	0.2552
2	2	-0.490	0.706	0.010008	0.006616	0.6552
3	3	-0.351	0.708	0.009899	0.003545	0.7083
4	4	-0.246	0.700	0.004708	-0.000725	-0.1515
5	5	-0.175	0.705	0.005194	-0.009116	-1.7530
5	5	-0.105	0.705	0.005556	-0.006851	-1.2330
6	6	-0.034	0.705	0.005065	-0.014917	-3.5505
7	7	0.035	0.787	0.005000	-0.010082	-3.2163
8	8	0.106	0.787	0.004808	-0.006554	-1.3408
9	9	0.175	0.708	0.004454	-0.002834	-0.6363
10	10	0.244	0.700	0.005342	-0.007722	-1.4455
11	11	0.315	0.708	0.005351	0.012635	2.3570
12	12	0.305	0.706	0.006304	0.011181	2.1000
13	13	0.456	0.706	0.006564	0.017430	3.1304
14	14	0.506	0.708	0.006443	0.030034	3.6812
15	15	0.506	0.708	0.006443	0.017000	1.8812
16	16	0.630	0.707	0.010017	0.017000	0.3582
17	17	0.770	0.707	0.010017	0.003048	-0.3582

THIS PAGE IS BEST QUALITY PRACTICABLE
FROM COPY FURNISHED TO DDC

Table 6. Cont. ider

VORTICITY AND CIRCULATION				VORTICITY AND CIRCULATION			
POINT	ROW	VC	AREA	POINT	ROW	VC	AREA
1	6	-0.700	0.02072	1	9	-0.700	0.043573
2	6	-0.490	0.01092	2	9	-0.490	0.02800
3	6	-0.350	0.01011	3	9	-0.351	0.020121
4	6	-0.245	0.00518	4	9	-0.245	0.01156
5	6	-0.175	0.00506	5	9	-0.174	0.01130
6	6	-0.104	0.005346	6	9	-0.105	0.01095
7	6	-0.034	0.00570	7	9	-0.035	0.01009
8	6	0.035	0.00570	8	9	0.035	0.01072
9	6	0.106	0.00570	9	9	0.104	0.01065
10	6	0.175	0.005372	10	9	0.174	0.01087
11	6	0.245	0.00491	11	9	0.245	0.01082
12	6	0.316	0.005203	12	9	0.315	0.01135
13	6	0.386	0.005491	13	9	0.386	0.010638
14	6	0.456	0.005513	14	9	0.455	0.010380
15	6	0.526	0.005266	15	9	0.525	0.010384
16	6	0.596	0.005153	16	9	0.595	0.021107
17	6	0.666	0.009809	17	9	0.665	0.022298

GAM
0.00005
0.001997
-0.00003
-0.00007
-0.003481
-0.004337
-0.003845
-0.00245
-0.002483
-0.003814
0.004845
0.01591
0.019747
0.012536
0.003635
0.002969
-0.003242

VORTIC
0.0226
0.0960
-0.0489
-0.0793
-0.3128
-0.402
-0.3525
-0.4892
-0.2467
-0.3590
0.4486
1.3256
1.8562
1.2078
0.2923
0.1402
-0.1454

VORTICITY AND CIRCULATION				VORTICITY AND CIRCULATION			
POINT	ROW	VC	AREA	POINT	ROW	VC	AREA
1	9	-0.700	0.04156	1	9	-0.700	0.04156
2	9	-0.490	0.021272	2	9	-0.490	0.021272
3	9	-0.351	0.021248	3	9	-0.351	0.021248
4	9	-0.246	0.010611	4	9	-0.246	0.010611
5	9	-0.175	0.010704	5	9	-0.175	0.010704
6	9	-0.104	0.010839	6	9	-0.104	0.010839
7	9	-0.035	0.010821	7	9	-0.035	0.010821
8	9	0.035	0.010515	8	9	0.035	0.010515
9	9	0.105	0.010324	9	9	0.105	0.010324
10	9	0.175	0.010074	10	9	0.175	0.010074
11	9	0.244	0.01092	11	9	0.244	0.01092
12	9	0.315	0.010516	12	9	0.315	0.010516
13	9	0.386	0.010945	13	9	0.386	0.010945
14	9	0.455	0.010548	14	9	0.455	0.010548
15	9	0.525	0.020876	15	9	0.525	0.020876
16	9	0.595	0.021910	16	9	0.595	0.021910
17	9	0.665	0.021910	17	9	0.665	0.021910

GAM
-0.003320
-0.001921
0.000427
0.001610
-0.000317
0.001138
0.000101
0.001774
0.000313
0.011340
0.020270
0.026117
0.024302
0.027773
0.021073
0.012893
-0.001394

VORTIC
-0.0793
-0.0903
0.0201
0.1517
-0.0296
0.1050
0.0094
0.1608
0.7906
1.0965
2.0120
2.3546
2.3110
2.5376
1.8978
0.6000
-0.0636

ROW 10: ZC = 1.43
PT. VC GAM VORTIC
6 .07 .0020 .45
7 .21 .0184 .96
8 .35 .0186 1.08
9 .49 .0078 .41
STOP

Table 7. Flow Field Velocities at 37.5° Pitch Angle and X = 6.3

MPT	RUN	IY	JZ	LUDIR	UT	P	U	V	W	U _{G1}	U _{G2}	RMSB	RMSG
43	023	8	1	1	2	2.9442	0.11079	0.51	0.74	0.081	0.051	278.3	278.3
IPT	RUN	1	X	Y	Z	U	0.744	0.081	0.816	241.5	278.3	761.7	241.6
		2	6.300	-0.979	0.501	0.840	0.724	0.081	0.824	252.5	318.3	756.8	252.5
		3	6.298	-0.700	0.504	0.840	0.716	0.124	0.854	266.2	357.7	759.9	266.6
		4	6.292	-0.561	0.500	0.840	0.671	0.178	0.861	282.9	415.9	743.2	282.4
		5	6.287	-0.491	0.504	0.840	0.670	0.234	0.856	292.6	459.1	729.0	292.8
		6	6.284	-0.420	0.497	0.840	0.623	0.248	0.843	263.2	449.6	708.0	263.2
		7	6.301	-0.351	0.498	0.840	0.593	0.154	0.835	-662.6	-147.2	451.7	-662.6
		8	6.305	-0.278	0.500	0.840	0.589	0.876	0.838		6.1	459.7	
MPT	RUN	20	1	1	2	36.340	16.663	0.46	0.78	0.088	0.046	241.4	241.4
		1	X	Y	Z	U	0.748	0.088	0.814	237.1	269.9	756.1	237.3
		2	6.303	-0.841	0.597	0.840	0.726	0.100	0.827	248.3	313.4	756.1	249.1
		3	6.304	-0.700	0.598	0.840	0.716	0.169	0.836	256.3	338.0	758.1	257.0
		4	6.302	-0.561	0.599	0.840	0.705	0.198	0.849	273.8	366.3	758.1	274.0
		5	6.302	-0.491	0.599	0.840	0.693	0.121	0.838	292.1	388.6	746.1	292.2
		6	6.304	-0.351	0.597	0.840	0.666	0.148	0.891	346.7	475.8	643.0	346.7
		7	6.300	-0.280	0.597	0.840	0.776	0.177	0.905	401.1	523.5	543.8	401.1
IPT	RUN	8	X	Y	Z	U	0.868	-0.077	0.188	-518.9	-575.8	549.8	-518.9
		9	6.301	-0.140	0.600	0.840	0.911	-0.188	0.055	574.8	716.0	543.8	574.8
		10	6.302	-0.070	0.598	0.840	1.033	-0.196	0.040	722.4	868.3	591.7	722.4
		11	6.302	-0.002	0.599	0.840	1.008	-0.131	0.032	694.5	792.1	591.7	694.5
		12	6.300	0.071	0.600	0.840	1.042	-0.142	0.035	774.3	880.3	599.8	774.3
		13	6.301	0.140	0.597	0.840	1.039	-0.178	-0.045	834.1	966.4	559.8	834.1
		14	6.305	0.211	0.554	0.840	1.065	-0.137	-0.074	912.0	1012.5	561.8	912.0
		15	6.301	0.279	0.552	0.840	1.090	-0.146	-0.022	952.7	1060.4	609.9	952.7
MPT	RUN	16	X	Y	Z	U	0.958	-0.401	0.042	-622.2	-736.7	609.9	-622.2
		17	6.302	0.351	0.597	0.840	1.058	-0.401	0.042	622.2	736.7	609.9	622.2
		18	6.303	0.421	0.597	0.840	0.998	-0.441	0.042	523.5	637.5	637.5	523.5
		19	6.304	0.491	0.597	0.840	0.957	-0.190	0.042	357.5	459.1	744.1	357.5

THIS PAGE IS BEST QUALITY PRACTICABLE
FROM COPY FURNISHED TO DDG

Table 7. Continued

68	018	22	6.307	0.830	0.709	0.830	0.041	0.563	-105.9	704.0	-105.9	-75.1	-75.1
69	018	23	6.294	0.800	0.806	0.823	0.005	0.593	-46.1	720.0	-46.1	-43.1	-43.1

MPT	RUM	IV	JZ	LUDIR	UT	P	U	UB1	UG1	UG2	RMSB	RMSG
92	018	23	5	1	36.394	16.712	0.144	175.3	283.4	744.1	175.4	283.4
70	018	1	6.309	0.891	0.897	0.728	0.092	185.3	253.4	744.1	185.3	253.4
71	018	2	6.308	0.890	0.895	0.730	0.131	171.4	269.4	744.1	171.4	269.4
72	018	3	6.308	0.899	0.895	0.730	0.118	187.3	297.4	744.1	187.3	297.4
73	018	4	6.310	0.859	0.891	0.718	0.218	191.3	355.5	744.1	191.3	355.5
74	018	5	6.306	0.419	0.895	0.726	0.150	175.4	287.4	744.1	175.4	287.4
75	018	6	6.306	0.350	0.897	0.719	0.110	211.3	315.5	748.1	211.3	315.5
76	018	7	6.306	0.280	0.894	0.738	0.207	121.5	277.4	746.1	121.5	277.4
77	018	8	6.306	0.209	0.897	0.701	0.238	139.5	319.5	746.1	139.5	319.5
78	018	9	6.306	0.140	0.902	0.681	0.304	140.1	359.4	676.0	140.1	359.4
79	018	10	6.307	0.070	0.895	0.702	0.144	140.1	41.1	625.9	140.1	41.1
80	018	11	6.301	0.000	0.900	0.735	0.011	181.8	13.5	625.9	181.8	13.5
81	018	12	6.307	0.070	0.892	0.756	0.010	181.8	13.5	547.8	181.8	13.5
82	018	13	6.307	0.139	0.896	0.756	0.156	181.8	13.5	547.8	181.8	13.5
83	018	14	6.313	0.209	0.896	0.890	0.156	181.8	13.5	547.8	181.8	13.5
84	018	15	6.301	0.281	0.888	0.935	0.245	181.8	13.5	547.8	181.8	13.5
85	018	16	6.305	0.350	0.893	0.935	0.245	181.8	13.5	547.8	181.8	13.5
86	018	17	6.307	0.421	0.893	0.916	0.332	181.8	13.5	547.8	181.8	13.5
87	018	18	6.312	0.500	0.890	0.921	0.332	181.8	13.5	547.8	181.8	13.5
88	018	19	6.306	0.560	0.890	0.888	0.332	181.8	13.5	547.8	181.8	13.5
89	018	20	6.306	0.600	0.857	0.888	0.003	181.8	13.5	547.8	181.8	13.5
90	018	21	6.312	0.641	0.889	0.845	0.020	181.8	13.5	547.8	181.8	13.5
91	018	22	6.299	0.681	0.889	0.845	0.056	181.8	13.5	547.8	181.8	13.5
92	018	23		0.981	0.905	0.813	0.053	181.8	13.5	547.8	181.8	13.5

MPT	RUM	IV	JZ	LUDIR	UT	P	U	UB1	UG1	UG2	RMSB	RMSG
17	022	17	6	1	36.214	16.762	0.089	137.6	204.1	750.1	138.2	204.1
1	022	1	6.299	0.121	0.999	0.763	0.089	144.3	219.1	750.1	144.3	219.1
2	022	2	6.300	0.081	1.000	0.760	0.100	150.6	247.0	750.1	150.6	247.0
3	022	3	6.303	0.151	0.998	0.747	0.137	150.6	258.3	750.1	150.6	258.3
4	022	4	6.303	0.221	0.998	0.736	0.166	150.6	345.3	746.1	150.6	345.3
5	022	5	6.301	0.291	0.997	0.723	0.207	150.6	433.6	746.1	150.6	433.6
6	022	6	6.301	0.361	1.000	0.671	0.160	150.6	521.9	748.1	150.6	521.9
7	022	7	6.301	0.431	1.002	0.665	0.177	150.6	609.3	690.0	150.6	609.3
8	022	8	6.307	0.501	1.000	0.764	0.160	150.6	697.6	690.0	150.6	697.6
9	022	9	6.307	0.571	1.000	0.853	0.263	150.6	785.9	567.8	150.6	785.9
10	022	10	6.307	0.641	0.997	0.697	0.103	150.6	873.2	567.8	150.6	873.2
11	022	11	6.307	0.711	0.991	0.655	0.103	150.6	961.5	567.8	150.6	961.5
12	022	12	6.306	0.781	0.991	0.744	0.106	150.6	1049.8	567.8	150.6	1049.8
13	022	13	6.306	0.851	0.995	0.831	0.297	150.6	1138.1	567.8	150.6	1138.1
14	022	14	6.316	0.921	0.995	0.821	0.297	150.6	1226.4	567.8	150.6	1226.4
15	022	15	6.309	0.991	0.990	0.790	0.297	150.6	1314.7	567.8	150.6	1314.7
16	022	16	6.309	1.061	0.990	0.888	0.066	150.6	1403.0	567.8	150.6	1403.0
17	022	17			0.990	0.888	0.066	150.6	1491.3	567.8	150.6	1491.3

—

Table 7. Continued

NPT	RUN	UT	LUDIR	JZ	Y	Z	UT	P
51	021	27.283	1	7	1	1	0.02	0.5136
IPT	021	1	1.120	0.757	0.757	0.757	0.02	0.5136
35	021	1	1.120	0.757	0.757	0.757	0.02	0.5136
36	021	2	1.120	0.757	0.757	0.757	0.02	0.5136
37	021	3	1.120	0.757	0.757	0.757	0.02	0.5136
38	021	4	1.120	0.757	0.757	0.757	0.02	0.5136
39	021	5	1.120	0.757	0.757	0.757	0.02	0.5136
40	021	6	1.120	0.757	0.757	0.757	0.02	0.5136
41	021	7	1.120	0.757	0.757	0.757	0.02	0.5136
42	021	8	1.120	0.757	0.757	0.757	0.02	0.5136
43	021	9	1.120	0.757	0.757	0.757	0.02	0.5136
44	021	10	1.120	0.757	0.757	0.757	0.02	0.5136
45	021	11	1.120	0.757	0.757	0.757	0.02	0.5136
46	021	12	1.120	0.757	0.757	0.757	0.02	0.5136
47	021	13	1.120	0.757	0.757	0.757	0.02	0.5136
48	021	14	1.120	0.757	0.757	0.757	0.02	0.5136
49	021	15	1.120	0.757	0.757	0.757	0.02	0.5136
50	021	16	1.120	0.757	0.757	0.757	0.02	0.5136
51	021	17	1.120	0.757	0.757	0.757	0.02	0.5136

MPT	RUN	IY	JZ	LUDIR	UT	P
34	021	17	8	1	26.100	16.557
IPT	18	021	1	1	200	0.693
19	021	2	303	-1.120	1.200	0.722
20	021	3	302	-0.980	1.203	0.738
21	021	4	304	-0.835	1.199	0.749
22	021	5	304	-0.830	1.198	0.744
23	021	6	302	-0.851	1.198	0.734
24	021	7	302	-0.820	1.190	0.688
25	021	8	304	-0.279	1.190	0.655
26	021	9	301	-0.140	1.195	0.545
27	021	10	306	-0.000	1.192	0.709
28	021	11	306	-0.141	1.190	0.844
29	021	12	301	-0.280	1.190	0.901
30	021	13	302	-0.561	1.198	0.877
31	021	14	306	-0.760	1.200	0.847
32	021	15	306	-0.840	1.198	0.780
33	021	16	304	-0.981	1.190	0.736
34	021	17	308	-1.055	1.195	0.736
			X	Y	Z	U
			6.303	-1.120	0.722	0.693
			6.302	-0.980	0.738	0.735
			6.302	-0.835	0.749	0.755
			6.304	-0.830	0.744	0.745
			6.304	-0.820	0.734	0.775
			6.302	-0.879	0.688	0.702
			6.304	-0.800	0.655	0.815
			6.306	-0.600	0.545	0.857
			6.306	-0.411	0.709	0.902
			6.303	-0.280	0.844	0.986
			6.301	-0.191	0.901	1.024
			6.302	-0.561	0.877	1.037
			6.306	-0.760	0.847	1.037
			6.306	-0.840	0.780	1.037
			6.304	-0.981	0.736	1.037
			6.308	-1.055	0.736	1.037
			UG1	UG2	UG3	UG4
			187.7	7.6	117.6	1.1
			111.1	7.4	117.6	1.1
			202.4	7.4	117.6	1.1
			387.7	7.8	123.4	1.1
			562.7	7.9	123.4	1.1
			751.5	7.9	123.4	1.1
			935.7	7.9	123.4	1.1
			1151.5	7.9	123.4	1.1
			1335.7	7.9	123.4	1.1
			1517.5	7.9	123.4	1.1
			1692.5	7.9	123.4	1.1
			1875.7	7.9	123.4	1.1
			2057.5	7.9	123.4	1.1
			2239.7	7.9	123.4	1.1
			2421.5	7.9	123.4	1.1
			2602.5	7.9	123.4	1.1
			2784.7	7.9	123.4	1.1
			2965.5	7.9	123.4	1.1
			3147.7	7.9	123.4	1.1
			3329.5	7.9	123.4	1.1
			3511.7	7.9	123.4	1.1
			3692.5	7.9	123.4	1.1
			3874.7	7.9	123.4	1.1
			4055.5	7.9	123.4	1.1
			4237.7	7.9	123.4	1.1
			4419.5	7.9	123.4	1.1
			4601.7	7.9	123.4	1.1
			4782.5	7.9	123.4	1.1
			4964.7	7.9	123.4	1.1
			5145.5	7.9	123.4	1.1
			5327.7	7.9	123.4	1.1
			5509.5	7.9	123.4	1.1
			5691.7	7.9	123.4	1.1
			5873.5	7.9	123.4	1.1
			6055.7	7.9	123.4	1.1
			6237.5	7.9	123.4	1.1
			6419.7	7.9	123.4	1.1
			6601.5	7.9	123.4	1.1
			6783.7	7.9	123.4	1.1
			6965.5	7.9	123.4	1.1
			7147.7	7.9	123.4	1.1
			7329.5	7.9	123.4	1.1
			7511.7	7.9	123.4	1.1
			7692.5	7.9	123.4	1.1
			7874.7	7.9	123.4	1.1
			8055.5	7.9	123.4	1.1
			8237.7	7.9	123.4	1.1
			8419.5	7.9	123.4	1.1
			8601.7	7.9	123.4	1.1
			8782.5	7.9	123.4	1.1
			8964.7	7.9	123.4	1.1
			9145.5	7.9	123.4	1.1
			9327.7	7.9	123.4	1.1
			9509.5	7.9	123.4	1.1
			9691.7	7.9	123.4	1.1
			9873.5	7.9	123.4	1.1
			10055.7	7.9	123.4	1.1
			10237.5	7.9	123.4	1.1
			10419.7	7.9	123.4	1.1
			10601.5	7.9	123.4	1.1
			10783.7	7.9	123.4	1.1
			10965.5	7.9	123.4	1.1
			11147.7	7.9	123.4	1.1
			11329.5	7.9	123.4	1.1
			11511.7	7.9	123.4	1.1
			11692.5	7.9	123.4	1.1
			11874.7	7.9	123.4	1.1
			12055.5	7.9	123.4	1.1
			12237.7	7.9	123.4	1.1
			12419.5	7.9	123.4	1.1
			12601.7	7.9	123.4	1.1
			12782.5	7.9	123.4	1.1
			12964.7	7.9	123.4	1.1
			13145.5	7.9	123.4	1.1
			13327.7	7.9	123.4	1.1
			13509.5	7.9	123.4	1.1
			13691.7	7.9	123.4	1.1
			13873.5	7.9	123.4	1.1
			14055.7	7.9	123.4	1.1
			14237.5	7.9	123.4	1.1
			14419.7	7.9	123.4	1.1
			14601.5	7.9	123.4	1.1
			14783.7	7.9	123.4	1.1
			14965.5	7.9	123.4	1.1
			15147.7	7.9	123.4	1.1
			15329.5	7.9	123.4	1.1
			15511.7	7.9	123.4	1.1
			15692.5	7.9	123.4	1.1
			15874.7	7.9	123.4	1.1
			16055.5	7.9	123.4	1.1
			16237.7	7.9	123.4	1.1
			16419.5	7.9	123.4	1.1
			16601.7	7.9	123.4	1.1
			16782.5	7.9	123.4	1.1
			16964.7	7.9	123.4	1.1
			17145.5	7.9	123.4	1.1
			17327.7	7.9	123.4	1.1
			17509.5	7.9	123.4	1.1
			17691.7	7.9	123.4	1.1
			17873.5	7.9	123.4	1.1
			18055.7	7.9	123.4	1.1
			18237.5	7.9	123.4	1.1
			18419.7	7.9	123.4	1.1
			18601.5	7.9	123.4	1.1
			18783.7	7.9	123.4	1.1
			18965.5	7.9	123.4	1.1
			19147.7	7.9	123.4	1.1
			19329.5	7.9	123.4	1.1
			19511.7	7.9	123.4	1.1
			19692.5	7.9	123.4	1.1
			19874.7	7.9	123.4	1.1
			20055.5	7.9	123.4	1.1
			20237.7	7.9	123.4	1.1
			20419.5	7.9	123.4	1.1
			20601.7	7.9	123.4	1.1
			20782.5	7.9	123.4	1.1
			20964.7	7.9	123.4	1.1
			21145.5	7.9	123.4	1.1
			21327.7	7.9	123.4	1.1
			21509.5	7.9	123.4	1.1
			21691.7	7.9	123.4	1.1
			21873.5	7.9	123.4	1.1
			22055.7	7.9	123.4	1.1
			22237.5	7.9	123.4	1.1
			22419.7	7.9	123.4	1.1
			22601.5	7.9	123.4	1.1
			22783.7	7.9	123.4	1.1
			22965.5	7.9	123.4	1.1
			23147.7	7.9	123.4	1.1
			23329.5	7.9	123.4	1.1
			23511.7	7.9	123.4	1.1
			23692.5	7.9	123.4	1.1
			23874.7	7.9	123.4	1.1
			24055.5	7.9	123.4	1.1
			24237.7	7.9	123.4	1.1
			24419.5	7.9	123.4	1.1
			24601.7	7.9	123.4	1.1
			24782.5	7.9	123.4	1.1
			24964.7	7.9	123.4	1.1
			25145.5	7.9	123.4	1.1
			25327.7	7.9	123.4	1.1
			25509.5	7.9	123.4	1.1
			25691.7	7.9	123.4	1.1
			25873.5	7.9	123.4	1.1
			26055.7	7.9	123.4	1.1
			26237.5	7.9	123.4	1.1
			26419.7	7.9	123.4	1.1
			26601.5	7.9	123.4	1.1
			26783.7	7.9	123.4	1.1
			26965.5	7.9	123.4	1.1
			27147.7	7.9	123.4	1.1
			27329.5	7.9	123.4	1.1
			27511.7	7.9	123.4	1.1
			27692.5	7.9	123.4	1.1
			27874.7	7.9	123.4	1.1
			28055.5	7.9	123.4	1.1
			28237.7	7.9	123.4	1.1
			28419.5	7.9	123.4	1.1
			28601.7	7.9	123.4	1.1
			28782.5	7.9	123.4	1.1
			28964.7	7.9	123.4	1.1
			29145.5	7.9	123.4	1.1
			29327.7	7.9	123.4	1.1
			29509.5	7.9	123.4	1.1
			29691.7	7.9	123.4	1.1
			29873.5	7.9	123.4	1.1
			30055.7	7.9	123.4	1.1
			30237.5	7.9	123.4	1.1
			30419.7	7.9	123.4	1.1
			30601.5	7.9	123.4	1.1
			30783.7	7.9	123.4	1.1
			30965.5	7.9	123.4	1.1
			31147.7	7.9	123.4	1.1
			31329.5	7.9	123.4	1.1
			31511.7	7.9	123.4	1.1
			31692.5	7.9	123.4	1.1
			31874.7	7.9	123.4	1.1
			32055.5	7.9	123.4	1.1
			32237.7	7.9	123.4	1.1
			32419.5	7.9	123.4	1.1
			32601.7	7.9	123.4	1.1
			32782.5	7.9	123.4	1.1
			32964.7	7.9	123.4	1.1
			33145.5	7.9	123.4	1.1
			33327.7	7.9	123.4	1.1
			33509.5	7.9	123.4	1.1
			33691.7	7.9	123.4	1.1
			33873.5	7.9	123.4	1.1
			34055.7	7.9	123.4	1.1
			34237.5	7.9	123.4	1.1

52

WPT	RUN	IV	JZ	LUDIR	UT	P	0.12829
17	020	17	10	2	3.1500		
1	020	1	6339	1.396	0.798	0.118	
2	020	2	6300	1.398	0.790	0.135	
3	020	3	6301	1.397	0.785	0.155	
4	020	4	6300	1.397	0.780	0.184	
5	020	5	6300	1.400	0.770	0.212	
6	020	6	6300	1.398	0.761	0.239	
7	020	7	6301	1.398	0.754	0.268	
8	020	8	6301	1.394	0.745	0.297	
9	020	9	6301	1.393	0.737	0.325	
10	020	10	6302	1.393	0.729	0.354	
11	020	11	6302	1.393	0.722	0.382	
12	020	12	6302	1.393	0.715	0.410	
13	020	13	6303	1.395	0.708	0.438	
14	020	14	6303	1.397	0.701	0.466	
15	020	15	6301	1.398	0.694	0.494	
16	020	16	6301	1.398	0.687	0.522	
17	020	17	6301	1.398	0.680	0.550	

THIS PAGE IS BEST QUALITY PRACTICABLE
FROM COPY FURNISHED TO DDG

Table 7. Continued

MPT	RUN	IV	J2	LUDIR	UT	P
23	019	23	11	2	36.391	17.024
IPT	RUN	I	X	Y	Z	U
1	019	1	6.299	-0.000	1.499	0.777
2	019	2	6.299	-0.039	1.501	0.767
3	019	3	6.299	-0.079	1.502	0.755
4	019	4	6.299	-0.119	1.501	0.743
5	019	5	6.299	-0.159	1.499	0.731
6	019	6	6.299	-0.199	1.498	0.719
7	019	7	6.299	-0.239	1.498	0.707
8	019	8	6.299	-0.279	1.497	0.695
9	019	9	6.299	-0.319	1.496	0.683
10	019	10	6.299	-0.359	1.495	0.671
11	019	11	6.299	-0.399	1.494	0.659
12	019	12	6.299	-0.439	1.493	0.647
13	019	13	6.299	-0.479	1.492	0.635
14	019	14	6.299	-0.519	1.491	0.623
15	019	15	6.299	-0.559	1.490	0.611
16	019	16	6.299	-0.599	1.489	0.599
17	019	17	6.299	-0.639	1.488	0.587
18	019	18	6.299	-0.679	1.487	0.575
19	019	19	6.299	-0.719	1.486	0.563
20	019	20	6.299	-0.759	1.485	0.551
21	019	21	6.299	-0.799	1.484	0.539
22	019	22	6.299	-0.839	1.483	0.527
23	019	23	6.299	-0.879	1.482	0.515

MPT	RUN	IV	J2	LUDIR	UT	P
34	023	17	12	2	36.289	16.832
IPT	RUN	I	X	Y	Z	U
1	023	1	6.299	-1.120	1.700	0.784
2	023	2	6.299	-1.160	1.701	0.772
3	023	3	6.299	-1.200	1.702	0.760
4	023	4	6.299	-1.240	1.703	0.748
5	023	5	6.299	-1.280	1.704	0.736
6	023	6	6.299	-1.320	1.705	0.724
7	023	7	6.299	-1.360	1.706	0.712
8	023	8	6.299	-1.400	1.707	0.700
9	023	9	6.299	-1.440	1.708	0.688
10	023	10	6.299	-1.480	1.709	0.676
11	023	11	6.299	-1.520	1.710	0.664
12	023	12	6.299	-1.560	1.711	0.652
13	023	13	6.299	-1.600	1.712	0.640
14	023	14	6.299	-1.640	1.713	0.628
15	023	15	6.299	-1.680	1.714	0.616
16	023	16	6.299	-1.720	1.715	0.604
17	023	17	6.299	-1.760	1.716	0.592
18	023	18	6.299	-1.800	1.717	0.580
19	023	19	6.299	-1.840	1.718	0.568
20	023	20	6.299	-1.880	1.719	0.556
21	023	21	6.299	-1.920	1.720	0.544
22	023	22	6.299	-1.960	1.721	0.532
23	023	23	6.299	-2.000	1.722	0.520

—

54

WPT	RUN	IY	JZ	LUDIR	UT	P
08	022	17	14	1	35.594	16.193
IPT	52	1	X	Y	Z	U
53	022	2	300	1.121	001	0.010
54	022	3	301	0.817	004	0.100
55	022	4	300	0.700	002	0.116
56	022	5	301	0.520	002	0.147
57	022	6	300	0.429	001	0.155
58	022	7	300	0.279	002	0.234
59	022	8	300	0.141	001	0.269
60	022	9	300	0.090	002	0.347
61	022	10	303	0.130	003	0.452
62	022	11	300	0.280	004	0.530
63	022	12	300	0.420	004	0.637
64	022	13	300	0.560	005	0.733
65	022	14	300	0.700	004	0.808
66	022	15	300	0.841	004	0.863
67	022	16	300	0.985	002	0.894
68	022	17	302	1.055	002	0.908

Table 7. Concluded

NPT	RUN	IV	J2	LVDIR	UT	P	UG1	UG2	RMSB	RMSG
SI	022	17	15	1	2	36.493	17.02:			
IPT	RUN	1	X	Y	Z		U			
35	022	1	6.304	-1.122	2.496		0.078	7.7	28.4	32.4
36	022	2	6.304	-0.981	2.496		0.071	7.7	28.4	32.4
37	022	3	6.304	-0.841	2.496		0.085	7.7	28.4	32.4
38	022	4	6.304	-0.699	2.496		0.104	7.7	28.4	32.4
39	022	5	6.304	-0.559	2.496		0.090	7.7	28.4	32.4
40	022	6	6.304	-0.421	2.496		0.107	7.7	28.4	32.4
41	022	7	6.304	-0.280	2.496		0.123	7.7	28.4	32.4
42	022	8	6.304	-0.141	2.496		0.108	7.7	28.4	32.4
43	022	9	6.304	0.001	2.496		0.104	7.7	28.4	32.4
44	022	10	6.304	0.140	2.496		0.134	7.7	28.4	32.4
45	022	11	6.304	0.282	2.496		0.149	7.7	28.4	32.4
46	022	12	6.304	0.421	2.496		0.211	7.7	28.4	32.4
47	022	13	6.304	0.559	2.496		0.195	7.7	28.4	32.4
48	022	14	6.304	0.701	2.496		0.165	7.7	28.4	32.4
49	022	15	6.304	0.840	2.496		0.115	7.7	28.4	32.4
50	022	16	6.304	0.980	2.496		0.134	7.7	28.4	32.4
51	022	17	6.303	1.055	2.496		0.134	7.7	28.4	32.4

NPT	RUN	IV	J2	LVDIR	UT	P	UG1	UG2	RMSB	RMSG
34	022	17	15	1	2	36.173	16.724			
IPT	RUN	1	X	Y	Z		U			
18	022	1	6.304	-1.118	2.496		0.047	7.7	28.4	32.4
19	022	2	6.304	-0.982	2.496		0.054	7.7	28.4	32.4
20	022	3	6.304	-0.842	2.496		0.050	7.7	28.4	32.4
21	022	4	6.304	-0.700	2.496		0.044	7.7	28.4	32.4
22	022	5	6.304	-0.559	2.496		0.027	7.7	28.4	32.4
23	022	6	6.304	-0.418	2.496		0.024	7.7	28.4	32.4
24	022	7	6.304	-0.279	2.496		0.026	7.7	28.4	32.4
25	022	8	6.304	-0.140	2.496		0.039	7.7	28.4	32.4
26	022	9	6.304	0.000	2.496		0.071	7.7	28.4	32.4
27	022	10	6.304	0.140	2.496		0.074	7.7	28.4	32.4
28	022	11	6.304	0.279	2.496		0.086	7.7	28.4	32.4
29	022	12	6.304	0.420	2.496		0.113	7.7	28.4	32.4
30	022	13	6.304	0.559	2.496		0.113	7.7	28.4	32.4
31	022	14	6.304	0.700	2.496		0.113	7.7	28.4	32.4
32	022	15	6.304	0.839	2.496		0.113	7.7	28.4	32.4
33	022	16	6.304	0.982	2.496		0.113	7.7	28.4	32.4
34	022	17	6.306	1.055	2.496		0.113	7.7	28.4	32.4

Table 8. Vorticities and Circulations for 37.5° Pitch Angle and $X = 5.3$

VORTICITY AND CIRCULATION			
POINT	ROW	VC	AREA
1	1	-0.910	0.550
2	1	-0.770	0.551
3	1	-0.630	0.550
4	1	-0.526	0.550
5	1	-0.456	0.550
6	1	-0.385	0.548
7	1	-0.315	0.549
VORTICITY AND CIRCULATION			
POINT	ROW	VC	AREA
1	2	-0.910	0.650
2	2	-0.770	0.650
3	2	-0.630	0.651
4	2	-0.526	0.649
5	2	-0.456	0.650
6	2	-0.385	0.651
7	2	-0.315	0.650
8	2	-0.245	0.651
9	2	-0.175	0.651
10	2	-0.105	0.652
11	2	-0.035	0.652
12	2	0.035	0.652
13	2	0.105	0.651
14	2	0.175	0.650
15	2	0.245	0.651
16	2	0.315	0.650
17	2	0.385	0.649
18	2	0.456	0.650
19	2	0.526	0.651
20	2	0.630	0.651
21	2	0.770	0.650
22	2	0.910	0.650
VORTICITY AND CIRCULATION			
POINT	ROW	VC	AREA
1	3	-0.910	0.753
2	3	-0.770	0.752
3	3	-0.630	0.750
4	3	-0.526	0.748
5	3	-0.456	0.748
6	3	-0.385	0.748
7	3	-0.315	0.748
8	3	-0.245	0.750
9	3	-0.175	0.750
10	3	-0.105	0.750
11	3	-0.035	0.750
12	3	0.035	0.749
13	3	0.105	0.749
14	3	0.175	0.751
15	3	0.245	0.751
16	3	0.315	0.750
17	3	0.385	0.751
18	3	0.456	0.751
19	3	0.526	0.751
20	3	0.630	0.748
21	3	0.770	0.749
22	3	0.910	0.749
VORTICITY AND CIRCULATION			
POINT	ROW	VC	AREA
1	4	-0.910	0.848
2	4	-0.770	0.848
3	4	-0.630	0.846
4	4	-0.526	0.845
5	4	-0.456	0.845
6	4	-0.385	0.846
7	4	-0.315	0.847
8	4	-0.245	0.848
9	4	-0.175	0.848
10	4	-0.105	0.847
11	4	-0.035	0.847
12	4	0.035	0.846
13	4	0.104	0.845
14	4	0.174	0.845
15	4	0.245	0.848
16	4	0.315	0.849
17	4	0.385	0.847
18	4	0.456	0.845
19	4	0.526	0.846
20	4	0.630	0.847
21	4	0.770	0.843
22	4	0.910	0.847
VORTICITY AND CIRCULATION			
POINT	ROW	VC	AREA
1	5	-0.910	0.948
2	5	-0.770	0.948
3	5	-0.630	0.946
4	5	-0.526	0.945
5	5	-0.456	0.945
6	5	-0.385	0.946
7	5	-0.315	0.947
8	5	-0.245	0.948
9	5	-0.175	0.948
10	5	-0.105	0.947
11	5	-0.035	0.947
12	5	0.035	0.946
13	5	0.105	0.945
14	5	0.175	0.945
15	5	0.245	0.948
16	5	0.315	0.949
17	5	0.385	0.947
18	5	0.456	0.945
19	5	0.526	0.946
20	5	0.630	0.947
21	5	0.770	0.943
22	5	0.910	0.947
VORTICITY AND CIRCULATION			
POINT	ROW	VC	AREA
1	6	-0.910	1.048
2	6	-0.770	1.048
3	6	-0.630	1.046
4	6	-0.526	1.045
5	6	-0.456	1.045
6	6	-0.385	1.046
7	6	-0.315	1.047
8	6	-0.245	1.048
9	6	-0.175	1.048
10	6	-0.105	1.047
11	6	-0.035	1.047
12	6	0.035	1.046
13	6	0.105	1.045
14	6	0.175	1.045
15	6	0.245	1.048
16	6	0.315	1.049
17	6	0.385	1.047
18	6	0.456	1.045
19	6	0.526	1.046
20	6	0.630	1.047
21	6	0.770	1.043
22	6	0.910	1.047
VORTICITY AND CIRCULATION			
POINT	ROW	VC	AREA
1	7	-0.910	1.148
2	7	-0.770	1.148
3	7	-0.630	1.146
4	7	-0.526	1.145
5	7	-0.456	1.145
6	7	-0.385	1.146
7	7	-0.315	1.147
8	7	-0.245	1.148
9	7	-0.175	1.148
10	7	-0.105	1.147
11	7	-0.035	1.147
12	7	0.035	1.146
13	7	0.105	1.145
14	7	0.175	1.145
15	7	0.245	1.148
16	7	0.315	1.149
17	7	0.385	1.147
18	7	0.456	1.145
19	7	0.526	1.146
20	7	0.630	1.147
21	7	0.770	1.143
22	7	0.910	1.147
VORTICITY AND CIRCULATION			
POINT	ROW	VC	AREA
1	8	-0.910	1.248
2	8	-0.770	1.248
3	8	-0.630	1.246
4	8	-0.526	1.245
5	8	-0.456	1.245
6	8	-0.385	1.246
7	8	-0.315	1.247
8	8	-0.245	1.248
9	8	-0.175	1.248
10	8	-0.105	1.247
11	8	-0.035	1.247
12	8	0.035	1.246
13	8	0.105	1.245
14	8	0.175	1.245
15	8	0.245	1.248
16	8	0.315	1.249
17	8	0.385	1.247
18	8	0.456	1.245
19	8	0.526	1.246
20	8	0.630	1.247
21	8	0.770	1.243
22	8	0.910	1.247
VORTICITY AND CIRCULATION			
POINT	ROW	VC	AREA
1	9	-0.910	1.348
2	9	-0.770	1.348
3	9	-0.630	1.346
4	9	-0.526	1.345
5	9	-0.456	1.345
6	9	-0.385	1.346
7	9	-0.315	1.347
8	9	-0.245	1.348
9	9	-0.175	1.348
10	9	-0.105	1.347
11	9	-0.035	1.347
12	9	0.035	1.346
13	9	0.105	1.345
14	9	0.175	1.345
15	9	0.245	1.348
16	9	0.315	1.349
17	9	0.385	1.347
18	9	0.456	1.345
19	9	0.526	1.346
20	9	0.630	1.347
21	9	0.770	1.343
22	9	0.910	1.347
VORTICITY AND CIRCULATION			
POINT	ROW	VC	AREA
1	10	-0.910	1.448
2	10	-0.770	1.448
3	10	-0.630	1.446
4	10	-0.526	1.445
5	10	-0.456	1.445
6	10	-0.385	1.446
7	10	-0.315	1.447
8	10	-0.245	1.448
9	10	-0.175	1.448
10	10	-0.105	1.447
11	10	-0.035	1.447
12	10	0.035	1.446
13	10	0.105	1.445
14	10	0.175	1.445
15	10	0.245	1.448
16	10	0.315	1.449
17	10	0.385	1.447
18	10	0.456	1.445
19	10	0.526	1.446
20	10	0.630	1.447
21	10	0.770	1.443
22	10	0.910	1.447
VORTICITY AND CIRCULATION			
POINT	ROW	VC	AREA
1	11	-0.910	1.548
2	11	-0.770	1.548
3	11	-0.630	1.546
4	11	-0.526	1.545
5	11	-0.456	1.545
6	11	-0.385	1.546
7	11	-0.315	1.547
8	11	-0.245	1.548
9	11	-0.175	1.548
10	11	-0.105	1.547
11	11	-0.035	1.547
12	11	0.035	1.546
13	11	0.105	1.545
14	11	0.175	1.545
15	11	0.245	1.548
16	11	0.315	1.549
17	11	0.385	1.547
18	11	0.456	1.545
19	11	0.526	1.546
20	11	0.630	1.547
21	11	0.770	1.543
22	11	0.910	1.547
VORTICITY AND CIRCULATION			
POINT	ROW	VC	AREA
1	12	-0.910	1.648
2	12	-0.770	1.648
3	12	-0.630	1.646
4	12	-0.526	1.645
5	12	-0.456	1.645
6	12	-0.385	1.646
7	12	-0.315	1.647
8	12	-0.245	1.648
9	12	-0.175	1.648
10	12	-0.105	1.647
11	12	-0.035	1.647
12	12	0.035	1.646
13	12	0.105	1.645
14	12	0.175	1.645
15	12	0.245	1.648
16	12	0.315	1.649
17	12	0.385	1.647
18	12	0.456	1.645
19	12	0.526	1.646
20	12	0.630	1.647
21	12	0.770	1.643
22	12	0.910	1.647
VORTICITY AND CIRCULATION			
POINT	ROW	VC	AREA
1	13	-0.910	1.748
2	13	-0.770	1.748
3	13	-0.630	1.746
4	13	-0.526	1.745
5	13	-0.456	1.745
6	13	-0.385	1.746
7	13	-0.315	1.747
8	13	-0.245	1.748
9	13	-0.175	1.748
10	13	-0.105	1.747
11	13	-0.035	1.747
12	13	0.035	1.746
13	13	0.105	1.745
14	13	0.175	1.745
15	13	0.245	1.748
16	13	0.315	1.749
17	13	0.385	1.747
18	13	0.456	1.745
19	13	0.526	1.746
20	13	0.630	1.747
21	13	0.770	1.743
22	13	0.910	1.747
VORTICITY AND CIRCULATION			
POINT	ROW	VC	AREA
1	14	-0.910	1.848
2	14	-0.770	1.848
3	14	-0.630	1.846
4	14	-0.526	1.845
5	14	-0.456	1.845
6	14	-0.385	1.846
7	14	-0.315	1.847
8	14	-0.245	1.848
9	14	-0.175	1.848
10	14	-0.105	1.847
11	14	-0.035	1.847
12	14	0.035	1.846
13	14	0.105	1.845
14	14	0.175	1.845
15	14	0.245	1.848
16	14		

Table 8. Continued

ROW 5: ZC = .95				
PT.	YC	GAM	VORTIC	
4	-35	-0.021	-0.1	
5	-21	+0.036	+0.3	
6	-07	-0.050	-0.4	
7	+07	-0.137	-1.0	
8	+21	-0.211	-1.6	
9	+35	-0.222	-1.6	
10	+49	-0.14	-1.0	

ROW 5: ZC = .95				
PT.	YC	GAM	VORTIC	
1	0.051	0.013972	0.000373	0.0267
2	0.091	0.013953	0.001151	0.0843
3	0.077	0.013980	0.001139	0.1255
4	0.030	0.013906	0.001169	0.0873
5	0.490	0.013517	0.003730	0.2752
6	0.351	0.014168	0.003593	0.2472
7	0.210	0.014215	0.013554	0.9684
8	0.070	0.013256	0.020722	1.5655
9	0.070	0.014238	0.020095	1.9670
10	0.210	0.014374	0.018781	1.3066
11	0.351	0.014202	0.006383	0.4455
12	0.491	0.014771	0.009585	0.6489
13	0.630	0.015516	0.025283	1.6927
14	0.771	0.014789	0.017214	1.1640
15	0.910	0.014511	0.006514	0.5935
16	1.018	0.007863	0.000617	0.0785

ROW 5: ZC = .95				
PT.	YC	GAM	VORTIC	
1	0.050	0.013974	0.00269	0.0195
2	0.090	0.013947	0.00518	0.0374
3	0.070	0.013995	0.00056	0.0040
4	0.030	0.013732	0.001093	0.0786
5	0.490	0.013691	0.000579	0.0423
6	0.350	0.013909	0.00425	0.6587
7	0.210	0.014449	0.015745	1.0897
8	0.070	0.014319	0.018521	1.3633
9	0.070	0.013789	0.046879	3.3988
10	0.210	0.013555	0.046302	3.4134
11	0.350	0.013991	0.022719	1.6238
12	0.491	0.014133	0.000487	0.0345
13	0.630	0.013616	0.001919	0.1409
14	0.770	0.013247	0.007857	0.5895
15	0.911	0.013578	0.008215	0.6540
16	1.018	0.007857	0.004125	0.05251

ROW 10: ZC = 1.45				
PT.	YC	GAM	VORTIC	
7	-21	.0052	.32	
8	-07	-0.159	-1.12	
9	.07	-0.144	-1.01	
10	.21	-0.026	-.19	
11	.35	-0.036	-.26	
12	.49	+0.030	+.22	
13	.63	+0.128	.90	
14	.77	-0.009	-.07	
15	.91	-.014	-1.0	

ROW 10: ZC = 1.45				
PT.	YC	GAM	VORTIC	
1	0.050	0.013920	0.00616	0.0452
2	0.090	0.013841	0.00251	0.0184
3	0.070	0.013777	0.00319	0.0232
4	0.030	0.014357	0.001332	0.0927
5	0.490	0.014110	0.00451	0.1828
6	0.350	0.013531	0.00546	0.5745
7	0.210	0.013161	0.01385	0.7899
8	0.070	0.013276	0.015865	1.1339
9	0.070	0.013958	0.011464	0.8266
10	0.210	0.013237	0.00463	0.3372
11	0.350	0.013394	0.001512	0.1137
12	0.490	0.013574	0.00343	0.2463
13	0.630	0.014657	0.000658	0.1800
14	0.770	0.013951	0.024303	1.7348
15	0.911	0.013951	0.00378	1.3147
16	1.018	0.007133		

ROW 10: ZC = 1.45				
PT.	YC	GAM	VORTIC	
1	0.050	0.014295	0.000343	0.0240
2	0.090	0.014548	0.000281	0.0192
3	0.070	0.014580	0.001278	0.0876
4	0.030	0.014319	0.001560	0.1090
5	0.490	0.014543	0.002571	0.1768
6	0.350	0.014125	0.002531	0.1792
7	0.210	0.013681	0.002241	0.6024
8	0.070	0.014506	0.023805	1.6534
9	0.070	0.014300	0.034011	2.3652
10	0.210	0.014289	0.028642	2.0059
11	0.351	0.014837	0.028537	1.9234
12	0.491	0.014289	0.018735	1.3112
13	0.630	0.014122	0.008389	0.5940
14	0.771	0.013925	0.000899	0.0646
15	0.911	0.014380	0.002087	0.1451
16	1.018	0.007693	0.000384	0.0500

Table 8. Concluded

ROW 11: ZC = 1.60			
PT.	YC	GAM	VORTIC
9	.07	.0067	.24
10	.21	.004	.14
11	.35	.0080	.29
12	.49	.0039	.14
13	.63	.0109	.39
14	.77	.0242	.85
15	.91	.0269	.96

VORTICITY AND CIRCULATION			
POINT ROW	YC	GAM	VORTIC
1	1.749	0.013417	0.00487
2	1.748	0.012859	0.00386
3	1.748	0.013211	-0.00837
4	1.748	0.014130	-0.001261
5	1.748	0.013745	-0.002724
6	1.748	0.014130	-0.006768
7	1.749	0.013859	-0.002884
8	1.748	0.013782	-0.015513
9	1.750	0.013586	-0.016719
10	1.751	0.013786	0.006082
11	1.750	0.013763	0.019209
12	1.749	0.014332	0.020134
13	1.748	0.013776	0.017082
14	1.748	0.013404	0.011106
15	1.747	0.013914	-0.004266
16	1.745	0.007665	-0.006693

VORTICITY AND CIRCULATION			
POINT ROW	YC	GAM	VORTIC
1	1.050	0.00487	0.0363
2	0.910	0.00386	0.0259
3	0.771	-0.00837	-0.0634
4	0.630	-0.001261	-0.0893
5	0.490	-0.002724	-0.1982
6	0.350	-0.006768	-0.0543
7	0.210	-0.002884	-0.2080
8	0.070	-0.015513	-1.1256
9	0.000	-0.016719	-1.2306
10	0.000	0.006082	0.4416
11	0.350	0.019209	1.4019
12	0.491	0.020134	1.4048
13	0.631	0.017082	1.2408
14	0.770	0.011106	0.8235
15	0.909	-0.004266	-0.3066
16	1.017	-0.006693	-0.0731

VORTICITY AND CIRCULATION			
POINT ROW	YC	GAM	VORTIC
1	1.900	0.028562	-0.04052
2	1.898	0.028030	-0.00058
3	1.895	0.028940	-0.001058
4	1.890	0.028508	0.001189
5	1.889	0.028222	-0.001672
6	1.900	0.028081	0.003094
7	1.900	0.028081	0.1072
8	1.899	0.028022	0.003530
9	1.901	0.028158	0.020478
10	1.902	0.028507	0.12157
11	1.901	0.028697	0.018351
12	1.902	0.028216	0.023831
13	1.901	0.028394	0.033281
14	1.901	0.029107	0.040314
15	1.901	0.028940	0.023067
16	1.899	0.015621	0.012330

VORTICITY AND CIRCULATION			
POINT ROW	YC	GAM	VORTIC
1	1.050	0.00487	0.0363
2	0.910	0.00386	0.0259
3	0.770	-0.00837	-0.0634
4	0.630	-0.001261	-0.0893
5	0.491	-0.002724	-0.1982
6	0.351	-0.006768	-0.0543
7	0.210	-0.002884	-0.2080
8	0.070	-0.015513	-1.1256
9	0.000	-0.016719	-1.2306
10	0.000	0.006082	0.4416
11	0.350	0.019209	1.4019
12	0.491	0.020134	1.4048
13	0.631	0.017082	1.2408
14	0.770	0.011106	0.8235
15	0.909	-0.004266	-0.3066
16	1.017	-0.006693	-0.0731

VORTICITY AND CIRCULATION			
POINT ROW	YC	GAM	VORTIC
1	1.051	0.00487	0.0363
2	0.911	0.00386	0.0259
3	0.771	-0.00837	-0.0634
4	0.629	-0.001261	-0.0893
5	0.489	-0.002724	-0.1982
6	0.349	-0.006768	-0.0543
7	0.210	-0.002884	-0.2080
8	0.071	-0.015513	-1.1256
9	0.070	-0.016719	-1.2306
10	0.210	0.006082	0.4416
11	0.350	0.019209	1.4019
12	0.490	0.020134	1.4048
13	0.630	0.017082	1.2408
14	0.770	0.011106	0.8235
15	0.910	-0.004266	-0.3066
16	1.018	-0.006693	-0.0731

VORTICITY AND CIRCULATION			
POINT ROW	YC	GAM	VORTIC
1	1.051	0.00487	0.0363
2	0.911	0.00386	0.0259
3	0.771	-0.00837	-0.0634
4	0.629	-0.001261	-0.0893
5	0.489	-0.002724	-0.1982
6	0.349	-0.006768	-0.0543
7	0.210	-0.002884	-0.2080
8	0.071	-0.015513	-1.1256
9	0.070	-0.016719	-1.2306
10	0.210	0.006082	0.4416
11	0.350	0.019209	1.4019
12	0.490	0.020134	1.4048
13	0.630	0.017082	1.2408
14	0.770	0.011106	0.8235
15	0.910	-0.004266	-0.3066
16	1.018	-0.006693	-0.0731

VORTICITY AND CIRCULATION			
POINT ROW	YC	GAM	VORTIC
1	1.051	0.00487	0.0363
2	0.911	0.00386	0.0259
3	0.771	-0.00837	-0.0634
4	0.629	-0.001261	-0.0893
5	0.489	-0.002724	-0.1982
6	0.349	-0.006768	-0.0543
7	0.210	-0.002884	-0.2080
8	0.071	-0.015513	-1.1256
9	0.070	-0.016719	-1.2306
10	0.210	0.006082	0.4416
11	0.350	0.019209	1.4019
12	0.490	0.020134	1.4048
13	0.630	0.017082	1.2408
14	0.770	0.011106	0.8235
15	0.910	-0.004266	-0.3066
16	1.018	-0.006693	-0.0731

VORTICITY AND CIRCULATION			
POINT ROW	YC	GAM	VORTIC
1	1.051	0.00487	0.0363
2	0.911	0.00386	0.0259
3	0.771	-0.00837	-0.0634
4	0.629	-0.001261	-0.0893
5	0.489	-0.002724	-0.1982
6	0.349	-0.006768	-0.0543
7	0.210	-0.002884	-0.2080
8	0.071	-0.015513	-1.1256
9	0.070	-0.016719	-1.2306
10	0.210	0.006082	0.4416
11	0.350	0.019209	1.4019
12	0.490	0.020134	1.4048
13	0.630	0.017082	1.2408
14	0.770	0.011106	0.8235
15	0.910	-0.004266	-0.3066
16	1.018	-0.006693	-0.0731

VORTICITY AND CIRCULATION			
POINT ROW	YC	GAM	VORTIC
1	1.051	0.00487	0.0363
2	0.911	0.00386	0.0259
3	0.771	-0.00837	-0.0634
4	0.629	-0.001261	-0.0893
5	0.489	-0.002724	-0.1982
6	0.349	-0.006768	-0.0543
7	0.210	-0.002884	-0.2080
8	0.071	-0.015513	-1.1256
9	0.070	-0.016719	-1.2306
10	0.210	0.006082	0.4416
11	0.350	0.019209	1.4019
12	0.490	0.020134	1.4048
13	0.630	0.017082	1.2408
14	0.770	0.011106	0.8235
15	0.910	-0.004266	-0.3066
16	1.018	-0.006693	-0.0731

VORTICITY AND CIRCULATION			
POINT ROW	YC	GAM	VORTIC
1	1.051	0.00487	0.0363
2	0.911	0.00386	0.0259
3	0.771	-0.00837	-0.0634
4	0.629	-0.001261	-0.0893
5	0.489	-0.002724	-0.1982
6	0.349	-0.006768	-0.0543
7	0.210	-0.002884	-0.2080
8	0.071	-0.015513	-1.1256
9	0.070	-0.016719	-1.2306
10	0.210	0.006082	0.4416
11	0.350	0.019209	1.4019
12	0.490	0.020134	1.4048
13	0.630	0.017082	1.2408
14	0.770	0.011106	0.8235
15	0.910	-0.004266	-0.3066
16	1.018	-0.006693	-0.0731

VORTICITY AND CIRCULATION			
POINT ROW	YC	GAM	VORTIC
1	1.051	0.00487	0.0363
2	0.911	0.00386	0.0259
3	0.771	-0.00837	-0.0634
4	0.629	-0.001261	-0.0893
5	0.489	-0.002724	-0.1982
6	0.349	-0.006768	-0.0543
7	0.210	-0.002884	-0.2080
8	0.071	-0.015513	-1.1256
9	0.070	-0.016719	-1.2306
10	0.210	0.006082	0.4416
11	0.350	0.019209	1.4019
12	0.490	0.020134	1.4048
13	0.630	0.017082	1.2408
14	0.770	0.011106	0.8235
15	0.910	-0.004266	-0.3066
16	1.018	-0.006693	-0.0731

VORTICITY AND CIRCULATION			
POINT ROW	YC	GAM	VORTIC
1	1.051	0.00487	0.0363
2	0.911	0.00386	0.0259
3	0.771	-0.00837	-0.0634
4	0.629	-0.001261	-0.0893
5	0.489	-0.002724	-0.1982
6	0.349	-0.006768	-0.0543
7	0.210	-0.002884	-0.2080
8	0.071	-0.015513	-1.1256
9	0.070	-0.016719	-1.2306
10	0.210	0.006082	0.4416
11	0.350	0.019209	1.4019
12	0.490	0.020134	1.4048
13	0.630	0.017082	1.2408
14	0.770	0.011106	0.8235
15	0.910	-0.004266	-0.3066
16	1.018	-0.006693	-0.0731

VORTICITY AND CIRCULATION			
POINT ROW	YC	GAM	VORTIC
1	1.051	0.00487	0.0363
2	0.911	0.00386	0.0259
3	0.771	-0.00837	-0.0634
4	0.629	-0.001261	-0.0893
5	0.489	-0.002724	-0.1982
6	0.349	-0.006768	-0.0543
7	0.210	-0.002884	-0.2080
8	0.071	-0.015513	-1.1256
9	0.070	-0.016719	-1.2306
10	0.210	0.006082	0.4416
11	0.350	0.019209	1.4019
12	0.490	0.020134	1.4048
13	0.630	0.017082	1.2408
14	0.770	0.011106	0.8235
15	0.910	-0.004266	-0.3066
16	1.018	-0.006693	-0.0731

VORTICITY AND CIRCULATION			
POINT ROW	YC	GAM	VORTIC
1	1.051	0.00487	0.0363
2	0.911	0.00386	0.0259
3	0.771	-0.00837	-0.0634
4	0.629	-0.001261	-0.0893
5	0.489	-0.002724	-0.1982
6	0.349	-0.006768	-0.0543
7	0.210	-0.002884	-0.2080
8	0.071	-0.015513	-1.1256
9	0.070	-0.016719	-1.2306
10	0.210	0.006082	0.4416
11	0.350	0.019209	1.4019
12	0.490	0.020134	1.4048
13	0.630	0.017082	1.2408
14	0.770	0.011106	0.8235
15	0.910	-0.004266	-0.3066
16	1.018	-0.006693	-0.0731

VORTICITY AND CIRCULATION			
POINT ROW	YC	GAM	VORTIC
1	1.051	0.00487	0.0363
2	0.911	0.00386	0.0259
3	0.771	-0.00837	-0.0634
4	0.629	-0.001261	-0.0893
5	0.4		

Table 9. Summary of Vortex Data

α X	22.5	37.5		
	6.3	2.8	4.9	6.3
First vortex originating from -Y side:				
ZC from velocity vectors	0.572	----	0.687	----
YC from velocity vectors	-0.107	----	-0.010	----
ZC using vorticity values	----	0.61	----	0.99
YC using vorticity values	----	-0.17	----	0.28
Γ on -Y side of $\Omega = 0$	-0.356	-0.151	-0.604	----
Γ inside $\Omega = -1$ contour	-0.28	----	-0.35	-0.41
Γ inside $\Omega = -0.5$ contour	----	-0.169	----	----
First vortex originating from +Y side:				
ZC from velocity vectors	0.677	0.680	----	----
YC from velocity vectors	0.171	0.216	----	----
ZC using vorticity values	----	----	1.05	2.20
YC using vorticity values	----	----	0.35	1.15
Γ on +Y side of $\Omega = 0$	0.339	0.291	0.53	----
Γ inside $\Omega = +1$ contour	0.298	----	----	----
Γ inside $\Omega = +0.5$ contour	----	0.306	0.44	----
Γ inside $\Omega = +0.2$ contour	----	----	----	0.51

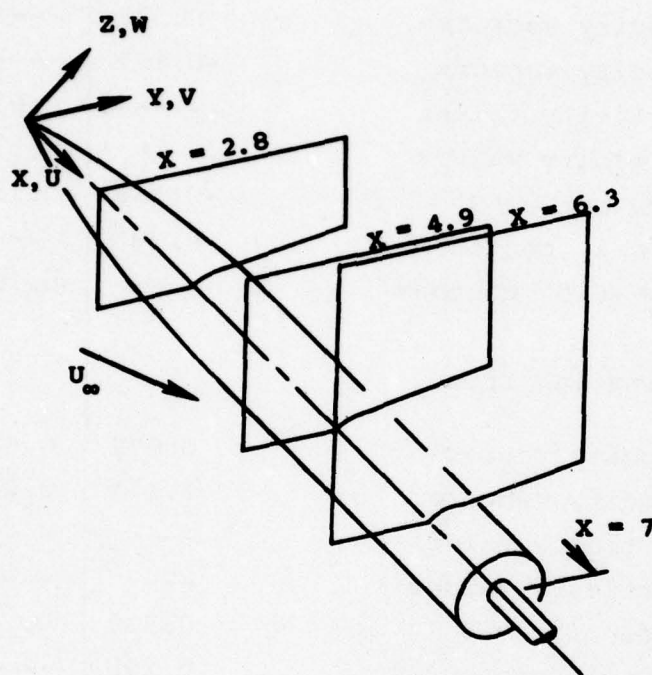


Figure 1.- Test model, coordinate system, and measurement planes.

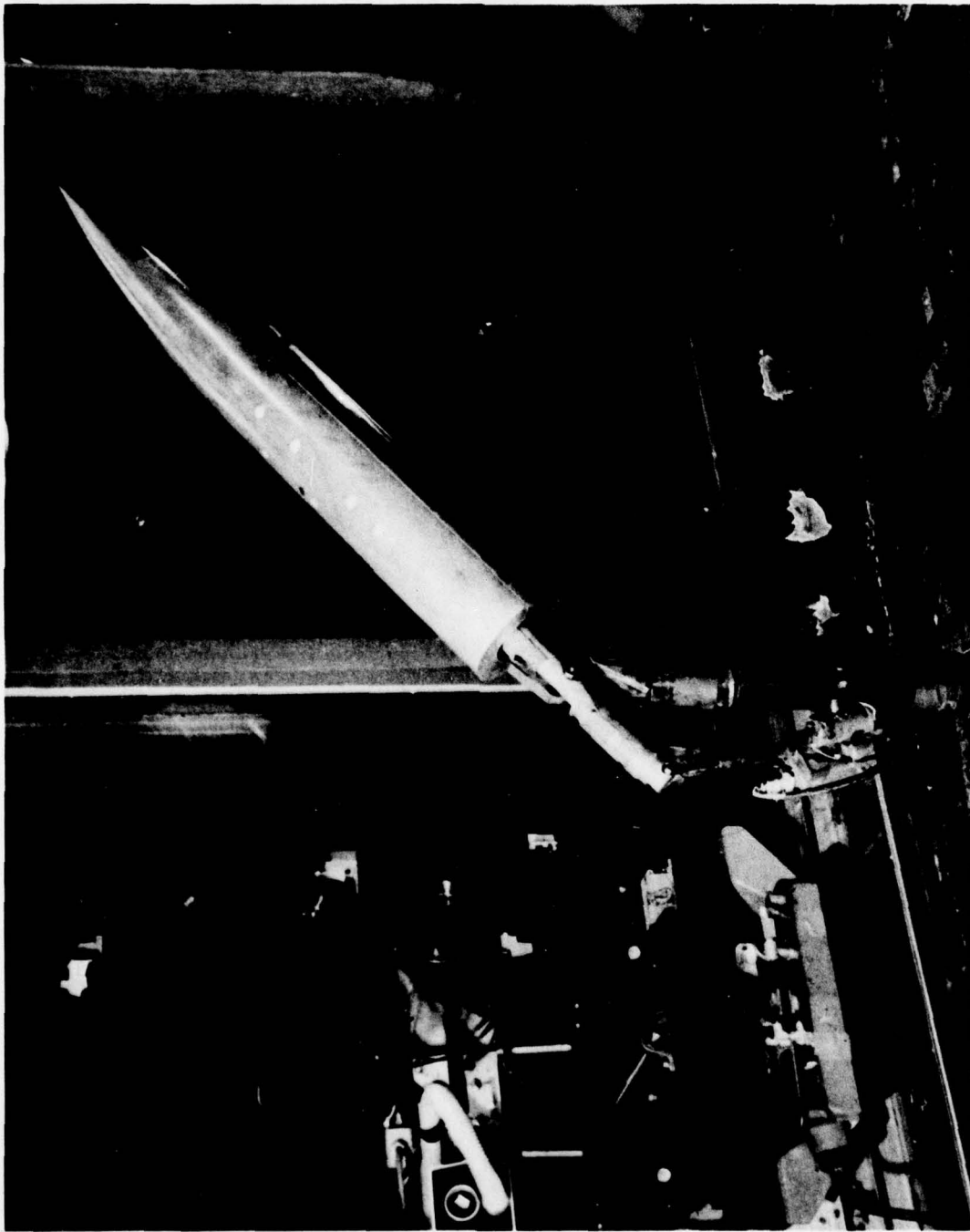


Figure 2.- Model mounted in the wind tunnel. Laser velocimeter system is seen through the window.

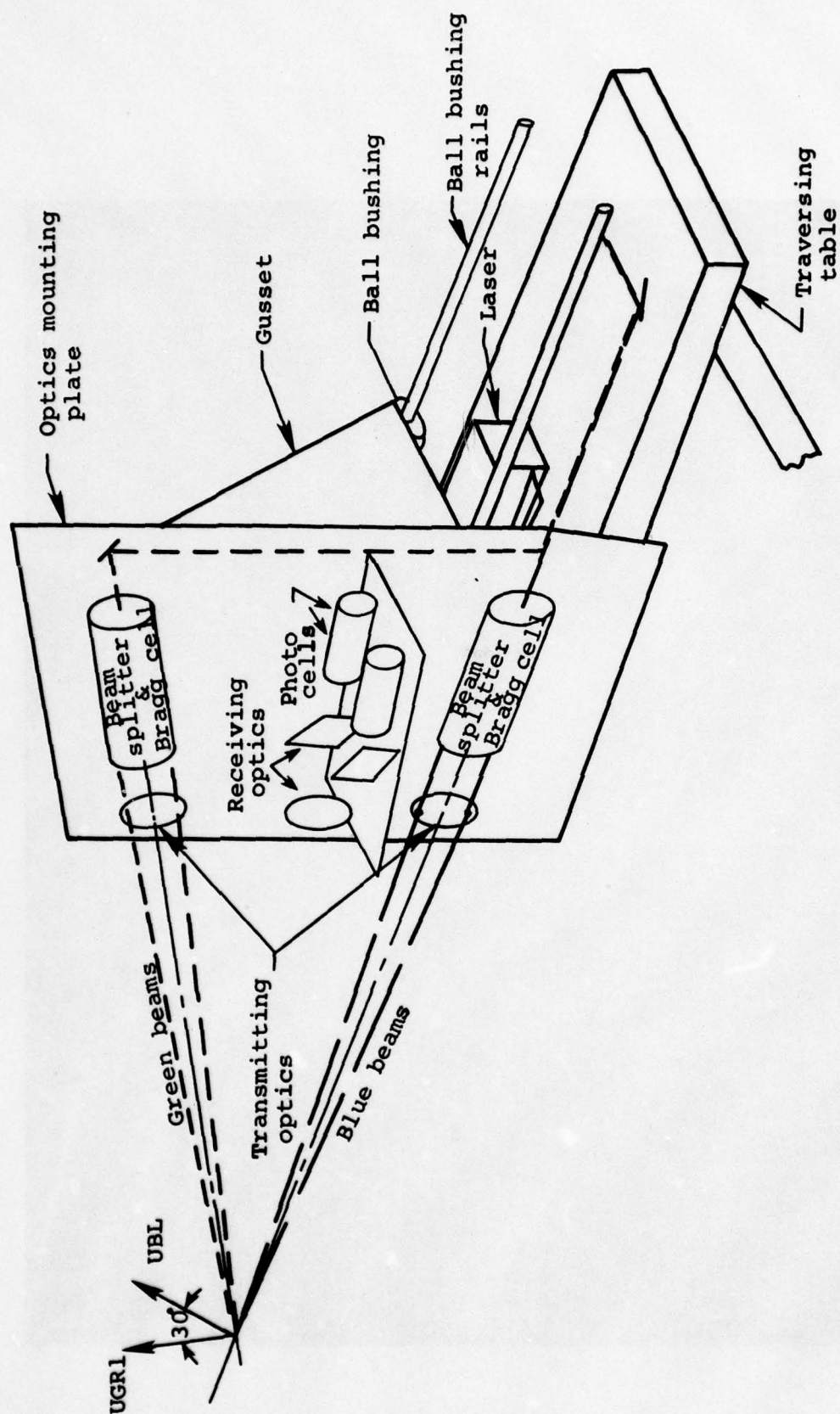


Figure 3.- Crossflow laser velocimeter.

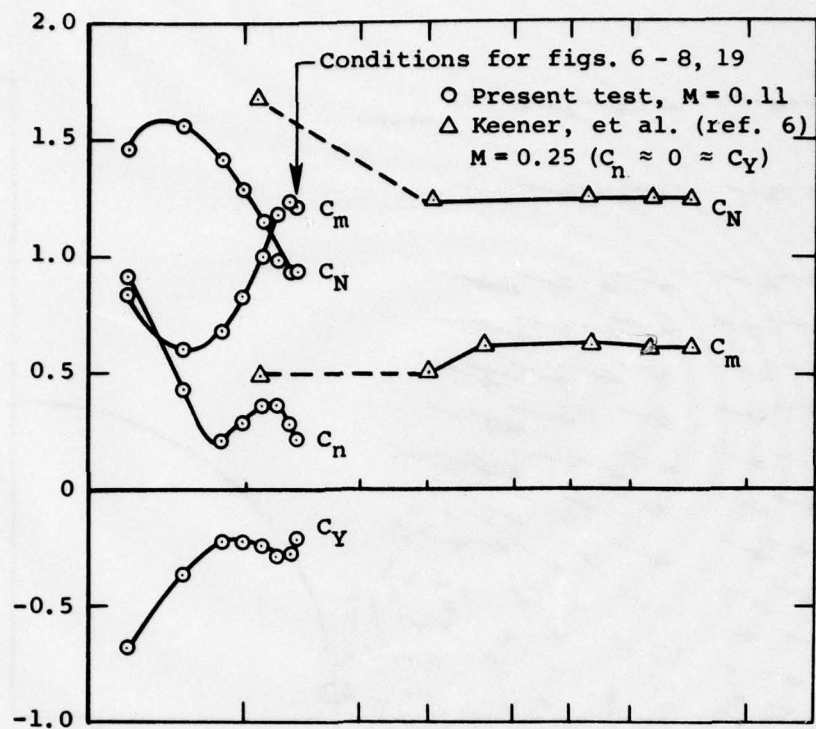


Figure 4.- Effect of crossflow Reynolds number on body forces and moments for 22.5° pitch angle.

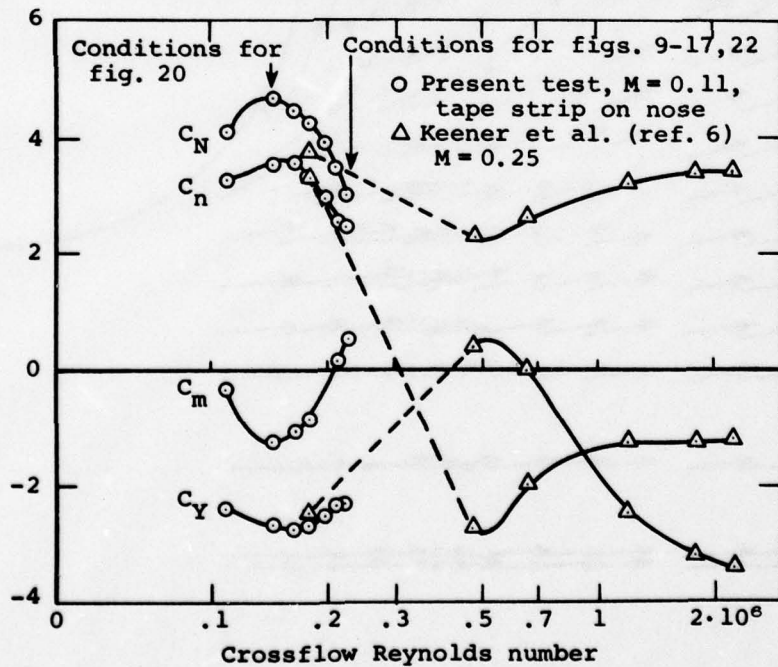


Figure 5.- Effect of crossflow Reynolds number on body forces and moments for 37.5° pitch angle.

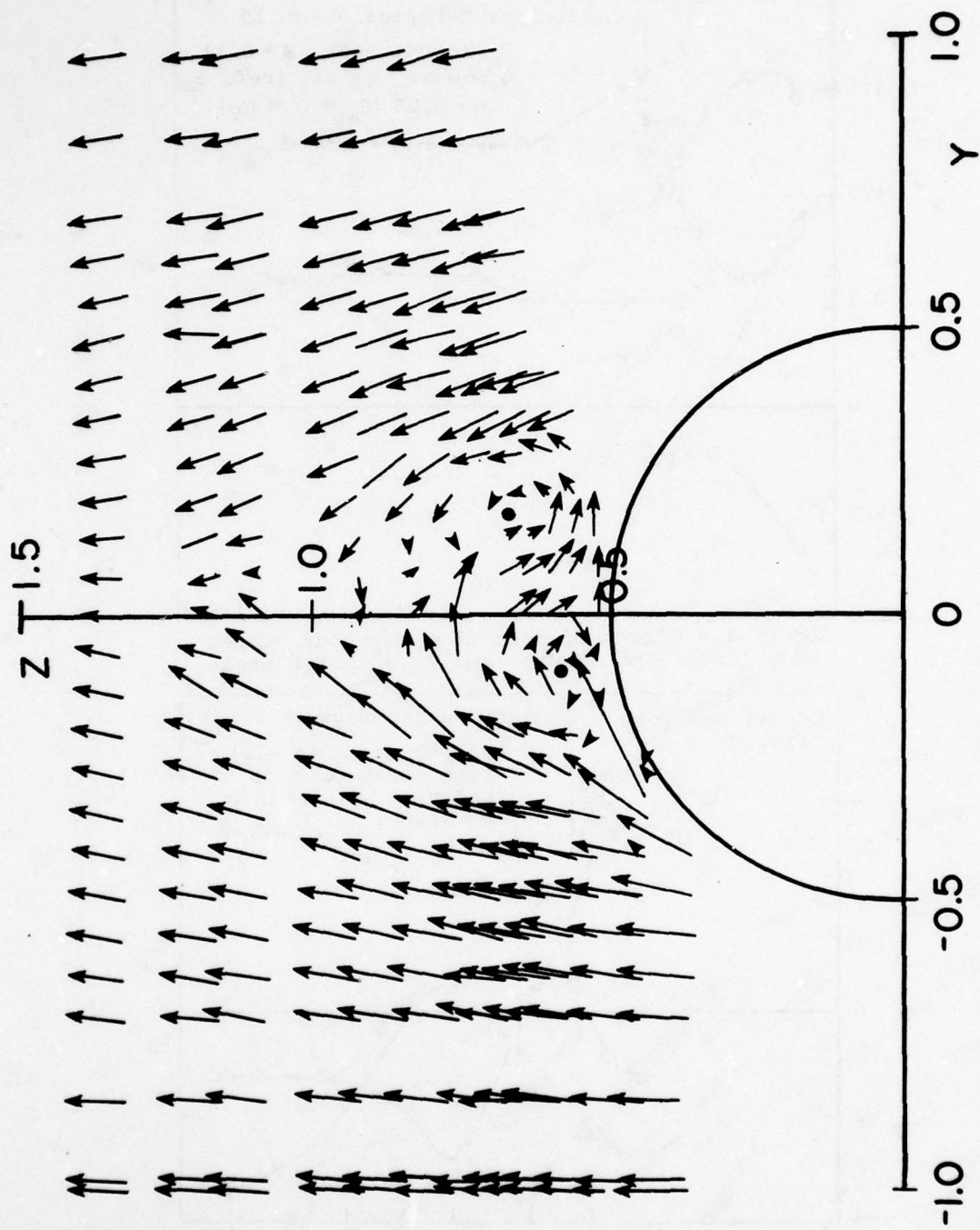


Figure 6.- Crossflow vectors at $X = 6.3$, for $\alpha = 22.5^\circ$.

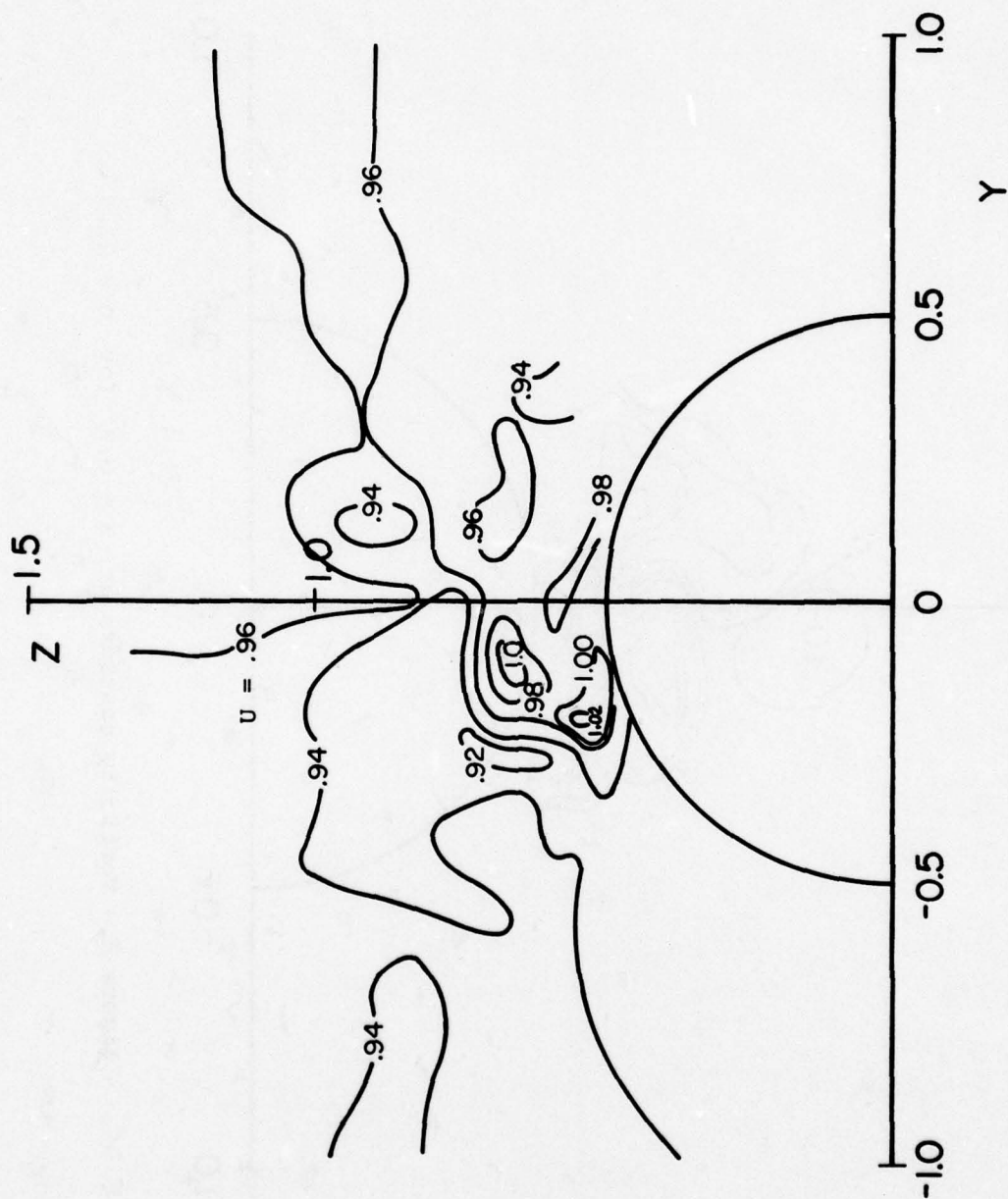


Figure 7.- Axial velocity contours at $X = 6.3$ for $\alpha = 22.5^\circ$.

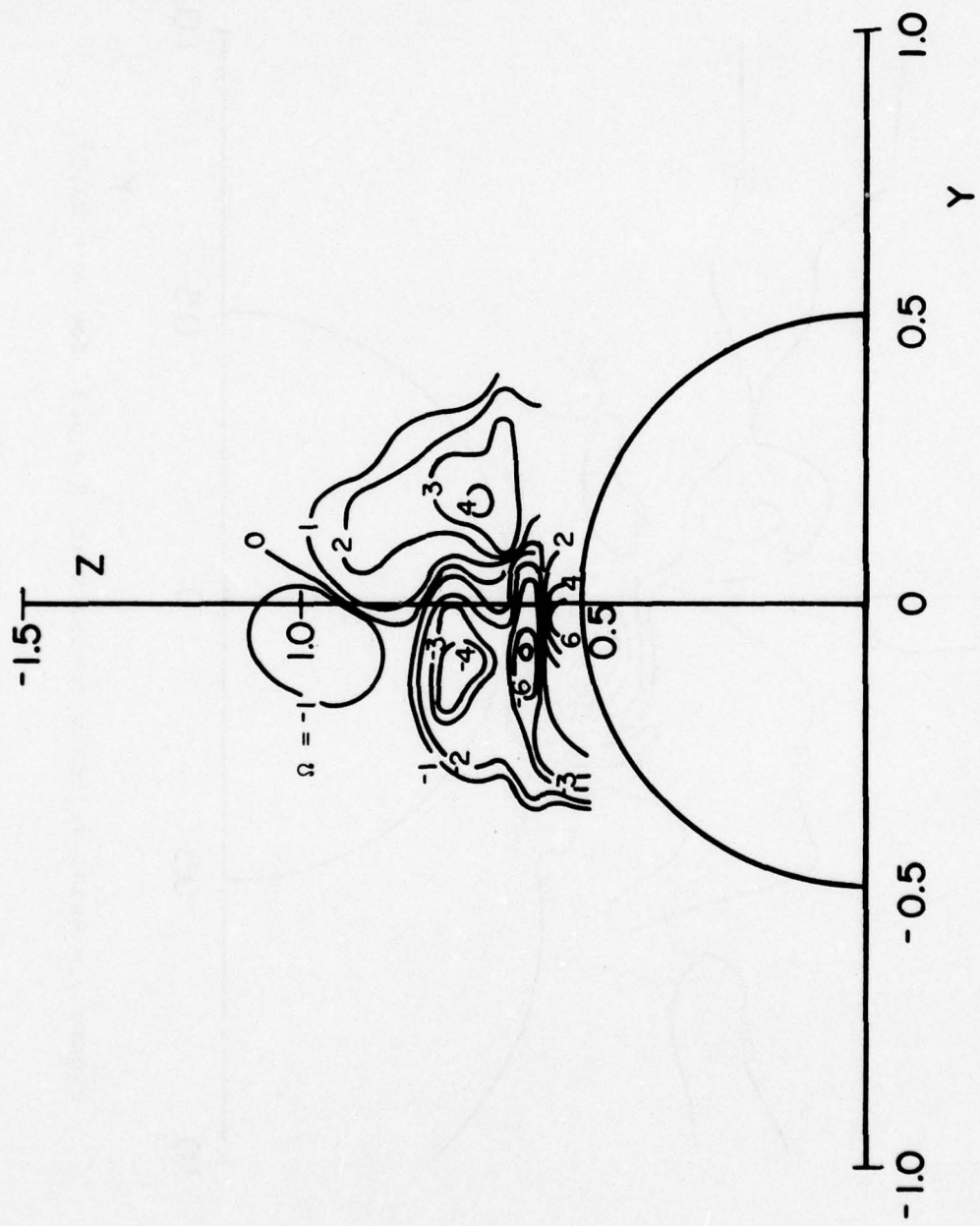


Figure 8.- Vorticity contours at $X = 6.3$ for $\alpha = 22.5^\circ$.

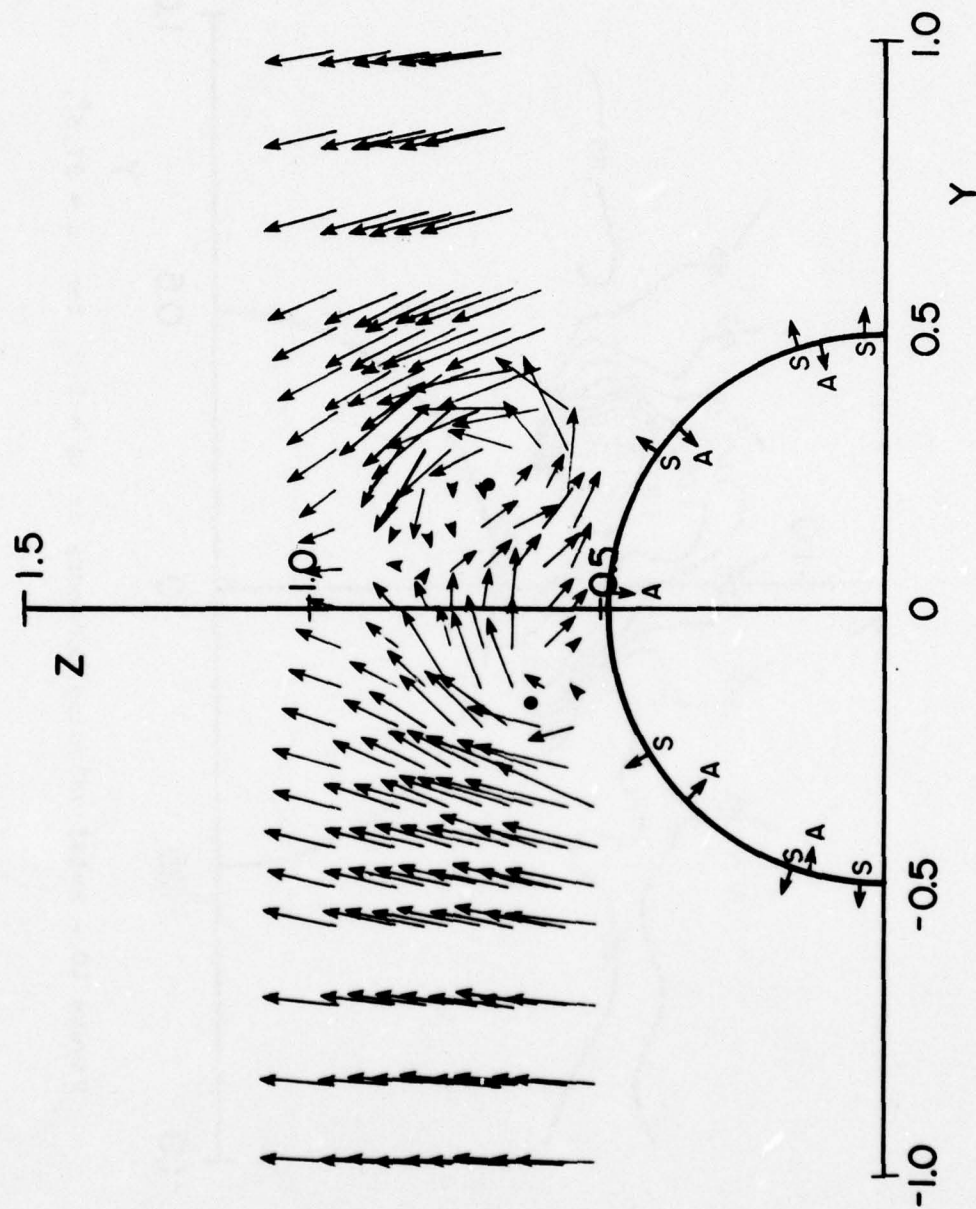


Figure 9.- Crossflow vectors at $X = 2.8$ for $\alpha = 37.5^\circ$.

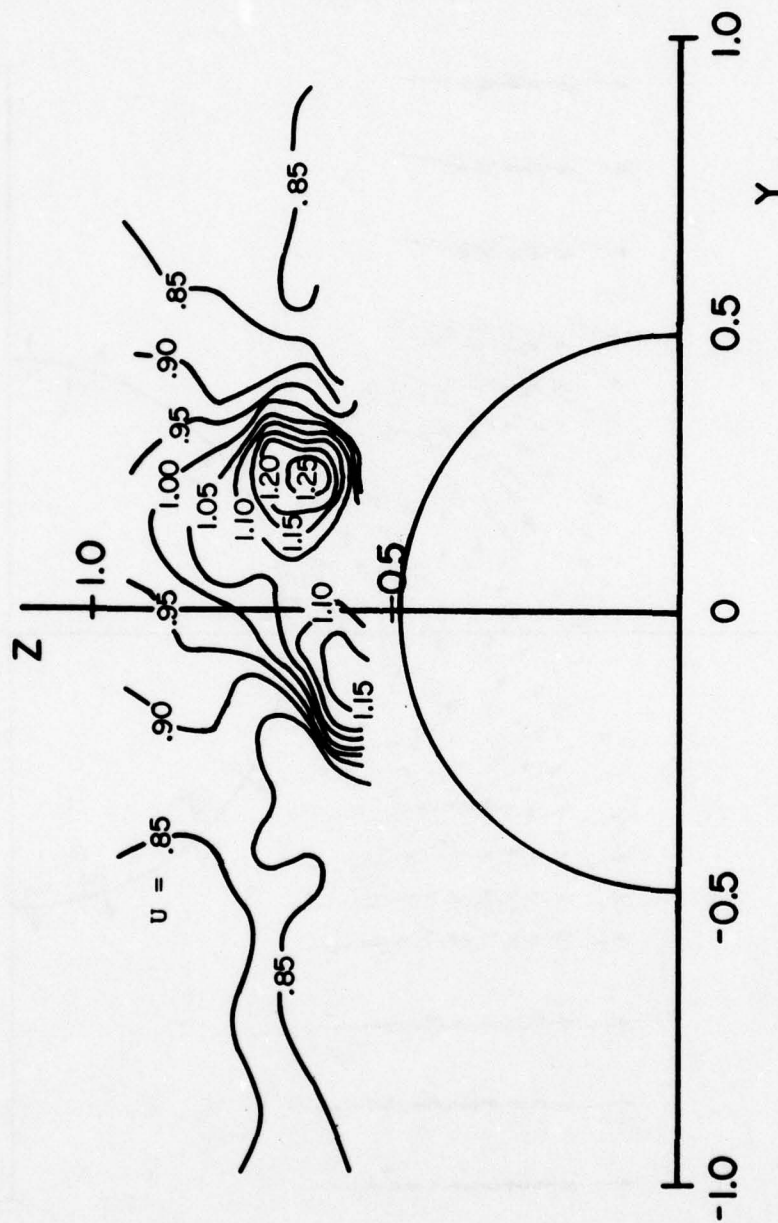


Figure 10.- Axial velocity contours at $X = 2.8$ for $\alpha = 37.5^\circ$.

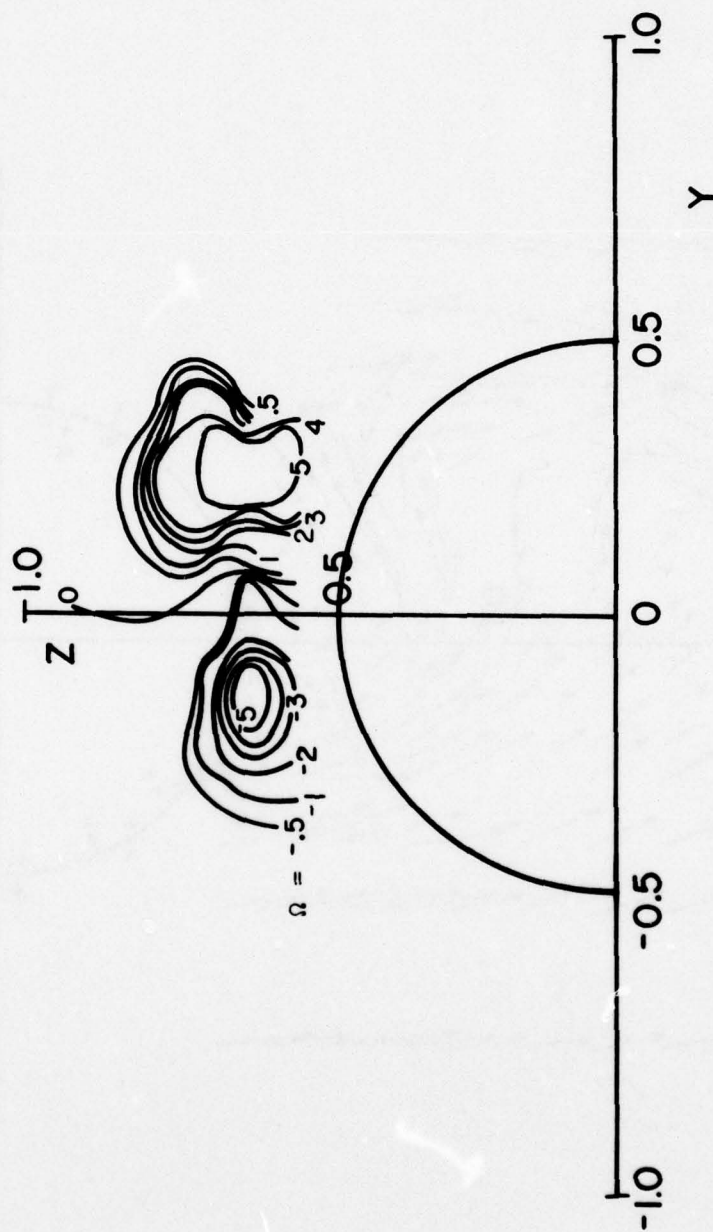


Figure 11.- Vorticity contours at $X = 2.8$ for $\alpha = 37.5^\circ$.

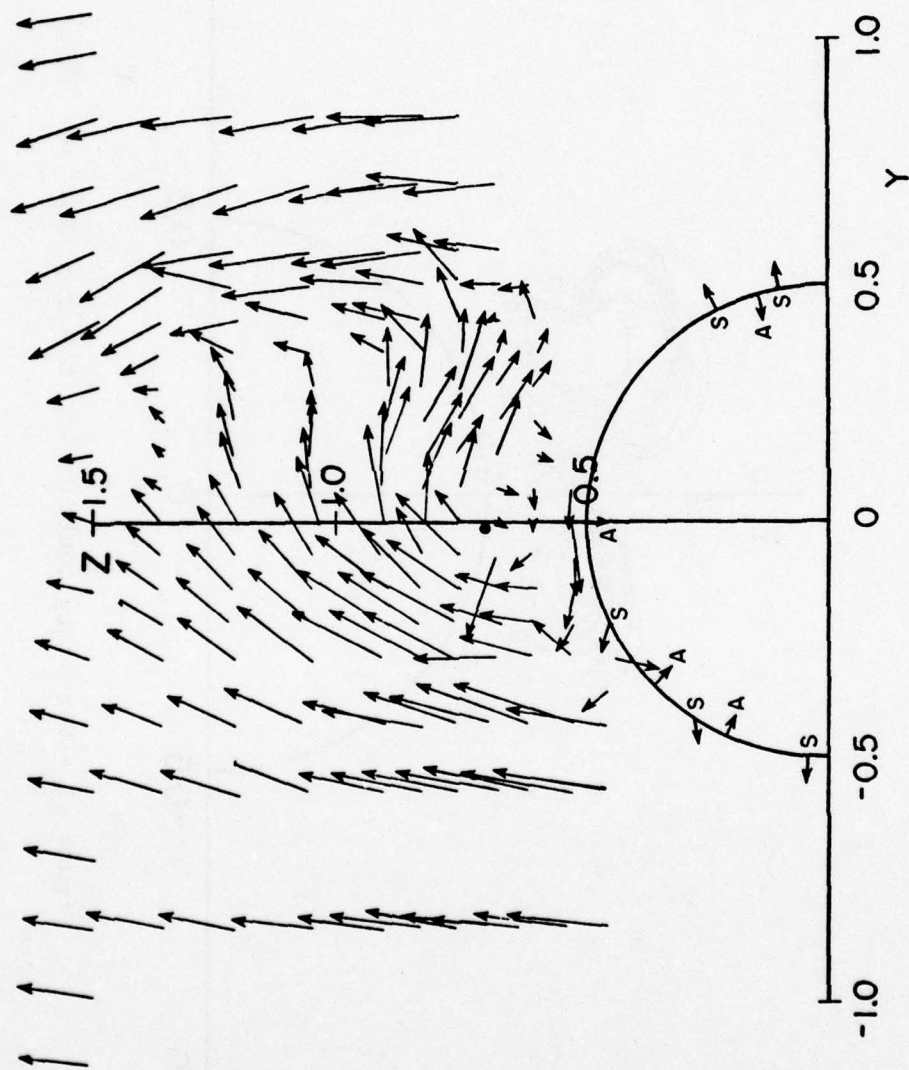


Figure 12.- Crossflow vectors at $X = 4.9$ for $\alpha = 37.5^\circ$.

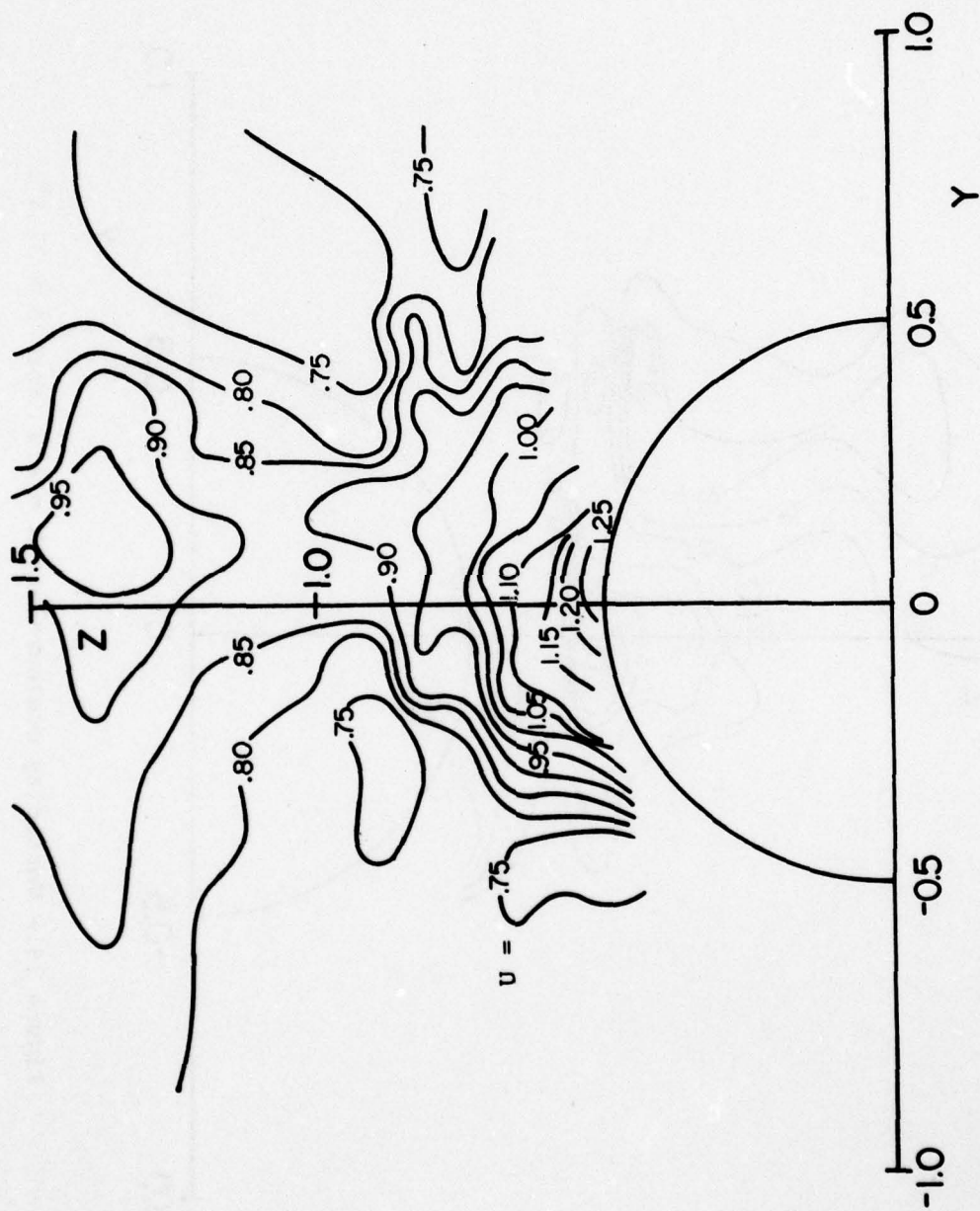


Figure 13.- Axial velocity contours at $X = 4.9$ for $\alpha = 37.5^\circ$.

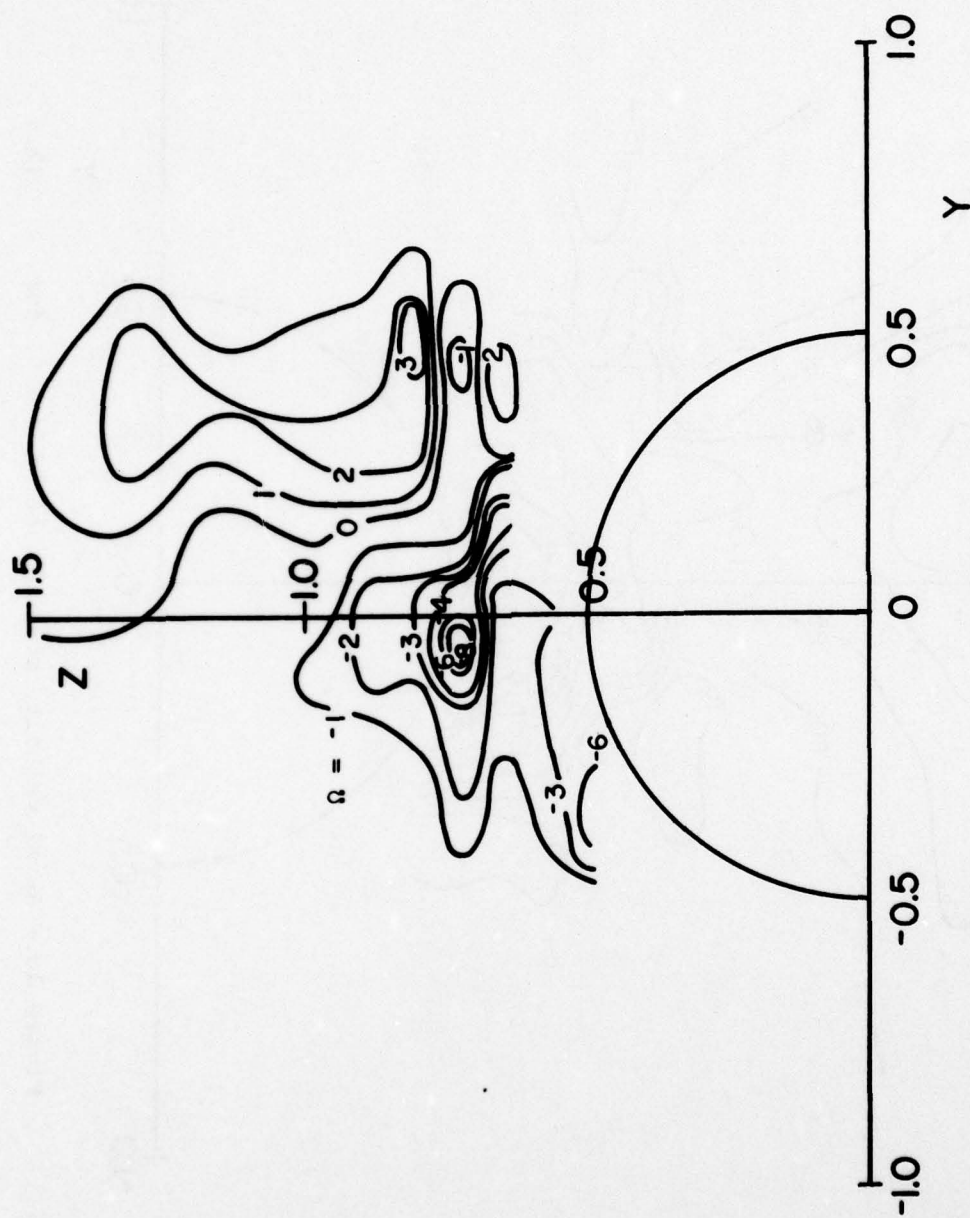


Figure 14.- Vorticity contours at $X = 4.9$ for $\alpha = 37.5^\circ$.

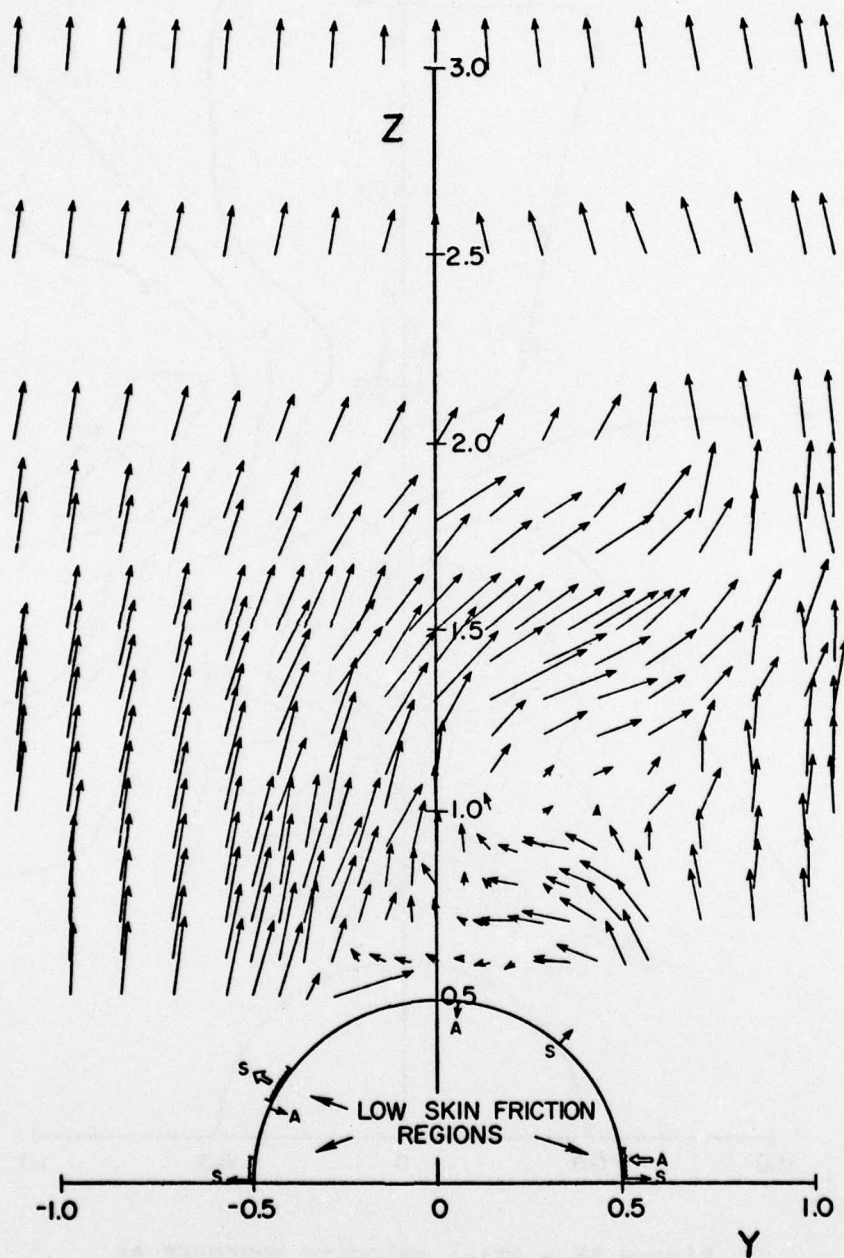


Figure 15.- Crossflow velocity vectors at $X = 6.3$ for $\alpha = 37.5^\circ$.

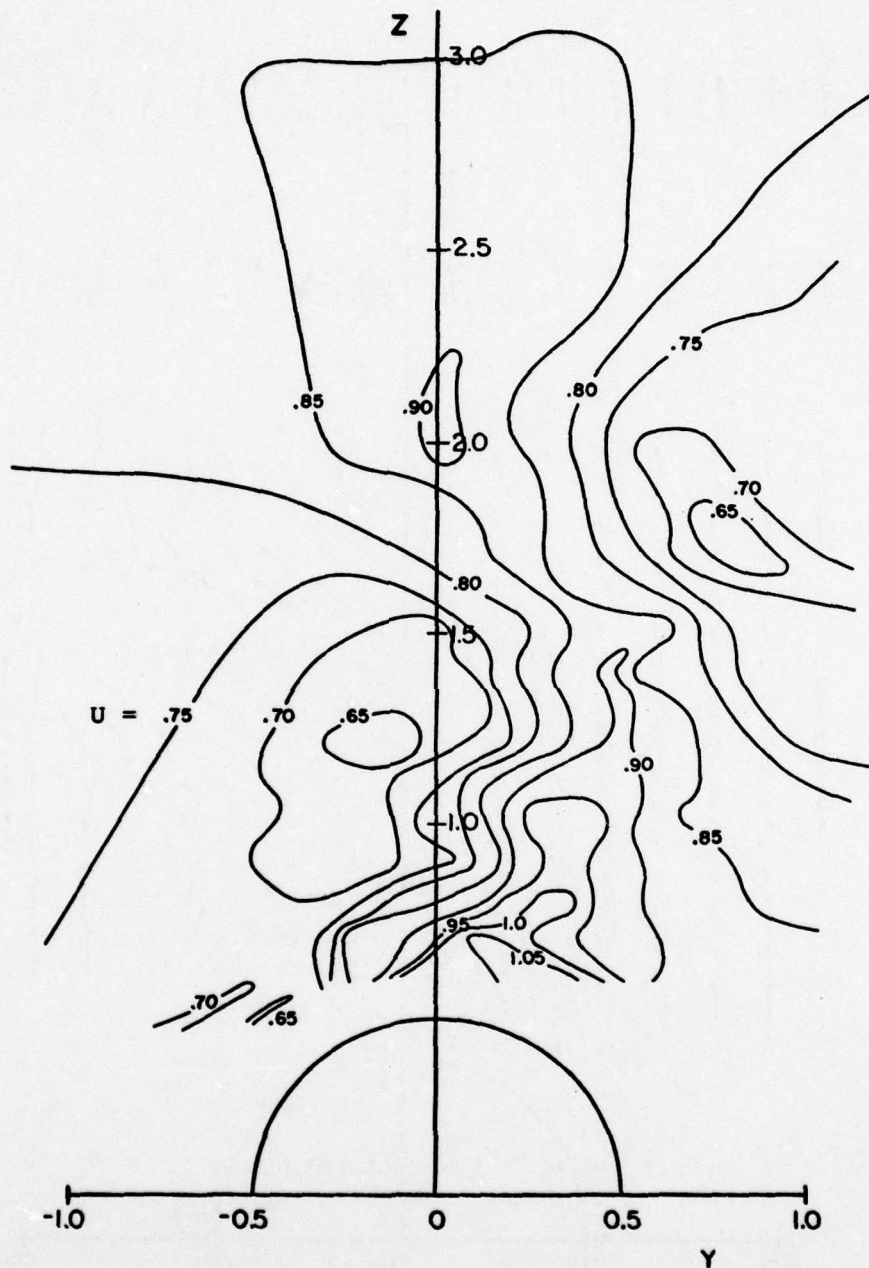


Figure 16.- Axial velocity contours at $X = 6.3$ for $\alpha = 37.5^\circ$.

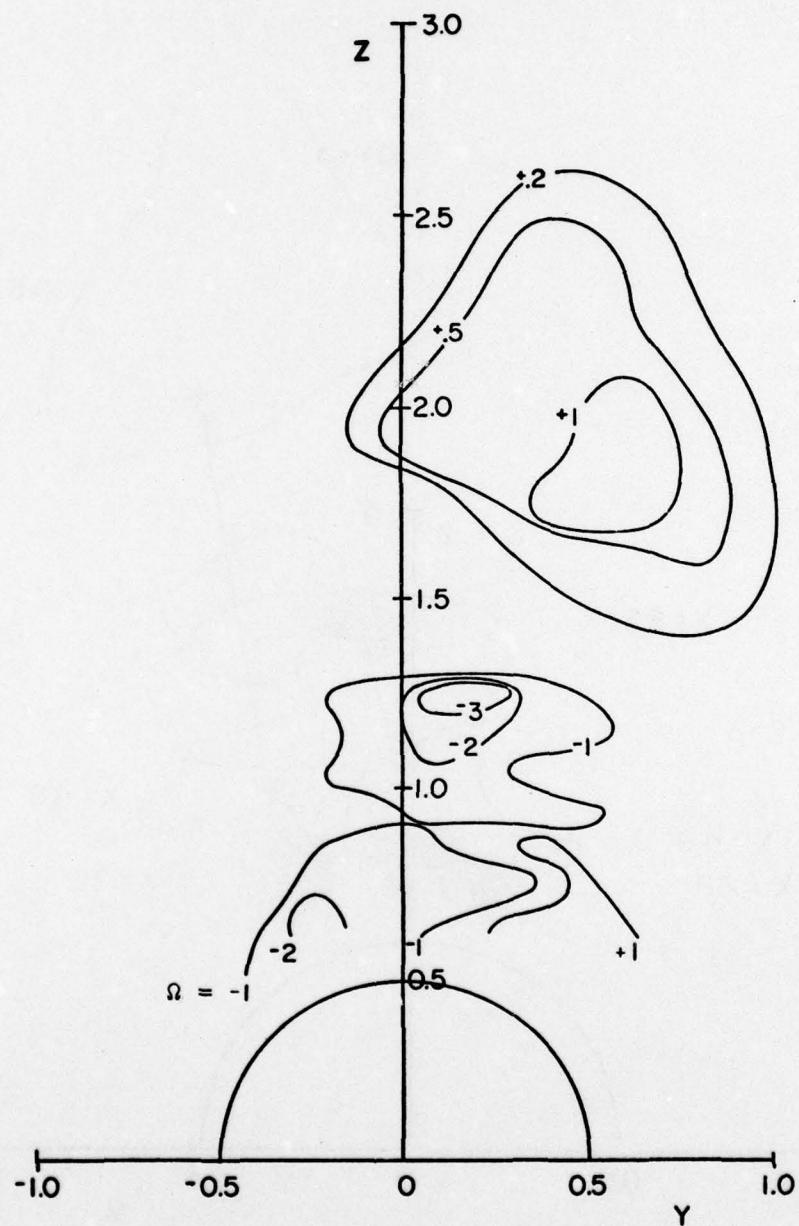


Figure 17.- Vorticity contours at
 $X = 6.3$ for $\alpha = 37.5^\circ$.

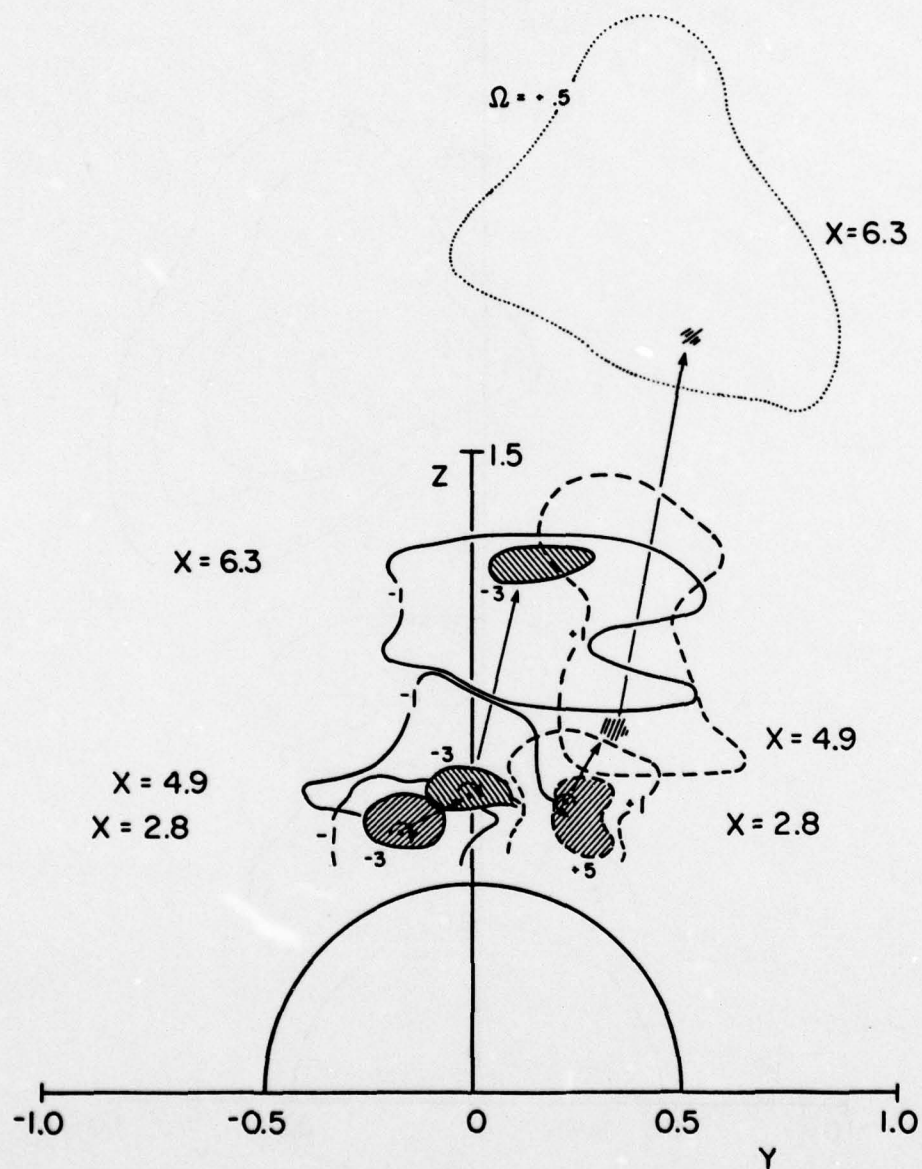
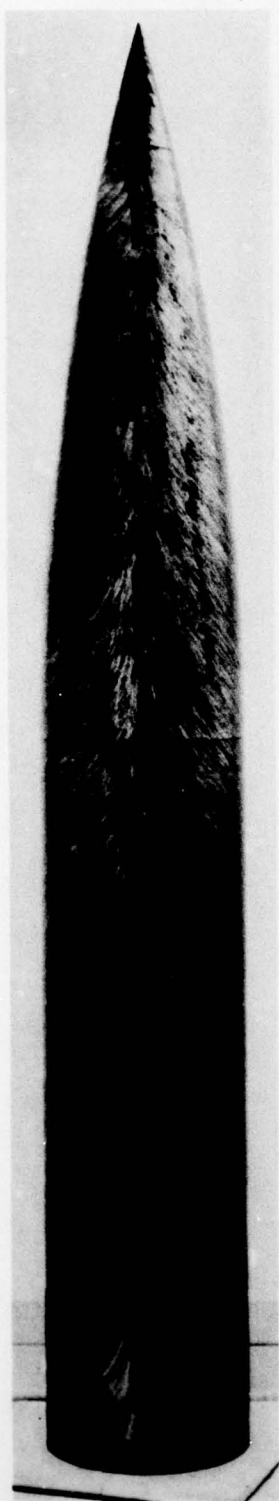
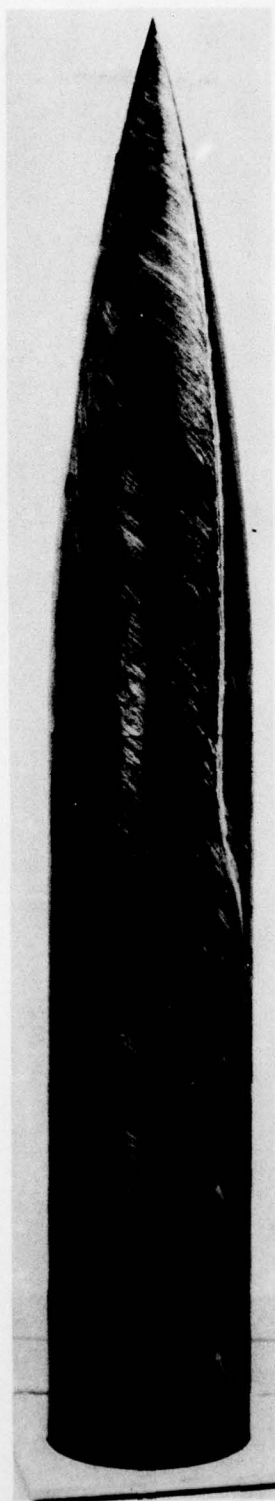


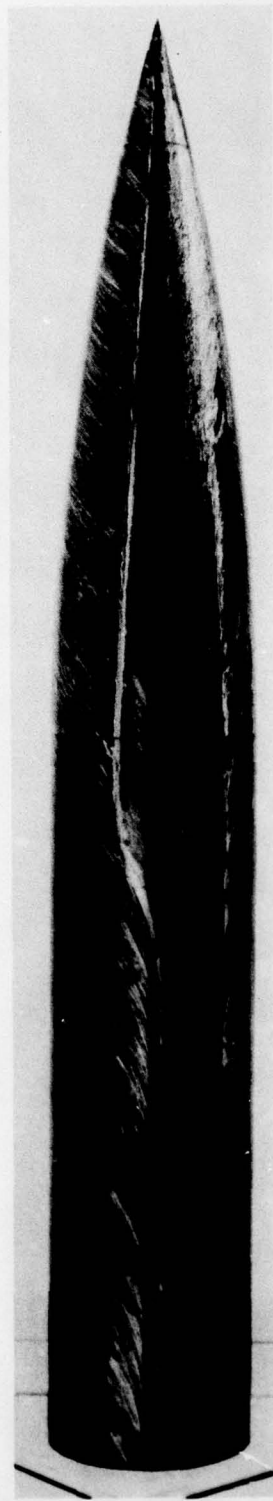
Figure 18.- Summary of vorticity contours at $\alpha = 37.5^\circ$.



$\theta = 0^\circ$



60°



120°

Figure 19.- Carbon black surface flow visualization,
 $\alpha = 22-1/2^\circ$; $Re_D = 0.37 \cdot 10^6$.



$\theta = 180^\circ$

78

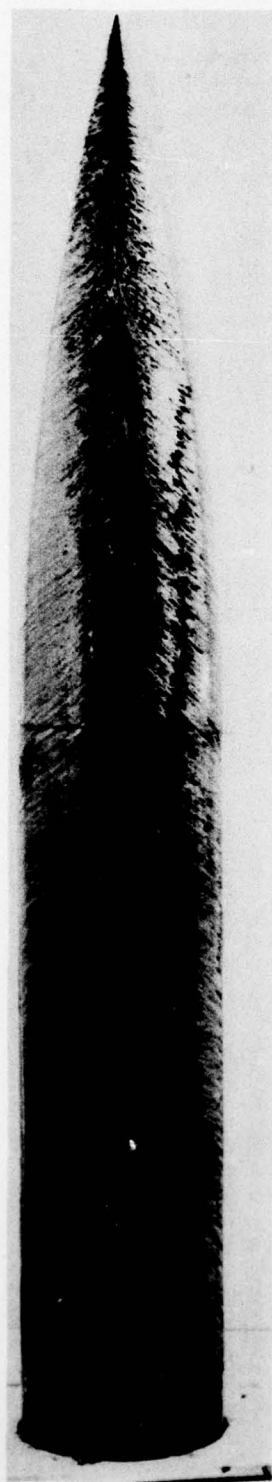


240°



300°

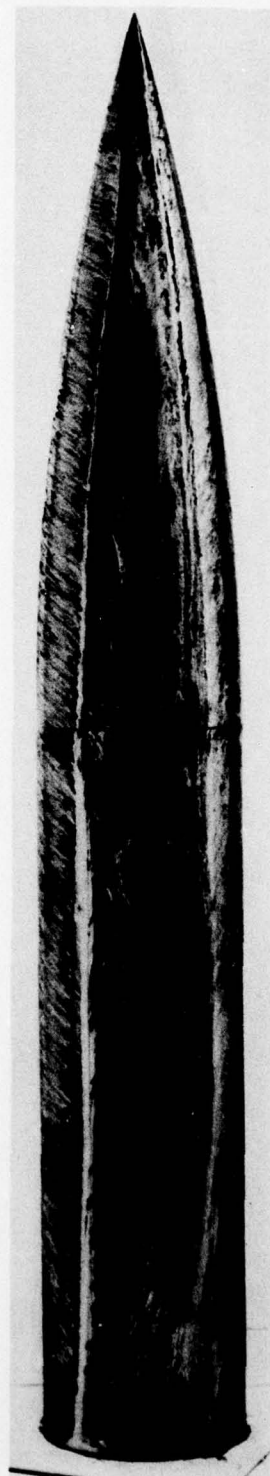
Figure 19.- Concluded.



$\theta = 0^\circ$

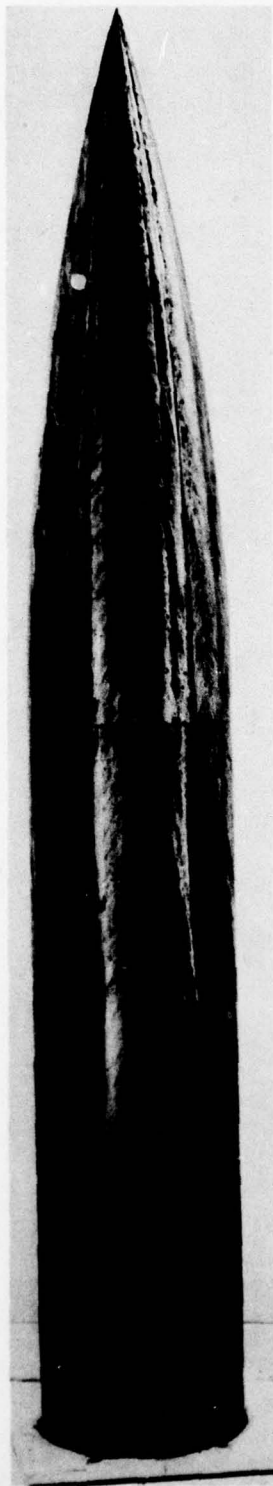


60°

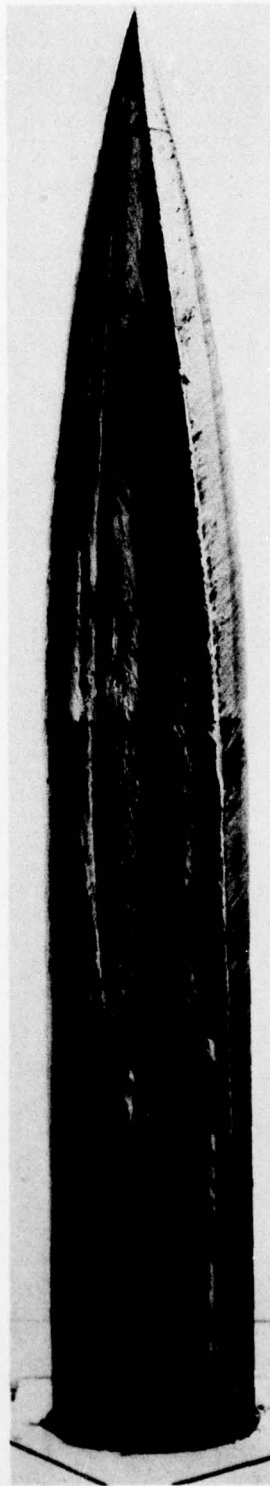


120°

Figure 20.- Carbon black surface flow visualization,
 $\alpha = 37.5^\circ$; $Re_D = 0.18 \cdot 10^6$, with tape strip on nose.



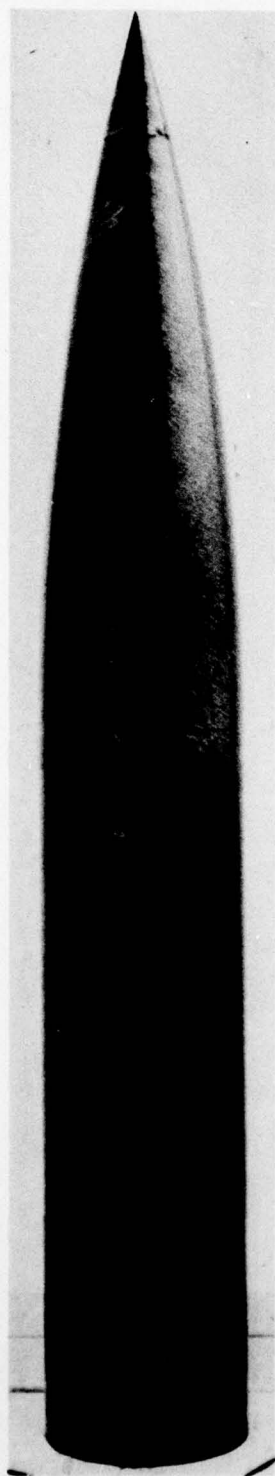
$\theta = 180^\circ$



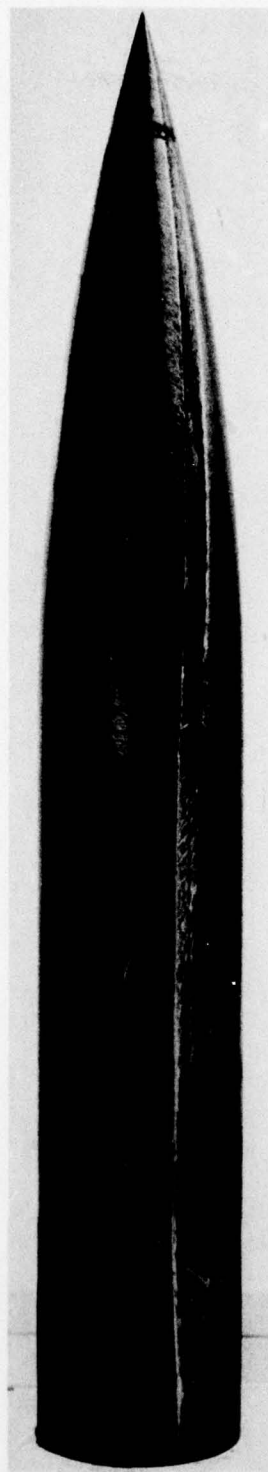
240°



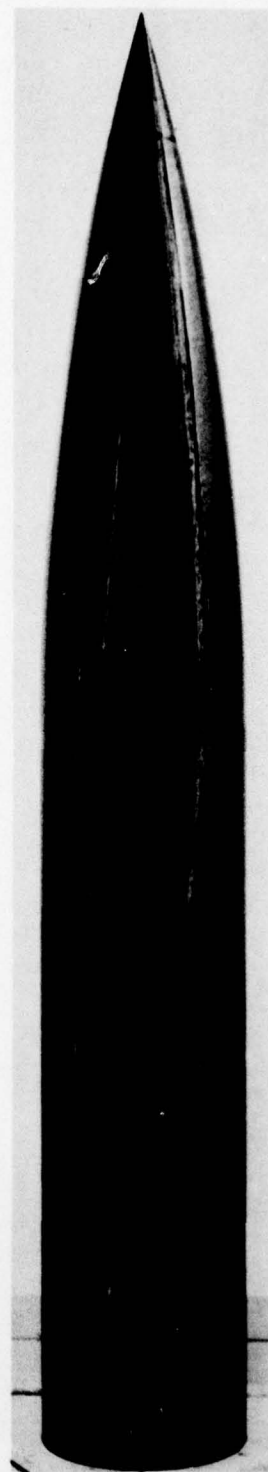
300°



$\theta = 0^\circ$

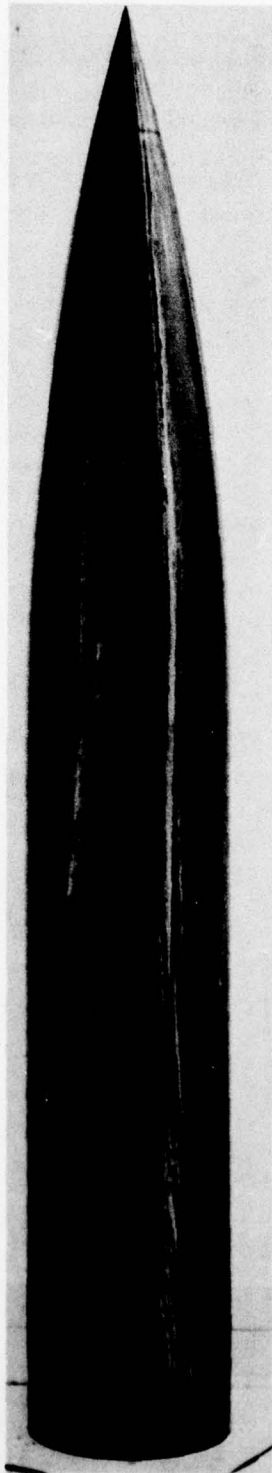


60°



120°

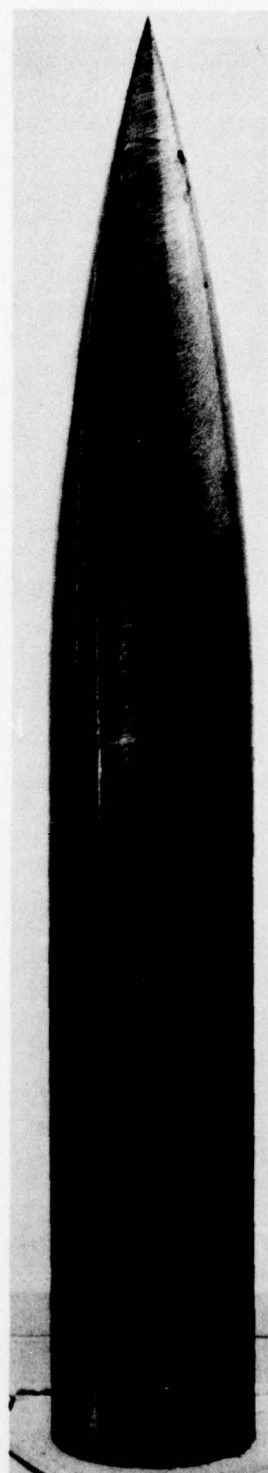
Figure 21.- Carbon black surface flow visualization, $\alpha = 37\text{-}1/2^\circ$;
 $Re_D = 0.37 \cdot 10^6$, without tape strip on nose.



$\theta = 180^\circ$



240°



300°

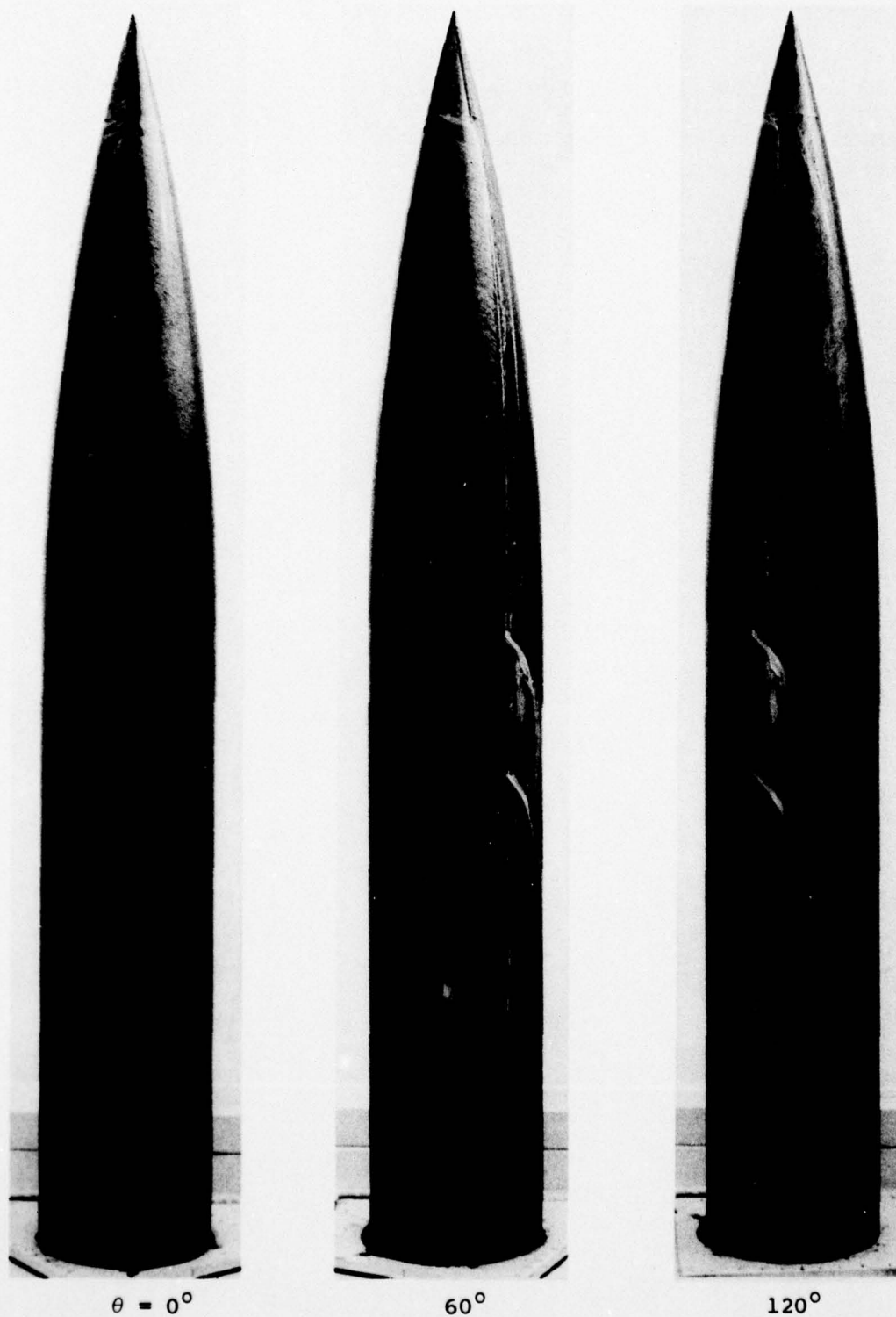
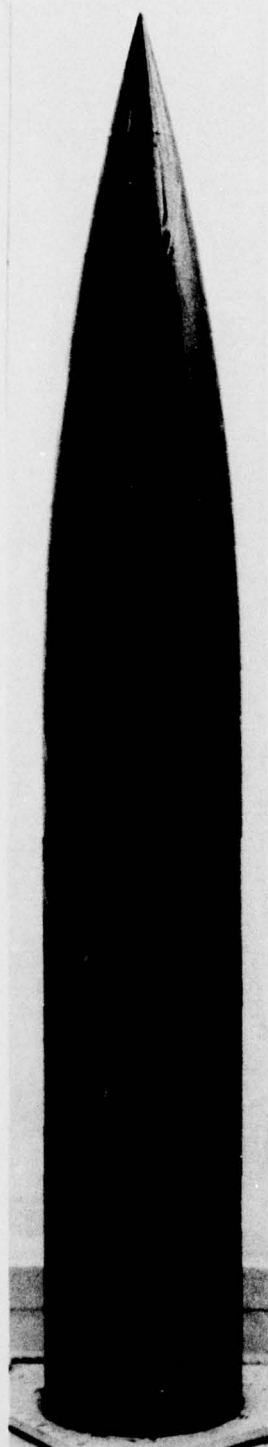
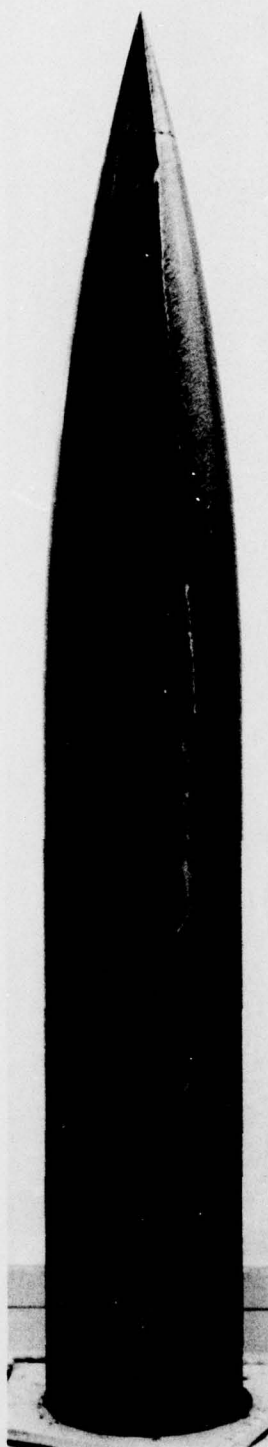


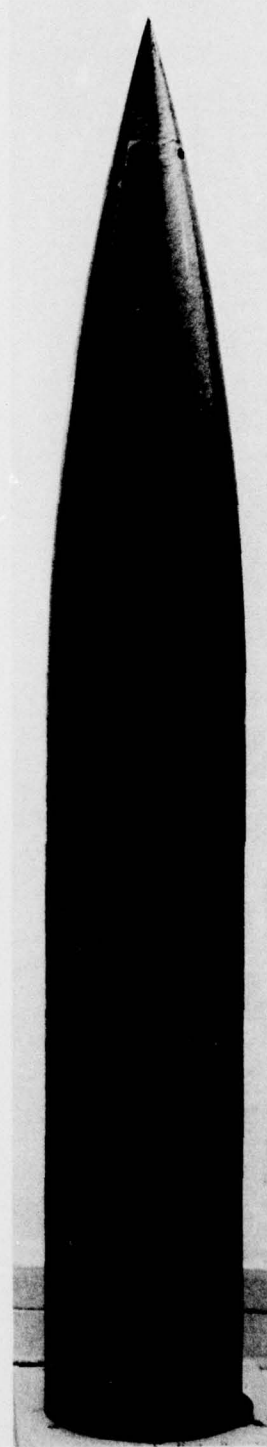
Figure 22.- Carbon black surface flow visualization,
 $\alpha = 37\text{-}1/2^\circ$; $Re = 0.37 \cdot 10^6$, with tape strip on nose.
 (Figures 9-18, 23 at same flow conditions)



$\theta = 180^\circ$



240°



300°

Figure 22.- Concluded.

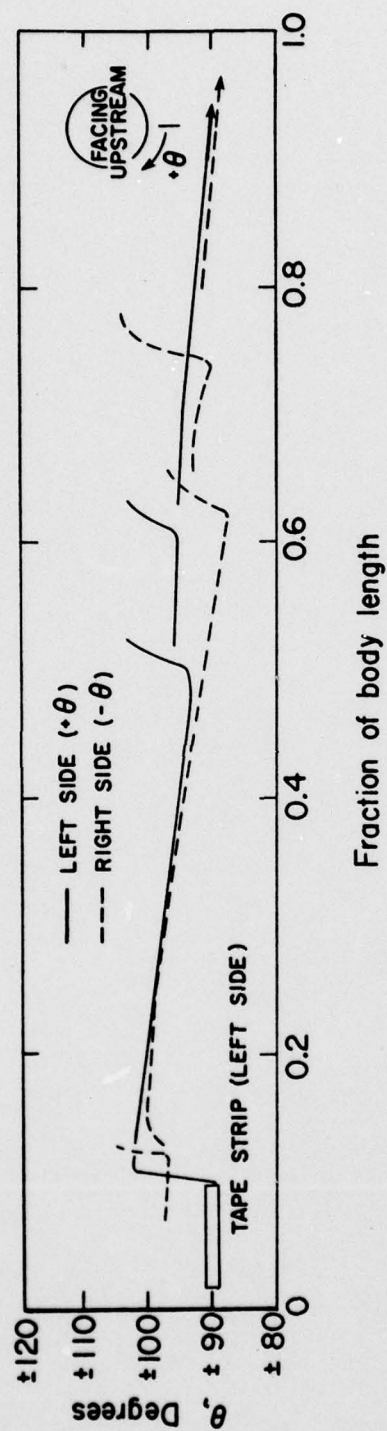


Figure 23.- Location of primary separation lines from photographs of Figure 22, $\alpha = 37-1/2^\circ$, $Re = 0.37 \cdot 10^6$, with tape strip.